# FLIGHT CONTROL DESIGN USING HYBRID INCREMENTAL NONLINEAR DYNAMIC INVERSION

Technische Universiteit Delft

YAĞIZ KUMTEPE

Master of Science Thesis

October 8, 2020

TU Delft
Delft University of Technology
Challenge the future

# Flight Control Design Using Hybrid Incremental Nonlinear Dynamic Inversion

For obtaining the degree of Master of Science in Aerospace Engineering at Delft University of Technology, to be defended publicly on Thursday October 08, 2020 at 14:00.

by

Yağız Kumtepe

October 8, 2020

| | | |
|---|---|---|
| Thesis committee: | Dr. ir. M. M. van Paassen, | TU Delft, Chair |
| | Dr. ir. E. Mooij, | TU Delft, Examiner |
| | Dr. ir. E. van Kampen, | TU Delft, Supervisor |
| | Ir. T.S.C. Pollack, | TU Delft, Supervisor |

An electronic version of this thesis is available at `http://repository.tudelft.nl/`.

Delft University of Technology

# ACKNOWLEDGMENTS

I would like to express my sincere gratitude to my supervisors Dr. Ir. Erik-Jan van Kampen and Ir. Tijmen Pollack. I had a very educational experience thanks to their feedback and guidance in our weekly discussions. I am grateful for the time that they contributed to the quality of the research, and for motivating me during such unprecedented times when I had to leave the Netherlands and stay at state quarantine.

I also would like to thank my friends, Alp for orienting me to the Netherlands very quickly, Hem for the discussions we had before the pandemic, and Nishant for his companionship during MSc.

My deepest thanks to my brother, mother, and father, who always supported me and made me feel their love that has become true motivation. Finally, special thanks to my dearest Cemre, who has been a great help for the completion of this thesis.

# CONTENTS

# LIST OF FIGURES

# List of Tables

# List of Symbols and Abbreviation

**Roman Symbols**

| | |
|---|---|
| $A$ | Acceleration |
| $a$ | Cost Function Weight |
| $b$ | Cost Function Weight |
| $b$ | Missile Control Effectiveness Coefficient |
| $C$ | Aerodynamic Coefficient |
| $d$ | Disturbance |
| $d$ | Reference Distance |
| $e$ | Error |
| $f$ | Vector Field |
| $g$ | Control Effectiveness Matrix |
| $H$ | Transfer Function |
| $h$ | Scalar Function |
| $I$ | Identity Matrix |
| $I$ | Inertia Tensor |
| $J$ | Cost Function |
| $k$ | Control Gain |
| $L$ | Lift |
| $M$ | Mach Number |
| $M$ | Moment |
| $m$ | Mass |
| $n$ | Noise |
| $Q$ | Dynamic Pressure |
| $q$ | Pitch Rate |
| $S$ | Surface Area |
| $s$ | Laplace Variable |
| $T$ | Thrust |
| $t$ | Time |
| $u$ | Control Input |

| | |
|---|---|
| $V$ | Velocity |
| $X$ | X-Axis |
| $x$ | State Vector |
| $Y$ | Y-Axis |
| $y$ | System Output |
| $Z$ | Z-Axis |

**Greek Symbols**

| | |
|---|---|
| $\alpha$ | Angle of Attack |
| $\Delta$ | Uncertain Subset / Increment |
| $\delta$ | Control Surface Deflection |
| $\epsilon$ | Root Mean Square of Tracking Error |
| $\gamma$ | Flight Path Angle |
| $\nu$ | Virtual Control |
| $\sigma$ | Standard Deviation |
| $\theta$ | Pitch Angle |

**Subscripts**

| | |
|---|---|
| 0 | Previous Value |
| $B$ | Body Coordinate Frame |
| $d$ | Desired Value |
| $d$ | Time Delay |
| $p$ | proportional |
| $yy$ | Around y-axis |
| act | Actuator |
| com | Command |
| des | Desired Value |
| m | Measurement |
| N | Noise Filter |
| q | Pitch Rate Sensor |
| ref | Reference |
| sync | Synchronization |

**Abbreviations**

| | |
|---|---|
| D/A | Digital to Analog Conversion |
| FBL | Feedback Linearization |

| | |
|---|---|
| FCC | Flight Control Computer |
| FCS | Flight Control System |
| INDI | Incremental Nonlinear Dynamic Inversion |
| LQR | Linear Quadratic Regulator |
| MAV | Micro Aerial Vehicle |
| MB | Model-Based |
| NDI | Nonlinear Dynamic Inversion |
| PID | Proportional Integral Derivative |
| RM | Reference Model |
| RMS | Root Mean Square |
| SB | Sensor-Based |
| SBB | Sensor-Based Backstepping |
| TF | Transfer Function |
| UAV | Unmanned Aerial Vehicle |
| VTOL | Vertical Take-off and Landing |

# 1

# INTRODUCTION

Balloons are one of the first kinds of human carrying aerial vehicles and yet their applications in the modern era are very limited. This is mainly due to their weak controllability. Controllability of a vehicle contributes to its value significantly. Aerial vehicles are free in all six degrees of freedom and therefore the control task is rather complex compared to, for instance, a system which is restricted to move only in one direction. In a piloted system, the full control task was initially performed by the pilot, causing an exhaustive workload. This was noticed very quickly and an automatic control system was designed in 1912, just nine years after the first flight by Wright brothers [9].

Over a hundred years, flight control systems have got more advanced. Yet it remains as a highly interesting subject due to its endless benefits to aerial vehicles. Advancing flight control systems can increase the ability to precisely and accurately position a vehicle throughout the mission. An example of this benefit is the development of reusable launch vehicles. Fig. 1.1 shows two boosters being safely and simultaneously landed. These vehicles are also part of a project to launch thousands of small satellites for a wide range of internet access [10]. The reusability of the launchers provides a solution for one of the main challenges of the field, efficiency.

Control systems are one of the essential components of aerospace vehicles. Time spent for the design for these systems is expected to be efficient as well. The aerospace industry comprises of a wide range of vehicles from civil aircraft to satellites, from rocket launchers to helicopters. The industry keeps growing and demands for new applications and new expectations emerge. For instance, drones find application in photography, search and rescue missions, surveillance, agriculture, etc. For these tasks new types of vehicles are designed and it is not efficient to spend extensive time and effort on a single type of vehicle. Accomplishment of efficiency in regards of design time is especially challenging because the tasks are expected to be completed even in the presence of unexpected events. The academics focus on advancing flight control systems in order to overcome this challenge [11]. Incremental Nonlinear Dynamic Inversion (INDI) is presented as one of the promising solutions to have a generic flight control system that can be easily applied to various types of vehicles and handle unexpected conditions [12]. It is also the main focus of this study.

This chapter presents an introduction for the thesis study, *Flight Control Design Using Hybrid Incremental Nonlinear Dynamic Inversion.* The next section, motivates the study by addressing current benefits of advanced automatic control systems in aerospace vehicles. The research questions are presented in Section 1.2 with definitions of the approaches used in the study. Lastly, the outline of the report is given in Section 1.3.

Figure 1.1: Landing of two side boosters of Falcon Heavy Test Mission on 6 February 2018 [1]

(a) Air Data System, SmartProbe

(b) Angle of Attack Sensor

Figure 1.2: Two common sensors widely used in air vehicles manufactured by Collins Aerospace [2]

## 1.1. RESEARCH MOTIVATION

This section aims to present general benefits and capabilities of flight control systems in order to emphasize the value added by these systems. The current drawbacks and challenges are stated. The section can be regarded as performance criteria because newly developed systems shall maintain the benefits stated here while eliminating the drawbacks.

In principle, flight control systems (FCS) include sensors provide information to flight control computer (FCC) about the current condition of the vehicle. Examples of these sensors, air data system and angle of attack sensor are shown in Fig. 1.2. FCC includes flight control laws and it determines the commands that need to be operated and send these to actuation mechanism of vehicle's control components. Primary task of FCS is to form a closed loop system that helps to have faster responses to input signals, supply a better tracking accuracy and to overcome some undesired effects such as atmospheric disturbances [11]. In other words, they increase the automation by helping or replacing pilot. The increase in automation mainly contributes to the safety and the economy of operation [13]. The significance of these issues are getting higher because more people are transported in commercial aircraft.

One of the developments that widened the benefits of FCS has been introduction of fly-by-wire mechanism that mainly contributes to flexibility of the control laws that can be implemented on FCS. This allows a control law to be applied to different systems without significant changes [14]. In addition, vehicles reach a higher level of automation by the help of advanced FCS. Accuracy of the model that is used for FCS design has vital importance for an automated flight. In the case of a model mismatch, the behavior of the system would not be as expected which leads to problems in performance. Although linear control techniques are well known and are relatively easier to ensure stability compared to nonlinear control methods, the flight dynamics are inherently nonlinear. Using a linear model increases the chance of model mismatches. Advancing flight control methods with nonlinear methods makes the actual system dynamics to be closer to the one that the controller is designed for, and reduces model mismatch problems.

Flight control systems improve the dynamical behavior of vehicles. For military aircraft, stability is compromised to increase maneuverability. Unstable characteristic is utilized to increase agility without the expense of increased control surface area. Stability augmentation system is supplied by FCS in order to achieve a stable closed-loop behavior and keep the agility of the aircraft. FCS also increases performance by actively providing gust suppression and auto trimming so that ride quality is improved for passengers as well. These benefits reduce the workload of pilots, avoid fatigue, and help them to focus on the tasks where precise control is required such as safe landing and take-off [15]. Although, the complexity may cause safety issues, the increased automation reduces human errors and accidents.

The atmospheric disturbance which can be categorized into convective turbulence, clear air turbulence and wind shear, may also cause many flight accidents and fatalities [16]. Therefore, reducing the effects of atmospheric disturbance should be one of the main concerns in the design of flight control systems. Another benefit of atmospheric disturbance reduction is to prevent structural fatigue. Fatigue in structure can threaten the integrity of the vehicle.

Aerospace vehicles operate under high loads which might cause structural damage. Any loss in the effectiveness of critical components jeopardizes the safety of the vehicle. On 4 October 1992, a cargo plane had structural damage and lost its control effectiveness. In August 1985, an aircraft crashed due to the breaking of a dome joint [17]. In some situations, although some of the control surfaces are lost, remaining ones may be sufficient to stabilize the vehicle. A study shows that the crash of El Al Flight 1862 could have been prevented by implementation of a fault-tolerant control system [18].

Advancing automatic flight control systems allows use of flexible materials. As propulsion systems improve, aircraft can reach higher speeds. This requires wings to be manufactured stiffer to ensure structural stability. Stiffer wings are heavier and thus cause consumption of more fuel. A solution to decrease wing weight is to use composite materials but they come at a cost of flexibility. Flexible structures deform under aerodynamic forces and moments causing interactions between structural dynamics and aerodynamics. Such adverse interactions introduce unwanted aeroelastic modes such as flutter which causes undamped oscillations and might lead to structural destruction. Recent developments in FCS make it possible to use highly flexible materials for aerial vehicle design and invalidate the assumption of a rigid body. For instance, the use of active flight control to suppress flutter is explored in the Flutter Free FLight Envelope eXpansion for ecOnomical Performance improvement (FLEXOP) project by experimenting on a test aircraft shown in Fig. 1.3 [3].

Modern FCS can help a different aircraft feel the same to the pilot by adjusting the control laws. Therefore, pilot training shortens and a pilot can be assigned to various types of aircraft. This decreases costs in the training and increases efficiency in the consumption of resources. A recent study shows that INDI control is suitable for the design of variable stability training aircraft [19].


Figure 1.3: FLEXOP Project Test Aircraft [3]

The precision in the position control has increased so that launch vehicles land safely [20]. Such a development significantly decreases the cost of manufacturing making many projects financially feasible.

Advanced flight control methods aim to contain the aforementioned benefits as much as possible. Those benefits come with the cost of increased complexity of the control design which is one of the major problems. More effort is required from engineers to design a complex system. Therefore, more resources and time need to be spent. As this is contradictory to the economic benefits of FCS, it is a problem in terms of certification as well. Before a new control law is implemented, it is required to be approved by authorities. Being recently developed, civilian use of adaptive controllers have certification problems since the criteria for this type of controller such as performance metrics, monitoring tools and analysis methods are not well established [21, 22].

Many of the flight control methods rely on the mathematical model of the system making them very vulnerable for model mismatches. Ideally, a generic flight control system would only require a primitive model to be uploaded to a new aircraft. The aerospace industry focuses on generic robust methods to limit the consumption of resources and efforts. INDI, as a flight control method, uses sensor information and determines the amount of control increment needed for good performance. It is robust to model uncertainties because it has emerged as a sensor-based control strategy. Data from the sensors would supply sufficient information and significantly decrease the need for a model. Hence, external disturbances and model mismatches can be compensated.

Relying on sensor measurement has consequences. Sensors have their own dynamics, noise, bias, drift, etc. which could be unintentionally regarded as external disturbances and model mismatch by the control system. Sensors might lose their functionality due to damage. This is one of the drawbacks of the INDI method and this research is dedicated to improve the method by using the aid of a system model. Some of the signals that are needed for feedback can be obtained from onboard models. Using the onboard model yields a method that is less dependent on sensor measurement. Therefore, the impact of a fault or damage on a sensor would be decreased. Differentiation would not be necessary when a model is used, thereby limiting the noise of a signal. The aim of this study is to utilize a system model in feedback signaling, to design a reliable flight controller that is robust to both sensor faults and model mismatches at the same time.

## 1.2. RESEARCH OBJECTIVES AND QUESTIONS

This section defines three different INDI approaches to prevent any possible confusion. Then, the main research question and sub-questions are presented for clarification of the objectives.

**Definition 1.1: Sensor-Based INDI**

Refers to the INDI method in the literature. Sensor-based feature of the model is emphasized to avoid confusions. It feeds back sensor measurement for linearization purposes.

**Definition 1.2: Model-Based INDI**

This method replaces the state derivative feedback that is obtained based on sensor measurement with the system's mathematical model. The method resembles Nonlinear Dynamic Inversion although the formulation follows through a modification of Sensor-Based INDI.

**Definition 1.3: Hybrid INDI**

Hybrid INDI uses sensor measurement and mathematical model simultaneously. The combination aims to maintain robust properties of both of the methods.

The main research question of this thesis is as follows

**"How can Sensor-Based INDI and Model-Based INDI be combined in order to formulate a robust Hybrid INDI such that the performance degradation due to model mismatches and sensor faults are decreased without compromising nominal performance?"**

This question is divided into multiple sub-questions that lead to answering the main question.

1. *What is the state of the art of INDI?*

   In order to observe the improvement by the model aiding, it is essential to first observe the existing performance results. In addition, the problems and shortcomings of the method should be investigated to focus on improving these areas. INDI has been studied for over ten years; therefore, a considerable amount of research is developed to improve it theoretically and practically. There could be various ways of model aiding to improve the performance for different theoretical and practical approaches. Studying these methods helps to widen the benefits of Hybrid INDI.

2. *How can Model-Based INDI be structured?*

   Although Model-Based INDI is formed to reduce the dependence on the sensor measurements, for the model to extract the needed information, sensor measurements should be supplied. The method has benefits such as being less vulnerable to sensor noise. The Model-Based INDI approach is expected to be integrated with Sensor-Based INDI. Therefore, both should be similar in some aspects. In this regard, listed sub-questions need consideration.

   (a) *How should the synchronization method be modified?*

   Ideally, control increment and state derivative feedback correspond to the same time. This is achieved by the synchronization of signals. First the synchronization method should be determined and then differences in the synchronization should be highlighted for a better combination.

   (b) *How should the noise filter be modified?*

   Sensor measurement contains noise. Noise filtering is a method to mitigate the effect of noise on the system to improve performance. As the sensor output is processed in a different manner, noise filter should be modified. Filtering techniques that is used for INDI might not be ideal for Model-Based INDI.

(c) *What other considerations should be taken for disturbance rejection or tracking performance?*

Command tracking and disturbance rejection are basic demands from a flight controller. It should be investigated whether additional modifications are needed.

3. *How do Model-Based INDI and Sensor-Based INDI perform compared to each other?*

(a) *What are the differences in the nominal performance?*

The nominal performances are expected to be similar. If this not the case, the reason for the difference should be identified.

(b) *How do the methods perform in robustness analysis?*

The two methods are robust against different issues. Factors such as, aerodynamic uncertainties, measurement delays and disturbance rejection should be investigated to identify and quantify their robust performance.

The results of questions 1- 3 highlight the main strengths of the two approaches. They are important to decide on hybridization of these approaches to maintain their benefits.

4. *What are the existing methods of hybrid controllers?*

(a) *What are the problems that are encountered with combining the control systems?*

(b) *Can these be applied to form Hybrid INDI?*

These questions require additional literature study. It is common to combine different control structures to form a hybrid method. These solutions should be checked and their feasibility for INDI application should be studied.

5. *How can Model-Based INDI and Sensor-Based INDI be combined into a hybrid method and what are the considerations of the combination?*

Ideally approaches are combined in in a way that they compensate each others' weaknesses while keeping their strengths.

(a) *How is the information from processed sensor signal integrated with the one coming from the onboard model?*

In the hybrid approach, same state derivative feedback is generated from two sources. It should be determined how to integrate these two signals. The options could be averaging signals' value or determining the regions where one of them is more reliable than the other and using the signal accordingly.

(b) *How are the signals synchronized?*

Hybrid approach combines two techniques with different synchronization methods. Therefore, it should be determined how to synchronize the control input with the feedback signal.

(c) *What is the effect of hybridization to stability margins?*

The hybrid method aims to have a larger stable region although instability might be also introduced in some regions which should be determined and restricted if possible.

6. *Which of the challenges of INDI is solved by Hybrid INDI and what are the challenges of Hybrid INDI?*

It is important to highlight the success of the method. Therefore, Hybrid INDI control design needs to be compared to each of its component methods. This can be done by time domain simulations and the performance comparisons can be presented. For further studies, any practical challenges or limitations should be listed.

The research questions are connected to each other in a way that answering one of them would be a requirement to continue for the others. The sub-questions also work as a guideline for answering the main research question. The questions are answered throughout the report and they are revisited in Chapter 6 to emphasize the answers.

## 1.3. REPORT OUTLINE

The outline of the report is as follows: Initially a scientific paper is presented in Chapter 2. The paper focuses on the main results of the research. In the paper, the Hybrid INDI approach is proposed based on the fusion of sensor measurement and model output by a complementary filter. The state derivative term in the INDI control law is replaced with state derivative estimation. The chapter presents robustness analysis against measurement delays. An attitude controller is designed for F-16 aircraft to test the performance of Hybrid INDI and time-domain simulation results are presented.

In Chapter 3 Nonlinear Dynamic Inversion (NDI) control method is presented. NDI is important because its drawbacks inspired INDI and it has a strong resemblance to Model-Based INDI. Chapter 4 is spared for the INDI method. The chapter contains broad literature survey of the method that includes developments in different perspectives. Studies that utilize both sensors and models are also presented in this chapter. Furthermore, hybrid controllers and methods to form a hybrid controller are investigated and their applicability to the INDI is discussed.

The preliminary results are presented in Chapter 5. Sensor-Based and Model-Based INDI controllers are derived specifically for the short period mode and closed-loop systems are formed including sensor dynamics and noise filters. Initially, the control design is improved by considering tracking error and disturbance rejection, optimizing proportional gains, and modifying feedforward controller. Then, time domain simulations are shown for robustness analysis of the methods which underline the differences of the approaches in terms of performance.

The main conclusions are presented in Chapter 6. The chapter discusses to what extent the research questions are answered by revising the research questions. Lastly, Chapter 7 states the limitations of Hybrid INDI approach and recommends future search to consider these limitations and highlights possible improvements.

# 2

# SCIENTIFIC PAPER

# Flight Control Design Using Hybrid Incremental Nonlinear Dynamic Inversion

Yagiz Kumtepe *
*Delft University of Technology, 2629HS Delft, The Netherlands*

**Incremental Nonlinear Dynamic Inversion (INDI) is a sensor-based control strategy, which has shown robustness against model uncertainties on various aerospace vehicles. The sensor-based nature of the method brings attractive properties which has made it popular in the last decade. INDI globally linearizes the system by making use of control input and state derivative feedback. The time lag between control input and state derivative is seen as one of the main challenges of the method. This has been partially solved by synchronization of actuator outputs with measurement, although the method is still vulnerable to unexpected measurement delays. This paper proposes Hybrid INDI approach to alleviate measurement delays and to reduce sensor dependence of INDI. The approach fuses the system model and sensor measurement via a complementary filter that produces angular acceleration estimation. The estimation responds fast to the system input thanks to the on-board model. It has also a low-frequency accuracy because of the sensor measurement. The method is found to retain good performance in case of model mismatches and measurement delays. An attitude controller is designed for the F-16 aircraft model and findings are verified with time-domain simulations.**

## Nomenclature

| | | |
|---|---|---|
| $b$, $\bar{c}$, $S$ | = | Wing span and mean aerodynamic chord, surface area |
| $C_l$, $C_m$, $C_n$ | = | Aerodynamic moment coefficients |
| $h$ | = | Altitude |
| $J$ | = | Inertia matrix, cost function |
| $\boldsymbol{K}$ | = | Control gains matrix |
| $L$, $M$, $N$ | = | Aircraft moments |
| $\boldsymbol{u}$ | = | Input vector |
| $V$ | = | Velocity |
| $\boldsymbol{y}$ | = | Output vector |
| $\boldsymbol{x}$ | = | State vector |
| $\alpha$, $\beta$ | = | Angle of attack and side slip angle |
| $\delta$ | = | Control surface deflection |
| $\epsilon$ | = | Root mean square of tracking error |
| $\zeta$ | = | Damping coefficient |
| $\boldsymbol{\theta}$ | = | Attitude angles |
| $\rho$ | = | Air density |
| $\phi$, $\theta$, $\psi$ | = | Roll angle, pitch angle, yaw angle |
| $\omega$, $p$, $q$, $r$ | = | Angular rates |
| $\omega_n$ | = | Natural frequency |
| Subscripts | | |
| $d$ | = | desired |
| $e$, $r$, $a$, th | = | elevator, rudder, aileron, thrust |
| $m$, $s$, $r$ | = | model, sensor and reference |
| sync, pf | = | synchronization and pre-filter |

*Graduate Student, Control and Simulation Division, Faculty of Aerospace Engineering

# I. Introduction

Ensuring global stability is one of the main aims of the flight control designers for good performance and safety of the system. Commonly used classical control approach, namely gain scheduling, does not guarantee the stability between the design points. In the 90s, Nonlinear Dynamic Inversion (NDI) was proposed as a promising substitute for gain scheduling since the linear control gains of NDI method do not need scheduling [1]. The control strategy has appealing properties such as global linearization of input-output relation, decoupling control channels, and being applicable to different types of vehicles with slight modifications. Requiring a full accurate system model is the main drawback of NDI. The workload of pilot increases dramatically in case of uncertainties and system failures because the control system becomes unstable. This problem is initially handled via blending robust control methods and online system identification [2].

To eliminate the drawbacks of NDI without compromising its above-mentioned appealing properties, Sieberling et al. proposed Incremental Nonlinear Dynamic Inversion (INDI) by reformulating the simplified NDI [3, 4]. INDI depends only on the control effectiveness model that makes it robust against the rest of the model parameters. The main advantage of the method is utilization of true acceleration of the system, which contains direct information about the system model including nonlinearities, flexible dynamics, and external disturbances such as wind gust. Having direct information about the system model is especially useful when the modeling is challenging and expensive. Incremental control system alleviates this challenge by counteracting unmodeled moments and forces as shown in the transition stage of a hybrid tailsitter UAV [5].

Being a sensor-based control technique, INDI is inherently robust against a wide range of faults and structural damages. Mainly there is no need to blend INDI with a robust control structure to achieve fault tolerance. The method showed its effectiveness against actuator faults [6]. The flight envelope of quadrotors is extended by INDI since the method is tolerant against actuator faults up to two rotors [7, 8]. Besides, INDI has been applied to various aerospace vehicles. Studies on helicopter and spacecraft dynamics showed the method's success on tracking performance and rejecting disturbances as well as the method's limitations based on sampling frequency and measurement delays [9, 10]. It is shown that the system oscillates unacceptably above 50 ms lag between helicopter dynamics and actuator, and low sampling frequency significantly degrades the performance [9].

The performance of INDI is impaired by measurement delays. INDI is partially model-independent with the cost of sensor measurement dependence. Sensors transmit information about model mismatches and disturbances but due to sampling frequency, noise filtering and additional processes, the measurement corresponds to a previous time sample. This is considered as one of the main challenges of INDI [11]. The use of angular accelerometers instead of gyroscopes is one of the methods to decrease the introduction of time lag and they are tested to be beneficial although they are not very common [12, 13]. Studies show that satisfactory performance is achieved when actuators are matched with measurement in time via a synchronization filter [14]. Flight tests are successfully performed using synchronous signals [11] even though the control systems are still vulnerable to unexpected delays. This paper aims to reduce the dependence of INDI control strategy on measurement by proposing a new INDI approach that is robust against measurement delays.

The main contributions of the paper are as follows: First, Model-Based INDI is presented as an incremental method, which is less dependent on measurements, to expose the capabilities of a full-model approach. Second, design and analysis of a complementary filter for angular acceleration estimation is presented. This filter fuses model output with sensor measurement keeping beneficial characteristics of both signals. The filter is used in the design of Hybrid INDI approach. Third, an analysis of Hybrid INDI is presented focusing on the synchronization method and performance when there are measurement delays. This analysis includes closed-loop pole migrations of the system and time-domain simulation comparisons of Hybrid INDI and Sensor-Based INDI. Lastly, Hybrid INDI is designed for F-16 aircraft to investigate and compare robustness of different INDI approaches against sensor delays and aerodynamic uncertainties.

The paper briefly discusses the theory and formulation of INDI in Sec. II. Sec. III introduces Hybrid INDI as well as the complementary filter used for the angular estimation, and shows improvements in robustness of Hybrid INDI compared to Sensor-Based INDI. Sec. IV explains the application of Hybrid INDI on by designing an attitude control. Various simulation results are presented and the INDI approaches are compared in terms of nominal performance, disturbance rejection, and handling measurement delays in Sec. V. Lastly, the conclusions are presented in Sec. VI.

# II. Incremental Nonlinear Dynamic Inversion

INDI is inspired by NDI, which is a subset of feedback linearization. The main principle of NDI is to linearize the input-output relation of a system by using state feedback and coordinate transformation rather than Jacobian linearization.

State transformation makes a nonlinear system to appear as linear. The dynamics of controlled variables are reduced to be simple integrator dynamics. Then, the system is controlled via linear control methods. The method works best when the model is fully accurate. Real systems are generally highly complex and obtaining their accurate model is difficult. INDI is proposed to reduce model dependency to the control effectiveness matrix [15]. This section introduces the key concepts of INDI. Two versions of INDI are presented, (i) Sensor-Based INDI that is referred to as the conventional INDI method in the literature, and (ii) Model-Based INDI, which is an incremental method that uses the system model.

### A. Sensor-Based INDI

A general nonlinear control-affine system has the form of

$$\dot{\boldsymbol{x}} = \boldsymbol{f}(\boldsymbol{x}) + \boldsymbol{g}(\boldsymbol{x})\boldsymbol{u}. \tag{1}$$

$$\boldsymbol{y} = \boldsymbol{h}(\boldsymbol{x}) \tag{2}$$

where state vector $\boldsymbol{x} \in R^n$, input vector $\boldsymbol{u} \in R^m$, output vector $\boldsymbol{y} \in R^p$, $\boldsymbol{f}$ represents system dynamics, $\boldsymbol{h}$ is a smooth vector and $\boldsymbol{g} \in R^{n \times m}$ a matrix with smooth vector field columns that represents state-dependent control matrix. The general nonlinear equation is approximated by Taylor series expansion at the current value of the state $\boldsymbol{x}_0$ and control input $\boldsymbol{u}_0$ as

$$\dot{\boldsymbol{x}} \approx \boldsymbol{f}(\boldsymbol{x}_0) + \boldsymbol{g}(\boldsymbol{x}_0)\boldsymbol{u}_0 + \frac{\partial}{\partial \boldsymbol{x}}\left[\boldsymbol{f}(\boldsymbol{x}) + \boldsymbol{g}(\boldsymbol{x})\boldsymbol{u}\right]_{\boldsymbol{u}_0,\boldsymbol{x}_0}(\boldsymbol{x} - \boldsymbol{x}_0) + \frac{\partial}{\partial \boldsymbol{u}}\left[\boldsymbol{f}(\boldsymbol{x}) + \boldsymbol{g}(\boldsymbol{x})\boldsymbol{u}\right]_{\boldsymbol{u}_0,\boldsymbol{x}_0}(\boldsymbol{u} - \boldsymbol{u}_0). \tag{3}$$

The second derivatives and higher order terms are assumed to be negligible, and they are not included. The summation of first two terms is simply $\dot{\boldsymbol{x}}_0$. In aerospace applications generally controls change much faster than the states. This leads to assumption of $\boldsymbol{x} = \boldsymbol{x}_0$, meaning that the change of the state between two time steps is negligible as a result of time scale separation between states and inputs. The validity of time scale separation is one of the requirements of INDI. The increment in control input is defined as $\Delta\boldsymbol{u} = \boldsymbol{u} - \boldsymbol{u}_0$. Then, Eq. (3) reduces to

$$\dot{\boldsymbol{x}} \approx \dot{\boldsymbol{x}}_0 + \boldsymbol{g}(\boldsymbol{x}_0)\Delta\boldsymbol{u}. \tag{4}$$

The incremental control law is formed based on the relation in Eq. (4). For this system, we assume that state variables are also the outputs i.e. $\dot{\boldsymbol{x}} = \dot{\boldsymbol{y}}$. A virtual control input is the input to the linearization loop and it is defined as $\boldsymbol{\nu} = \dot{\boldsymbol{x}}$. Virtual control value is designed by linear controllers based on the characteristics of desired state values. The design method is to be detailed in Sec. IV. With the adequate replacements the control increment is determined as

$$\Delta\boldsymbol{u} = \boldsymbol{g}^{-1}(\boldsymbol{x}_0)(\boldsymbol{\nu} - \dot{\boldsymbol{x}}_0). \tag{5}$$

The new control input is given based on the previous control input, control effectiveness matrix and virtual control input as

$$\boldsymbol{u} = \boldsymbol{u}_0 + \boldsymbol{g}^{-1}(\boldsymbol{x}_0)(\boldsymbol{\nu} - \dot{\boldsymbol{x}}_0). \tag{6}$$

As plant dynamics $\boldsymbol{f}(\boldsymbol{x})$ does not appear in the equation, the control law does not depend on it. Dependency of control law on model reduces to control effectiveness matrix with an expense of obtaining $\dot{\boldsymbol{x}}_0$. Sensor-Based INDI obtains this value based on sensor measurements. These measurements are not perfect and contains time lag, bias and noise in the real life applications. It may also not be possible to directly measure state derivatives $\dot{\boldsymbol{x}}$.

There has been several assumptions such as neglecting higher order terms and assuming negligible state change. The validity of the assumptions are studied in [9, 10]. The results show that sampling time is one of the factors that might reduce the performance. Using a low-sampling-rate flight computer causes the change in states to be non-negligible. There are different studies which derive INDI control without using time scale separation and show the stability of the method with less assumptions [16, 17].

### B. Model-Based INDI

Model-Based INDI is formulated based on the same procedure of Sensor-Based INDI. The Taylor series expansion given in Eq. (3) replaces the true dynamics, $\boldsymbol{f}(\boldsymbol{x}_0) + \boldsymbol{g}(\boldsymbol{x}_0)\boldsymbol{u}_0$, with $\dot{\boldsymbol{x}}_0$. For the derivation of Model-Based INDI, modeled dynamics, $\boldsymbol{f}_{\text{mod}}(\boldsymbol{x}_0) + \boldsymbol{g}_{\text{mod}}(\boldsymbol{x}_0)\boldsymbol{u}_0$, replace the true dynamics, and the same assumptions are applied. This yields control law as

$$\boldsymbol{u} = \boldsymbol{u}_0 + \boldsymbol{g}^{-1}(\boldsymbol{x}_0)\left[\boldsymbol{\nu} - \boldsymbol{f}_{\text{mod}}(\boldsymbol{x}_0) - \boldsymbol{g}_{\text{mod}}(\boldsymbol{x}_0)\boldsymbol{u}_0\right]. \tag{7}$$

The ideal scenario is $\boldsymbol{f}_{\text{mod}}(\boldsymbol{x}_0) = \boldsymbol{f}(\boldsymbol{x}_0)$ and $\boldsymbol{g}_{\text{mod}}(\boldsymbol{x}_0) = \boldsymbol{g}(\boldsymbol{x}_0)$. For this condition, further simplification of the equation removes the control increment, $\boldsymbol{u}_0$:

$$\boldsymbol{u} = \boldsymbol{u}_0 + \boldsymbol{g}^{-1}(\boldsymbol{x}_0)\boldsymbol{\nu} - \boldsymbol{g}^{-1}(\boldsymbol{x}_0)\boldsymbol{f}(\boldsymbol{x}_0) - \boldsymbol{u}_0 \tag{8}$$

$$\boldsymbol{u} = \boldsymbol{g}^{-1}(\boldsymbol{x}_0)\boldsymbol{\nu} - \boldsymbol{g}^{-1}(\boldsymbol{x}_0)\boldsymbol{f}(\boldsymbol{x}_0) \tag{9}$$

$$\boldsymbol{u} = \boldsymbol{g}^{-1}(\boldsymbol{x}_0)\big(\boldsymbol{\nu} - \boldsymbol{f}(\boldsymbol{x}_0)\big) \tag{10}$$

The simplified version of the Model-Based INDI is equivalent to NDI control law. The method is less dependent on sensor measurement but it requires the full system model.

## III. Hybrid Incremental Nonlinear Dynamic Inversion

Considering the angular rate control application of INDI, angular rates are regarded to be states and angular accelerations are state derivatives. Control law requires angular accelerations that are not readily available and angular accelerometers are not very common [15]. Aircraft are generally equipped with gyroscopes that measure angular rates. To obtain angular accelerations, angular rates are differentiated. Differentiation of a noisy signal magnifies the amplitude of the noise, which causes the need for additional noise filtering. Sensor dynamics itself and noise filtering introduce time lags to the measurements. This is seen as one of the main challenges of Sensor-Based INDI [14]. The proposed Hybrid INDI approach aims to solve this problem by fusing sensor measurement and system model with a complementary filter.

Hybrid INDI is designed to include characteristics of Model-Based and Sensor-Based INDI. The difference between approaches is the way to obtain the state derivative $\dot{\boldsymbol{x}}_0$. In Hybrid INDI, the signals are merged to complement each other in the frequency domain. Filter residual is referred to as state derivative estimation and denoted by $\hat{\dot{\boldsymbol{x}}}_0$. The estimation by the complementary filter is given by

$$\hat{\dot{\boldsymbol{x}}} = f(\boldsymbol{x}_s, \dot{\boldsymbol{x}}_m) \tag{11}$$

where $f$ is complementary function, $\boldsymbol{x}_s$ is the measurement of the state and $\boldsymbol{x}_m$ is the output of the on-board model. Replacing the state derivative in Eq. (6) with the state derivative estimate, yields the Hybrid INDI control law as

$$\boldsymbol{u} = \boldsymbol{u}_0 + \boldsymbol{g}^{-1}(\boldsymbol{x}_0)(\boldsymbol{\nu} - \hat{\dot{\boldsymbol{x}}}). \tag{12}$$

Hybrid INDI uses combination of gyroscope measurement $\boldsymbol{x}_s$ and model output $\boldsymbol{x}_m$. Gyroscope measurement is different from $\boldsymbol{x}_0$ because of measurement dynamics and noise filtering, and model output is different from $\boldsymbol{x}_0$ because the model is not equivalent to the real system and external disturbances are not reflected on $\boldsymbol{x}_m$.

### A. Complementary Filter for Angular Acceleration Estimation

Traditional complementary filters combine multiple signals to alleviate noise distortions. Signal with low-frequency noise characteristic is high pass filtered and added to low pass filtered signal with high-frequency noise characteristics. Setting the cut-off frequency of filters equal to each other complements the signals and an all-pass estimate is obtained. Complementary filters are well suited for measurements that are related by first-order dynamics [18]. Such complementary filters are commonly used in the aerospace field for attitude estimation by fusing gyroscope and linear accelerometers [19, 20]. A block diagram of a classical complementary filter is given at Fig. 1 where $y_1$ is the measurement of the state $x$ and $y_2$ is the measurement of the state derivative. The filter includes a controller $C(s)$, that is designed for estimation error dynamics and generally exploits the classical linear control method.

A similar complementary filter is proposed by Jiali and Jihong for the estimation of angular acceleration [21]. It utilizes angular rate measurements by gyroscopes and angular acceleration calculations by a mathematical model. The block diagram of the complementary filter is given in Fig. 2. Notice that the integral block is moved to the feedback signal since the estimation is for the state derivative instead of the state. The filter is designed as PI compensator where $e$ denotes the error between gyroscope measurement and estimation, and $i$ is the innovation signal.

The dynamics of the estimation is given in frequency domain as

$$\hat{\dot{\boldsymbol{x}}} = [\boldsymbol{x}_s - \hat{\dot{\boldsymbol{x}}}\frac{1}{s}][K_p + \frac{K_I}{s}] + \dot{\boldsymbol{x}}_m \tag{13}$$

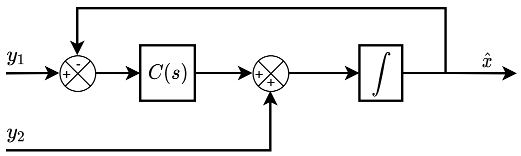


**Fig. 1 Block diagram of a classical complementary filter for attitude estimation [18]**

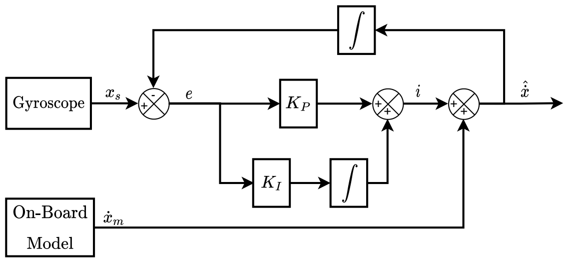


**Fig. 2 Block diagram of complementary filter for angular acceleration estimation**

defining the innovation and error dynamics as

$$I(s) = E(s)[K_p + \frac{K_I}{s}], \tag{14}$$

$$E(s) = \boldsymbol{x}_s - \frac{1}{s}\hat{\dot{\boldsymbol{x}}}. \tag{15}$$

The estimation is the sum of the model output and measurement innovation:

$$\hat{\dot{\boldsymbol{x}}} = I(s) + \dot{\boldsymbol{x}}_m. \tag{16}$$

Eq. 13 can be rearranged as well as

$$\hat{\dot{\boldsymbol{x}}} = S(s)\boldsymbol{x}_s + T(s)\dot{\boldsymbol{x}}_m \tag{17}$$

where

$$S(s) = \frac{K_p s + K_I}{s^2 + K_p s + K_I}s; \quad T(s) = \frac{s^2}{s^2 + K_p s + K_I} \tag{18}$$

$S(s)$ and $T(s)$ complement each other such that $\frac{1}{s}S(s) + T(s) = 1$. By the complementary filter, the sensor measurement is low pass filtered and the model output is high pass filtered. The filter contains low-frequency accuracy of the sensor measurement which includes external disturbances and model mismatches. The filter also contains the high-frequency prediction of the model. The system model responds fast to given inputs with a very low magnitude of noise which makes its high-frequency prediction valuable. The model mismatches act as slowly changing biases and due to their low-frequency characteristics, they are removed as well. The filter indirectly differentiates measurements and yet removes the high-frequency noise component. Applying the final value theorem shows that the error of estimation approaches to the error of the gyroscope [22]. In this way, the Hybrid approach can preserve Sensor-Based INDI's robustness against uncertainties. Equation 16 shows that without the innovation from the sensor measurement the estimation is only based on the model output and the control method becomes Model-Based INDI.

Crossover frequency and damping coefficient of the filter are set by linear controller gains, $K_I = \omega_n^2$ and $K_p = 2\zeta\omega_n$. The values are selected based on the characteristics of the signals. A lower $\omega_n$ filters more of the sensor noise, but the response to external disturbances and model mismatches become slower. Lowering $\zeta$ also removes more noise, but the response is not well-damped and causes oscillations. The integral gain, $K_I$, in classical complementary filters are included for to compensate gyroscope bias [18]. A constant bias in gyroscope does not affect angular acceleration in INDI applications because of differentiation [23]. The gains set the estimation characteristics, and they also affect the robustness against measurement delays.

### B. Synchronization

Sensor-Based INDI control law, given in Eq. 6, shows that the control input depends on the most recent state derivative, $\dot{\boldsymbol{x}}_0$. Sensors measure this value, and the signal is filtered to alleviate the noise. These dynamics cause $\dot{\boldsymbol{x}}_0$ not to be available for the use of controller. The available state derivative value is denoted as $\dot{\boldsymbol{x}}_f$ because it is the output of the noise filter. Using this value causes degradation in performance and yields oscillations. Studies show that the oscillatory motion of the INDI controlled system can be prevented by changing the modeled control effectiveness matrix by a factor [23, 24]. Increasing control effectiveness reduces control input since the control law reverses $\boldsymbol{g}$. It eventually makes the system less aggressive and more careful. A more common and theoretically proven method is the synchronization of the input signal with the expected measurement delay [14].

Assuming accurate knowledge actuator deflection angle means that the most recent value $\boldsymbol{u}_0$ is available and previous values are also achievable. In order to match the control input to the measurement, the input is filtered by the sensor and noise filter dynamics. In this way $\boldsymbol{u}_f$ is obtained and Sensor-Based INDI is rewritten as

$$\boldsymbol{u} = \boldsymbol{u}_f + \boldsymbol{g}^{-1}(\boldsymbol{x}_f)(\boldsymbol{\nu} - \dot{\boldsymbol{x}}_f). \tag{19}$$

Ensuring synchronous signals is regarded as the key for practical implementations of INDI [11]. As the state derivative matches with control input in time, dynamics that cause performance deterioration are eliminated [14]. These dynamics reappear when there is an unexpected additional lag in the signals. As the time mismatch between the signals increases, the tracking error also increases [25].

The synchronization of Hybrid INDI follows a similar procedure as in Sensor-Based INDI. In Sensor-Based INDI applications, the noise filter dynamics filter the control input. Hybrid INDI removes measurement noise by a complementary filter. The filter is utilized to fuse more than one signal therefore, direct application of it to the control input yields the same signal since the control input itself is the only source of the input. Instead, the low pass component of the filter is applied to the sensor measurement because the filter output approaches the measurement. A slightly modified version of $S(s)$ is given as

$$S'(s) = \frac{K_I}{s^2 + K_p s + K_I} \tag{20}$$

is used for synchronization. Note that, $S(s)$ is integrated because there is no need to differentiate the control input. Moreover, $K_p s$ in the numerator is removed because the term limits the phase shift that needs to be achieved in the control input. In addition, the measurement values are used in low frequencies and this term is not effective in the low frequency.

### C. Robustness Analysis of Hybrid INDI

In this section robustness and performance of Sensor-Based INDI and Hybrid INDI are compared with the focus on measurement delays. The analysis shows that Hybrid INDI is inherently more robust against measurement delays. Linearization by INDI and NDI aims to form an integrator dynamics between desired state derivative $\nu$ and actual state. A linear kinematic equation;

$$\dot{x} = u \tag{21}$$

is in the form of general nonlinear equation as in Eq. 1 where $f(x) = 0$ and $g(x) = 1$. This equation does not need linearization by INDI and helps to focus on time mismatches analysis instead of success of linearization. To form a closed loop system a sensor dynamics is added as

$$L'(s) = \frac{1}{t_1 s + 1} e^{-s\tau} \tag{22}$$

where $t_1$ is time constant and $\tau$ is unknown time delay. The actuator dynamics is given by

$$A(s) = \frac{1}{t_2 s + 1} \tag{23}$$

where $t_2$ is time constant of the actuator, selected to be 0.05. The noise filter $\frac{1}{s}S(s)$ as in Eq. 18 is included into the system. Gains for the noise and complementary filter are set to the same values for a fair comparison. For a real system, optimal performance is obtained with different values as shown in Sec. V. The synchronization filter comprises of sensor and noise filter dynamics. $L(s) = \frac{1}{t_1 s+1}$ is used in the synchronization because the time delay is assumed to be unknown. Synchronization filter is given by

$$H_{\text{sync}}(s) = L(s)S'(s) \tag{24}$$

where $S'(s)$ is given in Eq. 20. The block diagrams for Sensor-Based INDI and Hybrid INDI are given in Fig. 3.

In the nominal case, there is no unexpected time delay, i.e., $\tau = 0$. Figure 4 shows that Sensor-Based INDI outperforms Hybrid INDI in terms of step responses. Initial responses of both control systems are the same, then sensor innovation of the filter interferes, and the response slows down. The performance of Sensor-Based INDI is determined based on actuator dynamics since it is the only dynamics that is not canceled by the synchronization. This pole is

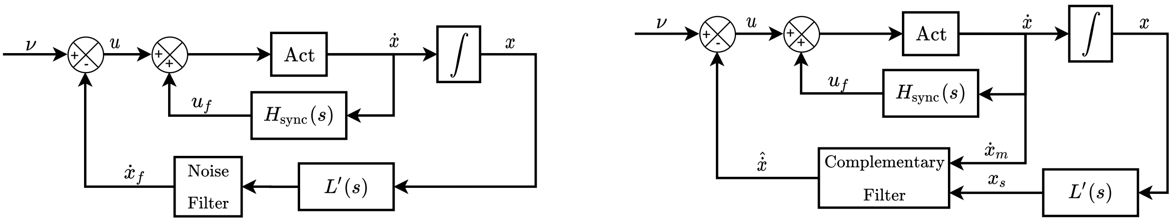


**(a) Sensor-Based INDI** **(b) Hybrid INDI**

**Fig. 3 Block Diagrams for Time Mismatch Robustness Analysis**

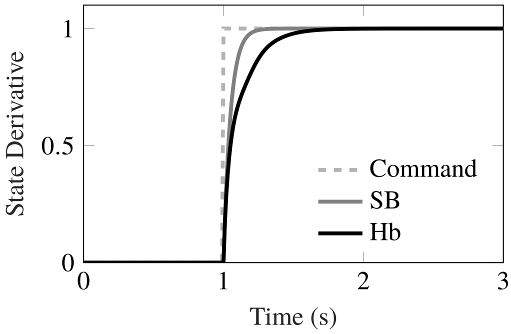


**Fig. 4 Nominal performances of Sensor-Based INDI (SB) and Hybrid INDI (Hb) are plotted. Measurements are not subject to additional delay.**

highlighted in Fig. 6a. For Hybrid INDI, the dynamics that belong to the complementary filter remain as well, which corresponds to highlighted complex poles in Fig. 6b. Thereby, the performance degradation in the nominal performance of Hybrid INDI is expected.

The damping coefficient, $\zeta$, of the filter should be designed based on the desired nominal performance. This value determines the smoothness of transition from Model-Based INDI to Sensor-Based INDI. Increasing damping coefficients slows the step response. Figure 5 shows the effect of damping coefficients on nominal performance. Migrations of significant poles are shown in Fig. 5a. The complex pair shifts from damping value of 0.18 to 0.55 as $\zeta$ increases from 0 to 1. A low $\zeta$ causes oscillations and a high value yields a long settling time. Three different step responses are shown in Fig. 5b. According to this analysis, a damping coefficient around 0.5 yields the best performance. The pole migration shows that the robustness against measurement delay is affected by $\zeta$. A lower damping coefficient causes a faster transition to the unstable region. Hence, this value is set to 0.7.

To show the robustness of Hybrid INDI against measurement delays, a pole migration analysis is performed. The time delay $\tau$ is increased up to 0.20 s by 0.02 s increments. The locations of significant poles are shown in Fig. 6a for

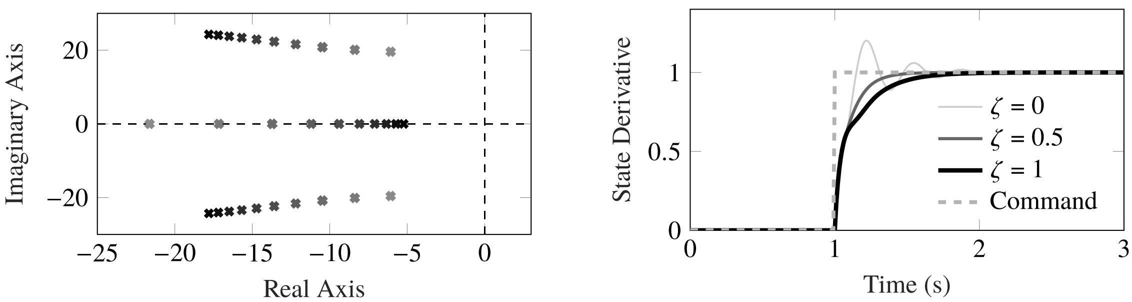


**(a) Complex poles moves left of the plane as damping increases** **(b) The effect of damping coefficient on step response**

**Fig. 5 Effect of damping coefficient of complementary filter on the closed-loop dynamics of Hybrid INDI**

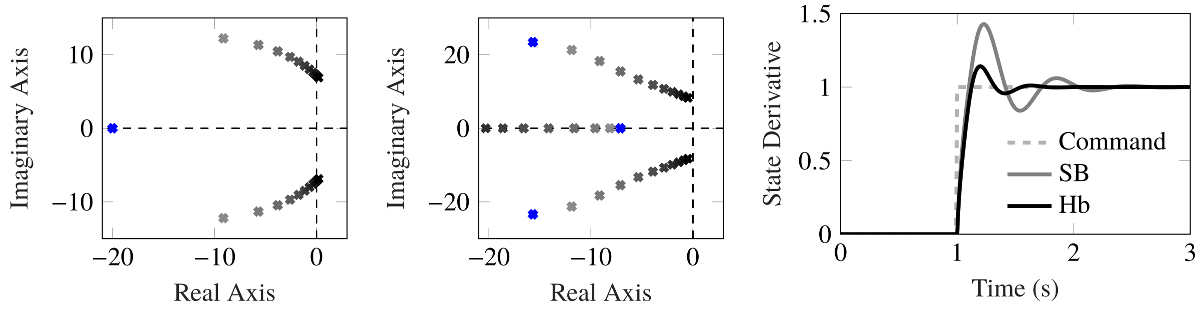


**(a) Sensor-Based INDI** **(b) Hybrid INDI** **(c) Step response**

**Fig. 6 Pole locations in complex plane for various measurement delay (a) Sensor-Based INDI, (b) Hybrid INDI. (c) shows time domain simulation results when measurement delay is 0.07s**

Sensor-Based INDI. It is shown that after 0.18 s of delay, the system becomes unstable. As shown in Fig. 6b, Hybrid INDI poles remain in the stable region. These results are verified by a time-domain simulation. Measurement delay is selected as $\tau = 0.07$ and the step responses of the systems are plotted in Fig. 6c. The results indicate that underestimation of measurement lag causes significant performance degradation for Sensor-Based INDI. For both systems, performance degrades but Hybrid INDI outperforms Sensor-Based INDI by achieving less overshoot and faster settling time.

Sensor-Based INDI does not get affected by overestimation of the measurement delay as much as underestimation. It is shown that INDI is more robust for actuator delays than the measurement delays [25]. A delayed application of actuator commands makes the system to be more careful about the actual state of the system. The reaction becomes safer and eliminates oscillations. This is equivalent to expecting a longer time delay or overestimating the measurement delays. By a modification in the synchronization filter, Sensor-Based INDI can be made robust for the measurement delays. The new synchronization filter is given as

$$H'_{\text{sync}}(s) = L(s)S'(s)e^{-s\tau_e} \tag{25}$$

where $\tau_e$ is the overestimation of the known time lag to deal with unexpected measurement delays. The modification helps the system to have a good performance when the specific unexpected delay is encountered. However, the nominal performance becomes undesirable. This observation is shown in Fig. 7 by setting $\tau_e = 0.07$ and keeping $\tau = 0$. The step responses indicate that the cost of designing Sensor-Based INDI as robust with this method is the degradation of the nominal performance. The Hybrid INDI method is robust against time mismatches inherently. Even though it loses nominal performances, Sensor-Based INDI loses more when it is modified to be robust against time mismatches.

### D. Hybrid INDI as Fault Tolerant System

This section introduces a variant of Hybrid INDI with a slight modification. Using Hybrid INDI together with a fault detection and isolation (FDI) system for sensor faults proposes an easy method to switch between controllers. Consider the state derivative estimation given as Eq. 16. The estimation is based on model output and innovation from the sensor. With a simple logic parameter, the innovation can be canceled if the FDI system detects a faulty sensor. To simulate a faulty sensor scenario, a fault in pitch rate measurement is used as specified in [26]. An oscillatory fault is introduced at $t = 1$ s and assuming the FDI algorithm takes two seconds to detect the fault, the innovation is from the sensor is canceled at $t = 3$ s. This transforms the control structure to Model-Based INDI without any additional change. The simulation result is shown in Fig. 8. It is shown that as soon as the fault is detected, the system starts to converge its steady-state value. In this simulation, the model is assumed to be accurate. Aircraft generally contain multiple IMU to prevent the effects of such faults. Small size aerial vehicles contain limited number of sensors and they can benefit from this application.

## IV. Hybrid INDI Flight Control Design for F-16 Aircraft

The objective of this study is to design an attitude controller for the F-16 aircraft model to robustly track the given pitch angle and roll angle commands while regulating the yaw angle. A cascaded control structure is presented based

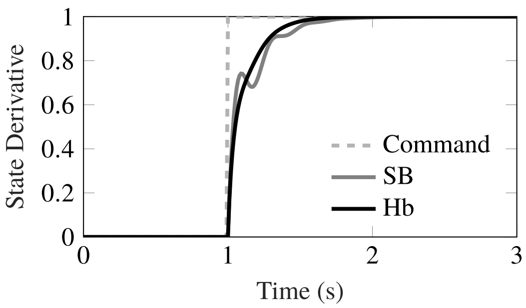


**Fig. 7 Nominal performance comparison, synchronization filter of Sensor-Based INDI is modified to be robust against time mismatches**

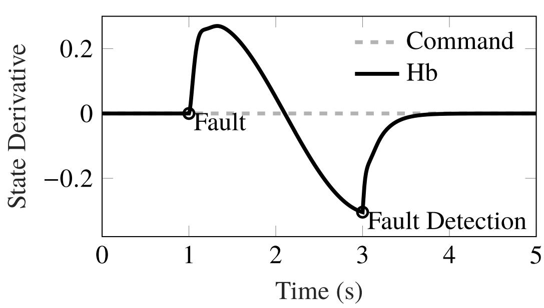


**Fig. 8 Fault is detected by FDI algorithm and the control system switches to Model-Based INDI**

on the time scale separation between angular rates and angular accelerations. The inner loop is designed for tracking desired angular rates, and the outer loop is designed to obtain the desired angular rates to achieve commanded attitude angles.

### A. Aircraft Model

The F-16 aircraft model by Russell [27] is used to test proposed control method. The model is valid within a constrained flight envelope for angle of attack $-10^\circ \leq \alpha \leq 45^\circ$, side slip angle $-30^\circ \leq \beta \leq 30^\circ$, velocity $300\,\text{ft/s} \leq V \leq 900\,\text{ft/s}$ and altitude $5000\,\text{ft} \leq h \leq 40000\,\text{ft}$. The model has three conventional control surfaces: elevator, rudder and aileron to generate pitch, yaw and roll moments. An engine mounted in the rear fuselage provides thrust. Actuators of the aircraft controls are modeled as first-order transfer functions. Characteristics of actuators are presented in Table 1. The actuator dynamics are assumed to be accurate. Additional sensors to measure actuator deflections are not used.

**Table 1 Aircraft Actuator Characteristics**

| Actuator | Upper Level Limit | Lower Level Limit | Rate Limits | Time Constant |
|---|---|---|---|---|
| Throttle ($\delta_{\text{th}}$) | 19000 lbf | 1000 lbf | ±10000 lbf/s | 1 s |
| Elevator ($\delta_{\text{e}}$) | 25° | -25° | $\pm 60^\circ/s$ | 0.0495 s |
| Rudder ($\delta_{\text{r}}$) | 30° | -30° | $\pm 120^\circ/s$ | 0.0495 s |
| Aileron ($\delta_{\text{a}}$) | 21.5° | -21.5° | $\pm 80^\circ/s$ | 0.0495 s |

The model is augmented with sensor models that are used in a high incidence aircraft model [28]. Sensor dynamics to measure body axes attitudes $(\phi, \theta, \psi)$ is

$$L_\theta(s) = \frac{1}{0.00104s^2 + 0.0323s + 1}. \tag{26}$$

Body axes angular rates $(p, q, r)$ are measured by sensors with dynamics of

$$L_\omega(s) = \frac{0.0001903s^2 + 0.005346s + 1}{0.0004942s^2 + 0.03082s + 1}, \tag{27}$$

Air data signals $(V_T, \alpha, \beta, h)$ are measured by

$$L_a(s) = \frac{1}{0.02s^2 + 1}. \tag{28}$$

All the sensors have additional dynamics to consider flight computer's computational delay and analog to digital conversion. In addition, air data and attitude sensors are filtered for anti-aliasing. Averaging dynamics are added to angular rate measurements. The details of these additional dynamics are found in [28]. Uncorrelated zero-mean white noise signals are added to the outputs of sensor measurements. The standard deviations of white noise are presented in Table 2 which are based on a previous study with the same aircraft model [29].

**Table 2 Standard Deviations of Measurement Noise**

| $V$ | $\alpha, \beta, \phi, \theta, \psi$ | $p$,$q$,$r$ | $h$ |
|---|---|---|---|
| $1\ \mathrm{m\,s^{-1}}$ | $0.1°$ | $0.01°\ \mathrm{s^{-1}}$ | 5 m |

The aircraft is modeled symmetric in x-z plane *i.e.* the moment of inertia $J_{xy} = J_{yz} = 0$. The inertia tensor is

$$J = \begin{bmatrix} J_{xx} & 0 & -J_{xz} \\ 0 & J_{yy} & 0 \\ -J_{xz} & 0 & J_{zz} \end{bmatrix}. \tag{29}$$

Total moment vector around body axes $\boldsymbol{M}$ is given by

$$\boldsymbol{M} = J\dot{\boldsymbol{\omega}} + \boldsymbol{\omega} \times J\boldsymbol{\omega}. \tag{30}$$

where angular rates $[p\ q\ r]^T$ are denoted by $\boldsymbol{\omega}$. The moments due to aerodynamics are denoted by $L$, $M$ and $N$, they represent rolling, pitching and yawing moments respectively, and given as

$$\boldsymbol{M} = \begin{bmatrix} L \\ M \\ N \end{bmatrix} = \frac{1}{2}\rho V^2 S \begin{bmatrix} b\, C_l \\ \bar{c}\, C_m \\ b\, C_n \end{bmatrix} \tag{31}$$

where $b$ is wing span, $\hat{c}$ is mean aerodynamic cord, $\rho$ is air density, $V$ is airspeed, $S$ is wing surface area, and $C_l$, $C_m$, $C_n$ are non-dimensional aerodynamic coefficients. The coefficients are gathered into data tables via wind tunnel tests [30]. The model utilizes coefficient tables given in [31] by linear interpolation. An overview of these values are represented as

$$C_l = C_{l_0}(\alpha,\beta) \ + \ C_{l_r}(\alpha)\frac{rb}{2V} \ + \ C_{l_p}(\alpha)\frac{pb}{2V} \ + \ C_{l_{\delta_a}}(\alpha,\beta)\delta_a \ + \ C_{l_{\delta_r}}(\alpha,\beta)\delta_r \tag{32}$$

$$C_m = C_{m_0}(\alpha,\delta_e) \ + \ C_{m_q}(\alpha)\frac{q\bar{c}}{2V} \ + \ C_z(\alpha,\beta,\delta_e,q)(X_{\mathrm{cgR}} - X_{\mathrm{cg}}) \tag{33}$$

$$C_n = C_{n_0}(\alpha,\beta) \ + \ C_{n_r}(\alpha)\frac{rb}{2V} \ + \ C_{n_p}(\alpha)\frac{pb}{2V} \ + \ C_{n_{\delta_a}}(\alpha,\beta)\delta_a \ + \ C_{n_{\delta_r}}(\alpha,\beta)\delta_r \tag{34}$$

where $C_z$ is total z-axis force coefficient and its effect on pitching moment is based on the difference between the reference center of gravity location, which is constant at $X_{\mathrm{cgR}} = 0.35\bar{c}$ and center of gravity location $X_{\mathrm{cg}}$. To bring the equations of motion in general nonlinear form as given in Eq. 1, control surface moments should be distinguished from moments due to airframe. The equations of $C_l$ and $C_n$ are control-affine, which makes the distinguishing straightforward; however, $C_m$ is control-nonaffine. To separate contribution of elevator deflection from $C_{m_0}$, the rate of change of coefficients with respect to $\delta_e$ is calculated. Effect of elevator deflection on $C_z$ is assumed to be negligible. The moments are rewritten as

$$\begin{bmatrix} L \\ M \\ N \end{bmatrix} = \frac{1}{2}\rho V^2 S \begin{bmatrix} b\, C_{l_{\delta_a}} & 0 & b\, C_{l_{\delta_r}} \\ 0 & \bar{c}\, C_m & 0 \\ b\, C_{n_{\delta_a}} & 0 & C_{n_{\delta_r}} \end{bmatrix} \begin{bmatrix} \delta_a \\ \delta_e \\ \delta_r \end{bmatrix} + \frac{1}{2}\rho V^2 S \begin{bmatrix} b\, C_{l_a} \\ \bar{c}\, C_{m_a} \\ b\, C_{n_a} \end{bmatrix} \tag{35}$$

where $C_{l_a}$, $C_{m_a}$, $C_{n_a}$ denote aerodynamic coefficients of the airframe. Equation (30) and Eq. (35) are combined to solve for angular acceleration $\dot{\boldsymbol{\omega}}$. This yields

$$\dot{\boldsymbol{\omega}} = J^{-1} \left\{ \frac{1}{2}\rho V^2 S \begin{bmatrix} b\, C_{l_a} \\ \bar{c}\, C_{m_a} \\ b\, C_{n_a} \end{bmatrix} - \boldsymbol{\omega} \times J\boldsymbol{\omega} \right\} + J^{-1}\frac{1}{2}\rho V^2 S \begin{bmatrix} b\, C_{l_{\delta_a}} & 0 & b\, C_{l_{\delta_r}} \\ 0 & \bar{c}\, C_m & 0 \\ b\, C_{n_{\delta_a}} & 0 & C_{n_{\delta_r}} \end{bmatrix} \begin{bmatrix} \delta_a \\ \delta_e \\ \delta_r \end{bmatrix}. \tag{36}$$

## B. Angular Rate Control

Angular rate controller is the inner loop of the control structure. The equation for angular acceleration given in Eq. (36) is in the form of general nonlinear equation as in Eq. (1) which is useful when the controller is designed. The controls are aileron, elevator and rudder. Engine thrust is kept constant. Control variables, virtual controls, and state derivative estimates are

$$\boldsymbol{u} = \begin{bmatrix} \delta_a \\ \delta_e \\ \delta_r \end{bmatrix}; \quad \boldsymbol{\nu_{\dot{\omega}}} = \begin{bmatrix} \nu_{\dot{p}} \\ \nu_{\dot{q}} \\ \nu_{\dot{r}} \end{bmatrix}; \quad \hat{\dot{\boldsymbol{\omega}}} = \begin{bmatrix} \hat{\dot{p}} \\ \hat{\dot{q}} \\ \hat{\dot{r}} \end{bmatrix}. \tag{37}$$

Control effectiveness matrix is inverted to apply Hybrid INDI approach as given by Eq. (12) which yields the control law as

$$\begin{bmatrix} \delta_a \\ \delta_e \\ \delta_r \end{bmatrix} = \begin{bmatrix} \delta_{a_0} \\ \delta_{e_0} \\ \delta_{r_0} \end{bmatrix} + \frac{J}{\frac{1}{2}\rho V^2 S} \begin{bmatrix} b\, C_{l_{\delta_a}} & 0 & b\, C_{l_{\delta_r}} \\ 0 & \bar{c}\, C_m & 0 \\ b\, C_{n_{\delta_a}} & 0 & C_{n_{\delta_r}} \end{bmatrix}^{-1} \left\{ \begin{bmatrix} \nu_{\dot{p}} \\ \nu_{\dot{q}} \\ \nu_{\dot{r}} \end{bmatrix} - \begin{bmatrix} \hat{\dot{p}} \\ \hat{\dot{q}} \\ \hat{\dot{r}} \end{bmatrix} \right\}. \tag{38}$$

Virtual input $\boldsymbol{\nu_{\dot{\omega}}}$ act as desired angular acceleration. Its dynamics is based on the error between desired angular rates and measured angular rates. The virtual angular acceleration input is given as

$$\boldsymbol{\nu_{\dot{\omega}}} = \boldsymbol{K_{P_\omega}}(\boldsymbol{\omega_d} - \boldsymbol{\omega_s}) + \boldsymbol{K_{D_\omega}}(\boldsymbol{\dot{\omega}_d} - \boldsymbol{\dot{\omega}_s}) + \boldsymbol{\dot{\omega}_d} \tag{39}$$

where $\boldsymbol{\omega_d}$ is the desired angular rates and they are the output of the outer loop, and $\boldsymbol{\omega_s}$ is measured angular rates. Derivative of desired angular rate and measurement is obtained based on derivative filter given as

$$H_{\mathrm{d}}(s) = \frac{s}{30s + 1}. \tag{40}$$

The linear controller consists of a set of proportional and derivative gains, i.e. the PD compensator is designed for the error dynamics, and a feedforward term based on the derivative of the desired angular rates is included. Depending on the required response characteristics, the feedback controller can be adjusted to be PI or PID compensator [25] as well. The feedforward term can be updated with an additional second derivative of the desired values [11, 32].

## C. Attitude Controller

The attitude controller controls roll, pitch, and yaw angles. According to time scale separation, angular rates are assumed to have reached their desired values very fast compared to the dynamics of the inner loop. Attitude control is based on NDI. The kinematic relation between attitude angles and angular rates are given as

$$\begin{bmatrix} \dot{\phi} \\ \dot{\theta} \\ \dot{\psi} \end{bmatrix} = \begin{bmatrix} 1 & \tan\theta\sin\phi & \tan\theta\cos\phi \\ 0 & \cos\phi & -\sin\phi \\ 0 & \sin\phi/\cos\theta & \cos\phi/\cos\theta \end{bmatrix} \begin{bmatrix} p \\ q \\ r \end{bmatrix}. \tag{41}$$

Applying NDI control law yields

$$\begin{bmatrix} p_d \\ q_d \\ r_d \end{bmatrix} = \begin{bmatrix} 1 & \tan\theta\sin\phi & \tan\theta\cos\phi \\ 0 & \cos\phi & -\sin\phi \\ 0 & \sin\phi/\cos\theta & \cos\phi/\cos\theta \end{bmatrix}^{-1} \begin{bmatrix} \nu_{\dot{\phi}} \\ \nu_{\dot{\theta}} \\ \nu_{\dot{\psi}} \end{bmatrix} \tag{42}$$

The virtual input $\boldsymbol{\nu_{\dot{\theta}}}$ is used as desired attitude angle derivatives. It is based on the error dynamics between the attitude angle commands and measured attitude angles. The relation is given as

$$\boldsymbol{\nu_{\dot{\theta}}} = \boldsymbol{K_{P_\theta}}(\boldsymbol{\theta_r} - \boldsymbol{\theta_s}) + \boldsymbol{\dot{\theta}_r} \tag{43}$$

where $\boldsymbol{\theta_r}$ is reference attitude angle commands and $\boldsymbol{\theta_s}$ is the measured attitude angles. To define the desired closed loop dynamics and to avoid unachievable control inputs, these commands are pre-filtered. The filter is designed to track commands as fast as the system dynamics allow. First-order lag filter is given as

$$H_{\mathrm{pf}}(s) = \frac{1}{0.25s + 1} \tag{44}$$

Setting a lower bandwidth decreases the response time of the system and a high bandwidth reaches to actuator limits easier then the system cannot respond any faster.

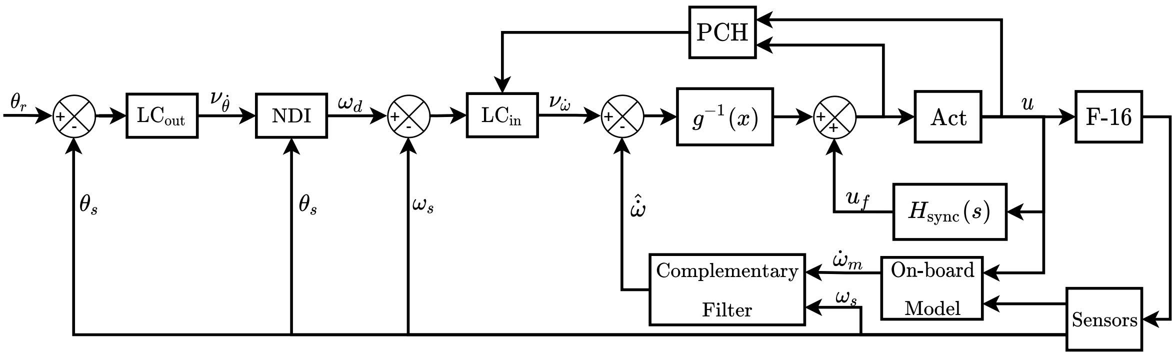


**Fig. 9 Overall block diagram of Hybrid INDI**

### D. Actuator Saturation

The control laws given in Eq. 38 and Eq. 42 do not consider actuator limits. The performance of INDI degrades as the actuators are saturated [9]. Pseudo Control Hedging (PCH) is one of the methods to avoid actuator saturation. The method calculates the amount of control input that cannot be reached due to the actuator limits and feeds the value to the angular rate controller. The angular rates are then limited based on this value. The inner loop requires a reference model to be set, which adds an extra tunable set of parameters that are designed to achieve good performance. The hedging can also be fed to the outer loop. This is not preferred in this study since it requires an additional integration and there is no improvement in performance. PCH is effective in removing actuator saturation but it causes slower responses. To maintain a fast response, a limited saturation is allowed by selecting the PCH gain as 20 for all channels. The details of PCH in INDI applications can be found in [11, 25].

### E. Controller Overview

The overall block diagram of Hybrid INDI is given in Fig. 9. The control gains $\boldsymbol{K_{P_\theta}}$, $\boldsymbol{K_{P_\omega}}$ and $\boldsymbol{K_{D_\omega}}$ are three by three diagonal matrices. In order to tune these parameters, an optimization algorithm is used. The objectives of the optimization are root mean square of tracking error of attitude angles and control effort spend by actuators. The control effort is based on additional deflection of the actuator at each time step, and it is calculated as

$$\delta_E = \sum_{i=1}^{3} \sum_{k=0}^{N} |\delta_i(k) - \delta_i(k-1)|\, dt \tag{45}$$

where $i$ is used for control surfaces and $N$ is the number of sampled data. RMS of tracking error $\epsilon$ is given by

$$\epsilon^2 = \frac{\sum_{l=1}^{3} \sum_{k=0}^{N} \left(\boldsymbol{\theta}_r(k) - \boldsymbol{\theta}(k)\right)^2}{N} \tag{46}$$

where $l$ denotes control channels of the system. The cost function is simply sum of these two parameters:

$$J = \delta_E + \epsilon \tag{47}$$

By this method, a single metric to evaluate the performance of the control system is obtained. Additional terms can be added based on performance requirements. For instance, a metric to detect oscillations is proposed in [33]. The gains are found by minimizing the cost function and they are given in the Table 3.

Selection of noise filtering in Sensor-Based INDI applications is challenging since more noise filtering means more time lag and slower response [5]. Similarly, the bandwidth of the complementary filter determines noise alleviation as well as response time and model mismatch cancellation. A balance between these perspectives should be found. The limits for bandwidth are selected based on the time scale separation. Angular accelerations are faster than the attitude angles. Desired attitude angle characteristics are determined by the prefilter given by Eq. 44. Setting the bandwidth below this value naturally slows down the attitude response. Therefore, the lower limit for the bandwidth is set to 4 rad/s. Similarly, angular accelerations to respond faster than the actuators do not affect the performance. Hence, the upper limit is set to the bandwidth of actuators, which is given as 20.2 rad/s in Table 1. Between these values, the balanced

**Table 3 Linear Control Gains**

| | $K_{P_\theta}$ | $K_{P_\omega}$ | $K_{D_\omega}$ | PCH |
|---|---|---|---|---|
| Roll | 1.17 | 6.68 | 0.3 | 20 |
| Pitch | 1.60 | 4.28 | 0 | 20 |
| Yaw | 1.22 | 3.73 | 1 | 20 |

value is found at 8 rad/s. Two main factors for the selection of this value becomes noise filtering and response time. Ideally, with a lower value, more noise is filtered, but this means that the response time is compromised. The damping coefficient of the filter is set to 0.7 for a nice transition from model-based estimation to sensor-based estimation and sufficient robustness against time mismatches. Hence, the filter gains are determined to be $K_I = 64$ and $K_P = 11.2$.

## V. Simulation Results

This section presents the simulation results of the F-16 aircraft model with the control system described in Sec. IV. Sampling frequency is fixed at 100 Hz for all simulations. The operating point is selected at altitude of 10000 ft and velocity is equal to 500 ft/s, in steady flight. The aircraft is trimmed at this operating point and the resulting values are listed in Table 4.

**Table 4 Aircraft trim values**

| $\delta_{\mathrm{th}}$ | $\delta_{\mathrm{e}}$ | $\delta_{\mathrm{a}}$ | $\delta_{\mathrm{r}}$ | $\alpha$ | $V_T$ | $h$ |
|---|---|---|---|---|---|---|
| 2081 lbf | −2.25° | 0 | 0 | 3.60° | 500 ft/s | 10000 ft |

The estimation value is compared with sensor measurement value by using a second order filter,

$$H_{\mathrm{NF}}(s) = \frac{40^2 s}{s^2 + 56s + 40^2} \tag{48}$$

which differentiates angular rates and filters noise. This filter is used for the Sensor-Based INDI simulations as well, and it is designed based on the best nominal performance. The noise below 40 rad/s is sufficient to be removed; therefore, there is no need to introduce additional time lag.

To show the differences between INDI approaches, nominal performance is investigated. The aircraft is commanded with pitch angle doublet. Pitch accelerations, tracking performance, and elevator deflection are shown in Fig. 10 focusing on different time ranges. Figure 10a shows actual angular acceleration, model output, complementary filter output, and sensor-based acceleration calculation and focuses on the time of initial command. First, notice that the hybrid variant of the acceleration has the highest noise value. This noise is allowed not to slow down the system response. The on-board model matches with the actual aircraft dynamics since no uncertainty is introduced. A difference between the model output and the actual value is caused by a one-time step delay of control inputs to the model to consider actuator modeling calculation. The model also uses the aircraft measurements without any noise filtering. Therefore, there is a slight time lag due to sensor dynamics. In addition, aerodynamic moments due to system states mismatch with the actual value due to noisy measurement. Sensor-based angular acceleration is the shifted version of actual value. They match well except the time lag between them. The hybrid angular acceleration increases with the model output that increases without any time delay. Then, it starts to converge to the sensor-based acceleration until the model output decreases. For higher magnitudes of commands, the estimation is expected to converge to sensor measurement. Using Hybrid INDI makes the system to respond earlier than the measured states. The magnitude of the value is lower than the real value as well. These are the reasons that the oscillations are eliminated in the Hybrid INDI approach.

Figure 10c compares elevator deflections of Hybrid INDI and Sensor-Based INDI. Around $t = 1.2$ s elevator deflection reverses since the angular rate reaches its desired value. Hybrid INDI experiences this change at a lower magnitude. This explains why a slower response is expected from the Hybrid INDI, and less control effort is spent. Figure 10b shows responses of INDI approaches to doublet command in pitch angle. Both of the responses show similar characteristics such that after one oscillation they settle down. The settling time of Hybrid INDI is slightly higher causing its RMS error to increase. The performance criteria were set to be the sum of RMS error and control effort. The cost value of both approaches is almost the same at the nominal conditions.

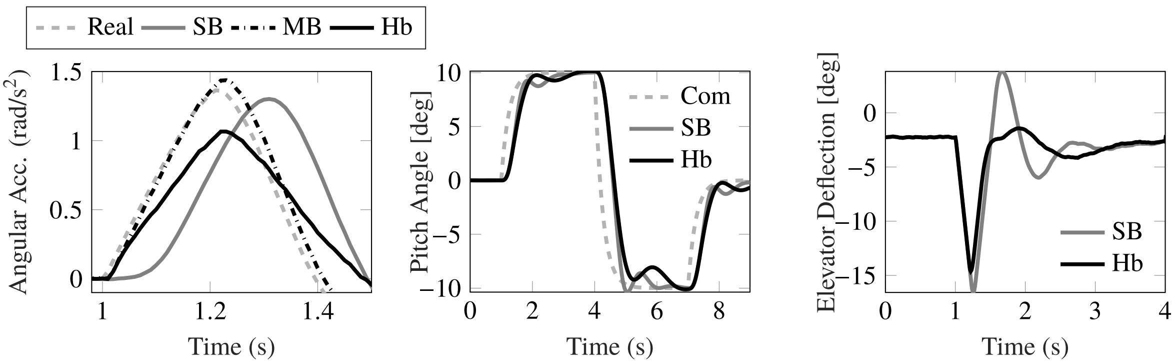


**(a) Pitch accelerations** **(b) Pitch angle tracking performance** **(c) Elevator deflection**

**Fig. 10 Response to pitch angle command in nominal conditions sensor and noise filter dynamics are included**

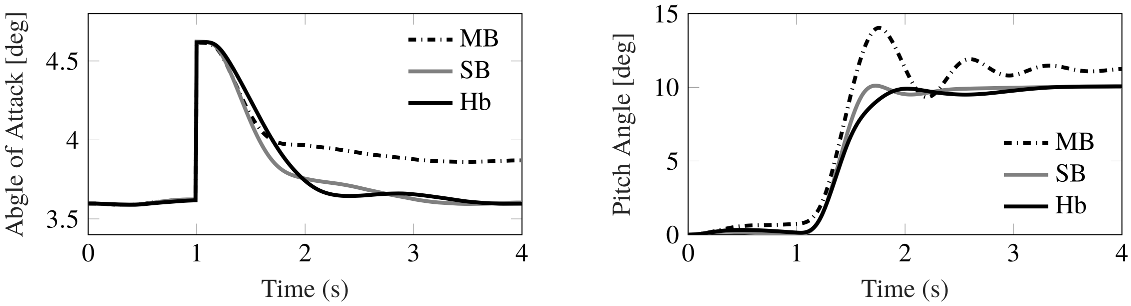


**(a) Step disturbance as wind gust** **(b) Aerodynamic uncertainties 50% increased coefficients**

**Fig. 11 Robustness comparison of INDI approaches**

Two simulations are performed to investigate disturbance rejection and system robustness against aerodynamic uncertainty. The results are shown in Fig. 11. In order to simulate a constant wind, a step input is introduced to the system at 1 s and added to the angle of attack measurement. The results of the angle of attack regulation control problem are shown in Fig. 11a. All approaches initially respond to the disturbance similarly. After a short time, Sensor-Based and Hybrid INDI remove the effect of disturbance by setting the angle of attack to its steady-state value. Although, the rejection characteristics are different the settling time of the methods is the same. Model-Based INDI cannot remove the disturbance and the angle of the attack remain to 0.4° above the trim value since $\boldsymbol{f}_{\text{mod}}$ does not match with real aircraft dynamics and the difference between them acts as bias given to the control law. In terms of robustness against aerodynamic uncertainty, Hybrid INDI is successful as seen in Fig. 11b. A step input is commanded in the pitch channel and the modeled aerodynamic coefficients are increased by 50%. The response of Sensor-Based INDI and Hybrid INDI does not deviate much from their nominal performances even if the performance of Model-Based INDI significantly degrades, a large overshoot and oscillations are observed, and a large tracking error remains.

To test Hybrid INDI robustness against measurement delays, a transport delay of 0.05 s is introduced in angular rate measurement, while maintaining the model mismatches with aerodynamic coefficients that are increased 50%. A doublet input is given in pitch and roll angles as shown in Fig. 12. The results show that Hybrid INDI is robust against measurement delays, and deviation from the nominal performance is very little. Oscillations occur with Sensor-Based INDI. Lateral modes are more vulnerable to time delays. For instance, the roll angle oscillates with a magnitude up to 4° of roll angle although the pitch plane is exited. The response of hybrid INDI does not have oscillations. Simulations with increasing time delays show that SB-INDI becomes unstable when the transport delay is 0.07 s. Hybrid INDI stays in the stable region up to 0.13 s.

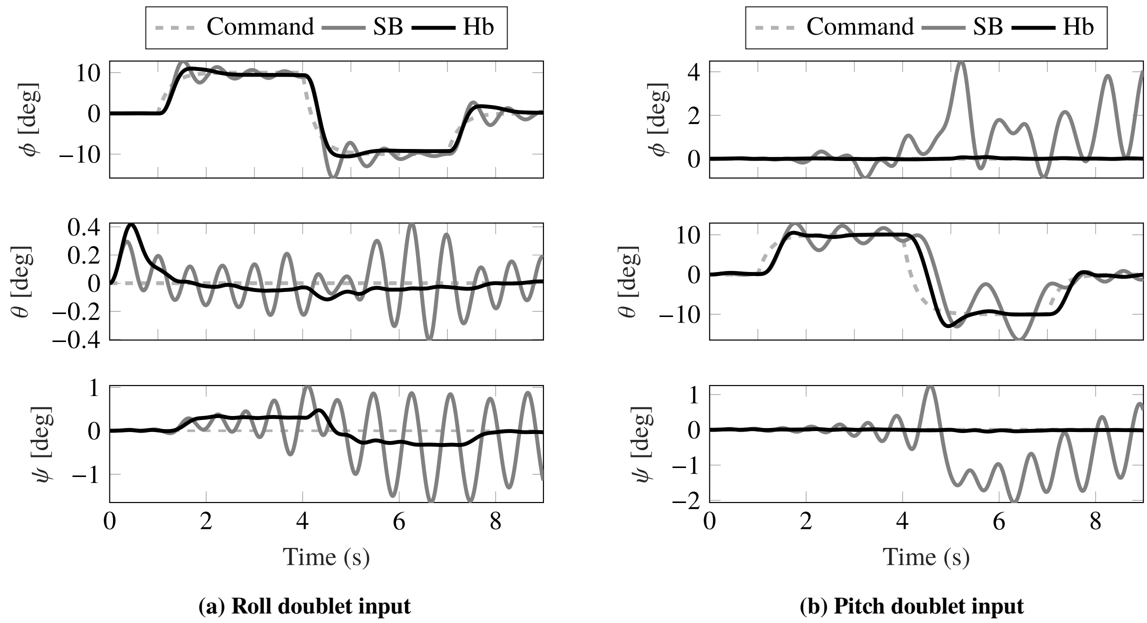


**Fig. 12 Tracking performances in existence of measurement delays and aerodynamic uncertainties**

# VI. Conclusion

This paper has presented a new approach of INDI by modifying the linearization loop via a complementary filter. The filter supplies an angular acceleration estimation based on sensor measurement and on-board model output. By formulating Hybrid INDI it is shown that the approach includes characteristics of both Model-Based INDI and Sensor-Based INDI. The fast response of on-board model is presented as the key feature for the elimination of drawbacks of sensor measurement delays. Hybrid INDI persists to be robust against model mismatches and external disturbances by utilizing low frequency characteristics of measurements.

The effectiveness of the Hybrid INDI has been demonstrated by two types of simulation analysis. The initial analysis considers a simple system and only the linearization loop of INDI is investigated. This analysis compares Sensor-Based INDI and Hybrid INDI in terms of tracking performance in nominal conditions, and in the existence of measurement delays. Consequently, it is shown that Hybrid INDI yields less overshoot and faster settling time when the measurements delays are underestimated. Further details are presented about the synchronization filter, which is given as a modified transfer function of the complementary filtering of sensor measurement. Moreover, change in closed loop characteristics with respect to filter gains and measurement delays are presented.

This analysis is validated by designing an attitude controller for the F-16 aircraft using Hybrid INDI, and showing its robustness against measurement delays and its ability to maintain the sensor-based nature of INDI. Simulation results indicated that Hybrid INDI loses very little tracking performance in nominal conditions. This is compensated by having low control effort. Simulation scenarios with uncertainties in aerodynamic coefficient indicates that the on-board model of Hybrid INDI does not have to be accurate for the control system to be robust against model mismatches. This finding is strengthened by the successful rejection of gust disturbance. Finally, measurement delays are introduced and the aircraft is commanded by doublets of pitch angle and roll angle. As a result, Hybrid INDI insignificantly deviates from the nominal performance whereas the performance of Sensor-Based INDI becomes undesirable due to oscillations in the commanded channel as well as other channels.

Hybrid INDI is not without drawbacks which future studies might overcome. One of the main limitations of Hybrid INDI approach is the noise filtering capability. The bandwidth of the filter design is determined based on the trade-off between the noise filtering and fast response. To achieve the same noise filtering of Sensor-Based INDI, the bandwidth of the complementary filter is required to be set to lower value which slows the response of the system dramatically. The noisy angular acceleration estimation is directly reflected to the actuator. The actuator itself filters the noise as well and the magnitude of the noise is very low such that the control effort is not affected. However, in real life applications, this limitation might lead to actuator failures. A future study can investigate the importance of the excess of noise and focus on mitigating it.

Different hybridization or estimation techniques could be used for Hybrid INDI. One possible modification that is worth investigating is to use angular accelerometers instead of gyroscopes. In this study, an angular acceleration estimation method is used for Hybrid INDI since this method has advantages such as being simple and easily adaptable to system requirements. The use of accelerometers can be implemented with a slight change in the complementary filter. A future study may consider Kalman filtering as one of the possible methods which exploits both measurement and model simultaneously.

A variant of Hybrid INDI is presented as a fault-tolerant system. The approach includes a logical switch that is fed by an FDI algorithm, which can switch the system to become Model-Based INDI by avoiding sensor measurement innovation. This variant is not tested in the F-16 aircraft application because of a lack of FDI algorithm. A future study may implement an FDI algorithm to show the applicability of this feature on an aerospace system.

## References


[1] Enns, D., Bugajski, D., Hendrick, R., and Stein, G., "Dynamic inversion: An evolving methodology for flight control design," *International Journal of Control*, Vol. 59, No. 1, 1994, pp. 71–91. https://doi.org/10.1080/00207179408923070.

[2] McFarland, M. B., and D'Souza, C. N., "Missile flight control with dynamic inversion and structured singular value synthesis," *Guidance, Navigation, and Control Conference, 1994*, 1994, pp. 544–550. https://doi.org/10.2514/6.1994-3604.

[3] Smith, P. R., "A simplified approach to nonlinear dynamic inversion based flight control," *23rd Atmospheric Flight Mechanics Conference*, 1998, pp. 762–770.

[4] Smith, P., and Berry, A., "Flight test experience of a non-linear dynamic inversion control law on the VAAC Harrier," *Atmospheric Flight Mechanics Conference*, 2000, pp. 132–142.

[5] Smeur, E. J., Bronz, M., and de Croon, G. C., "Incremental Control and Guidance of Hybrid Aircraft Applied to a Tailsitter Unmanned Air Vehicle," *Journal of Guidance, Control, and Dynamics*, Vol. 43, No. 2, 2020, pp. 274–287. https://doi.org/10.2514/1.g004520.

[6] Lu, P., van Kampen, E.-J., de Visser, C., and Chu, Q. P., "Aircraft fault-tolerant trajectory control using Incremental Nonlinear Dynamic Inversion," *Control Engineering Practice*, Vol. 57, 2016, pp. 126–141. URL http://dx.doi.org/10.1016/j.conengprac.2016.09.010.

[7] Sun, S., Wang, X., Chu, Q., and de Visser, C., "Incremental Nonlinear Fault-Tolerant Control of a Quadrotor with Complete Loss of Two Opposing Rotors," *arXiv preprint*, 2020. URL http://arxiv.org/abs/2002.07837.

[8] Sun, S., Sijbers, L., Wang, X., and De Visser, C., "High-Speed Flight of Quadrotor Despite Loss of Single Rotor," *IEEE Robotics and Automation Letters*, Vol. 3, No. 4, 2018, pp. 3201–3207. https://doi.org/10.1109/LRA.2018.2851028.

[9] Simplício, P., Pavel, M. D., Van Kampen, E.-J., and Chu, Q. P., "An acceleration measurements-based approach for helicopter nonlinear flight control using incremental nonlinear dynamic inversion," *Control Engineering Practice*, Vol. 21, No. 8, 2013, pp. 1065–1077.

[10] Acquatella, P. B., Falkena, W., Van Kampen, E.-J., and Chu, Q. P., "Robust nonlinear spacecraft attitude control using incremental nonlinear dynamic inversion," *AIAA Guidance, Navigation, and Control Conference*, 2012, p. 4623.

[11] Grondman, F., Looye, G. H., Kuchar, R. O., Chu, Q. P., and van Kampen, E.-J., "Design and flight testing of incremental nonlinear dynamic inversion based control laws for a passenger aircraft," *AIAA Guidance, Navigation, and Control Conference, 2018*, 2018, p. 0385. https://doi.org/10.2514/6.2018-0385.

[12] Cakiroglu, C., van Kampen, E.-J., and Chu, Q. P., "Robust incremental nonlinear dynamic inversion control using angular accelerometer feedback," *AIAA Guidance, Navigation, and Control Conference, 2018*, 2018, p. 1128. https://doi.org/10.2514/6.2018-1128.

[13] Keijzer, T., Looye, G., Chu, Q., and van Kampen, E.-J., "Flight testing of incremental backstepping based control laws with angular accelerometer feedback," *AIAA Scitech 2019 Forum*, 2019, p. 0129. https://doi.org/10.2514/6.2019-0129.

[14] Smeur, E. J., Chu, Q. P., and De Croon, G. C., "Adaptive incremental nonlinear dynamic inversion for attitude control of micro air vehicles," *Journal of Guidance, Control, and Dynamics*, Vol. 39, No. 3, 2016, pp. 450–461. https://doi.org/10.2514/1.G001490.

[15] Sieberling, S., Chu, Q. P., and Mulder, J. A., "Robust flight control using incremental nonlinear dynamic inversion and angular acceleration prediction," *Journal of Guidance, Control, and Dynamics*, Vol. 33, No. 6, 2010, pp. 1732–1742. https://doi.org/10.2514/1.49978.

[16] Wang, X., van Kampen, E.-J., Chu, Q. P., and Lu, P., "Stability Analysis for Incremental Nonlinear Dynamic Inversion Control," *Journal of Guidance, Control, and Dynamics*, Vol. 42, No. 5, 2019, pp. 1116–1129. https://doi.org/10.2514/1.G003791, URL https://arc.aiaa.org/doi/10.2514/1.G003791.

[17] Wang, X., Van Kampen, E.-J., Chu, Q. P., and De Breuker, R., "Flexible aircraft gust load alleviation with incremental nonlinear dynamic inversion," *Journal of Guidance, Control, and Dynamics*, Vol. 42, No. 7, 2019, pp. 1519–1536. https://doi.org/10.2514/1.G003980.

[18] Mahony, R., Hamel, T., and Pflimlin, J.-M., "Nonlinear Complementary Filters on the Special Orthogonal Group," *IEEE Transactions on Automatic Control*, Vol. 53, No. 5, 2008, pp. 1203–1219. https://doi.org/10.1080/00207179.2012.693951.

[19] Euston, M., Coote, P., Mahony, R., Kim, J., and Hamel, T., "A complementary filter for attitude estimation of a fixed-wing UAV," *IEEE/RSJ International Conference on Intelligent Robots and Systems, IROS*, IEEE, 2008, pp. 340–345. https://doi.org/10.1109/IROS.2008.4650766.

[20] Wu, J., Zhou, Z., Chen, J., Fourati, H., and Li, R., "Fast Complementary Filter for Attitude Estimation Using Low-Cost MARG Sensors," *IEEE Sensors Journal*, Vol. 16, No. 18, 2016, pp. 6997–7007. https://doi.org/10.1109/JSEN.2016.2589660.

[21] Jiali, Y., and Jihong, Z., "An angular acceleration estimation method based on the complementary filter theory," *IEEE Instrumentation and Measurement Technology Conference*, Vol. 2016-July, 2016, pp. 1–6.

[22] Yoo, T. S., Hong, S. K., Yoon, H. M., and Park, S., "Gain-scheduled complementary filter design for a MEMS based attitude and heading reference system," *Sensors*, Vol. 11, No. 4, 2011, pp. 3816–3830. https://doi.org/10.3390/s110403816.

[23] Smeur, E. J., de Croon, G. C., and Chu, Q. P., "Cascaded incremental nonlinear dynamic inversion for MAV disturbance rejection," *Control Engineering Practice*, Vol. 73, No. November 2017, 2018, pp. 79–90. https://doi.org/10.1016/j.conengprac.2018.01.003, URL https://doi.org/10.1016/j.conengprac.2018.01.003.

[24] Pavel, M. D., Shanthakumaran, P., Chu, Q., Stroosma, O., Wolfe, M., and Cazemier, H., "Incremental Nonlinear Dynamic Inversion for the Apache AH-64 Helicopter Control," *Journal of the American Helicopter Society*, Vol. 65, No. 2, 2020, pp. 1–16. https://doi.org/10.4050/JAHS.65.022006.

[25] van't Veld, R. C., van Kampen, E.-J., and Chu, Q. P., "Stability and robustness analysis and improvements for incremental nonlinear dynamic inversion control," *AIAA Guidance, Navigation, and Control Conference, 2018*, 2018, p. 1127. https://doi.org/10.2514/6.2018-1127.

[26] Lu, P., Van Eykeren, L., Van Kampen, E., Devisser, C. C., and Chu, Q. P., "Aircraft inertial measurement unit fault identification with application to real flight data," *Journal of Guidance, Control, and Dynamics*, Vol. 38, No. 12, 2015, pp. 2467–2475. https://doi.org/10.2514/1.G001247.

[27] Russell, R. S., "Non-linear F-16 Simulation using Simulink and MATLAB," Tech. rep., University of Minnesota, 2003.

[28] Terlouw, J. C., Scala, S., Muir, E., Moormann, D., Lambrechts, P., Hyde, R., Bennani, S., and Schuring, J., "GARTEUR Robust Flight Control Design Challenge Problem Formulation and Manual: the High Incidence Research Model (HIRM)," Tech. rep., GARTEUR, 1996.

[29] van Gils, P., van Kampen, E.-J., de Visser, C. C., and Chu, Q. P., "Adaptive incremental backstepping flight control for a high-performance aircraft with uncertainties," *AIAA Guidance, Navigation, and Control Conference*, 2016, p. 1380. https://doi.org/10.2514/6.2016-1380.

[30] Nguyen, L. T., Ogburn, M. E., Gilbert, W. P., Kibler, K. S., Brown, P. W., and Deal, P. L., "Simulator study of stall/post-stall characteristics of a fighter airplane with relaxed longitudinal static stability," Tech. rep., NASA, 1979.

[31] Stevens, B., Lewis, F., and Johnson, E., *Aircraft Control and Simulation: Dynamics, Controls Design, and Autonomous Systems*, Wiley, 2015.

[32] Lombaerts, T., Kaneshige, J., Schuet, S., Hardy, G., Aponso, B., and Shish, K., "Nonlinear dynamic inversion based attitude control for a hovering quad tiltrotor evtol vehicle," *AIAA Scitech 2019 Forum*, 2019, pp. 1–26. https://doi.org/10.2514/6.2019-0134.

[33] Mooij, E., "Robust Control of a Conventional Aeroelastic Launch Vehicle," *AIAA Scitech 2020 Forum*, 2020, p. 1103. https://doi.org/10.2514/6.2020-1103.

The following three chapters, Chapter 3-5 have been graded for preliminary thesis report. Therefore, these chapters are not be considered for final grading.

# 3

# NONLINEAR DYNAMIC INVERSION

## 3.1. BACKGROUND INFORMATION

Achieving the necessities of next generation systems requires consideration of full nonlinear model. Linear models of aerospace systems are approximate so that they are limited in performance. However, analysis and design of linear systems are considered to be better developed compared to nonlinear systems [23]. Therefore, divide and conquer approach is used where nonlinear control system design is decomposed into linear subsystems by linearization at several expected operating points. This method is called gain scheduling and it is one of the most popular and successfully applied nonlinear control design approach in aerospace field.

Gain scheduling covers overall flight regime by tuning control gains for the specific operating conditions and nonlinear control is obtained by interpolation of the gains. This allows obtaining satisfactory control performance over flight envelope. Incorporating with linear robust control design techniques is one of the main advantages of gain scheduling. In order to robustify gain scheduling, its application is blended with $H_\infty$ control design, $\mu$ synthesis and scheduling with linear fractional transformations [24, 25].

Gain scheduling uses linearized models of a system so that any kind of linear control method such as PID tuning, LQR or pole placement can be applied. This makes gain scheduling very appealing. There are also some challenges such as selection of meaningful scheduling parameters. Slowly varying parameters, for instance mach number, angle of attack and dynamic pressure, are generally preferred. The parameter does not have to be one of the states but complexity of interpolation and computational power requirement increase as more parameters are used. The design process is time consuming because it is challenging to decide linearization points, there is possibility of loss of stability within the points and there is need for repetition of procedure as the parameters of the model is updated. Some of the remedies of these problems are addressed in [26]. Nevertheless, *ad hoc* nature of the technique is time consuming for the design engineer and need for a more generic approach remained [27].

Nonlinear Dynamic Inversion (NDI) has emerged as a promising substitute of gain scheduling. One of the main motivations is to ensure stability and performance over the entire flight region. This is a challenge for gain scheduling in between operation points. NDI is a subset of Feedback Linearization (FBL) that is specifically applied to obtaining input-output linearization. Theory of feedback linearization is pioneered by Brockett and Krener who aimed to extend results of linear control studies to nonlinear case in the late seventies [28–30]. The theory is treated extensively in nonlinear control system design books [31–33].

The linearization refers to process of making the input-output response of a nonlinear system linear by using state feedback and coordinate transformation rather than Jacobian linearization. Forming a simpler state representation helps to find the solution easier. State transformation makes nonlinear system to appear as linear. Then, the system is controlled by linear control methods. The dynamics of controlled variables are reduced to be simple integrator dynamics. Moreover, the need to linearize the system in several points as in gain scheduling is eliminated and a single linear control gain is sufficient to ensure stability and performance. In general, control design is an iterative process, but NDI can be easily adapted to the changes in the parameters of the system. The performance is satisfactory in large region of state space but not well defined in singular points. In addition, selecting the gain values diagonally in a system with multiple inputs and outputs decouples control axes. This helps significantly for the control of coupled systems. These benefits of the method and its feasibility for aerospace systems are proved by practical applications of NDI in aerospace field for several systems that require high maneuverability [34–37].

There are some limitations to the applications of NDI. The technique works best when the model is accurately known. In many situations model cannot be accurately known and uncertainties need to be considered. Hence, robustness is not guaranteed in existence of model uncertainties. Sensitivity to model inaccuracies and the need for stable internal dynamics will be explained further and the application method of NDI will be clarified.

## 3.2. INPUT - OUTPUT LINEARIZATION

The concept of NDI is applied directly on the systems in companion form. These systems are a subset of feedback linearizable systems. It is also possible to use NDI after finding a linear relationship between the input of the system and the states. Not every system is suitable for this direct application since the system may not be in companion form or there may be a nonlinear relationship with the states and output. This is generally the case in aerospace applications and in this project. A general nonlinear state space representation is given as

$$\underline{\dot{x}} = \underline{f}(\underline{x}) + \underline{g}(\underline{x})u \tag{3.1a}$$

$$y = h(\underline{x}) \tag{3.1b}$$

where $\underline{x}$ is $n$-dimensional state vector, since a single input single output (SISO) system is considered $u$ and $y$ are scalar control input and system output, respectively, $\underline{f}$ and $\underline{g}$ are $n$-dimensional smooth nonlinear vector fields and $h$ is a scalar smooth nonlinear vector field. The term $\underline{g}$ is referred as control effectiveness because it determines the effect of the control input on the states. The main challenge of the control problem is that the output variable $y$ is desired to be controlled whereas the designer can only determine the value of the input $u$. The input does not appear directly the equation of output as seen in Eq. 3.1. Hence, the basic idea of input-output linearization is based on finding a direct relationship between the output and the input of the system. The approach to find this relation is to differentiate the output function until the input is apparent in the equation.

Lie derivative is a mathematical operation that eases application of NDI. Since successive differentiation is required to find the relation of input and output, number of differentiation may cause excessive number of terms. Lie derivative is used to reduce the number of terms and to generate an expression for undefined number of differentiation.

Assume that $h(\underline{x})$ is as defined in Eq. 3.1, a smooth scalar function such that $\mathbb{R}^n \to \mathbb{R}$ and $\underline{f}(\underline{x})$ is a smooth vector field that $\mathbb{R}^n \to \mathbb{R}^n$. The first order directional derivative of $h(\underline{x})$ along the direction of $\underline{f}(\underline{x})$ is called first order Lie derivative of $h(\underline{x})$ in the direction of $\underline{f}(\underline{x})$. The definition is shown as

$$\nabla h(\underline{x})\underline{f}(\underline{x}) = L_f h(\underline{x}) \tag{3.2}$$

where $\nabla$ is gradient operator and therefore the first terms is

$$\nabla h(\underline{x}) = \frac{\partial h(\underline{x})}{\partial \underline{x}}. \tag{3.3}$$

The strength of Lie derivative is to show high order directional derivatives in a compact way such as

$$\begin{aligned}
&L_f^1 h(\underline{x}) = \nabla h(\underline{x})\underline{f}(\underline{x})\\
&L_f^2 h(\underline{x}) = \nabla[L_f^1 h(\underline{x})]\underline{f}(\underline{x}) = L_f^1[L_f^1 h(\underline{x})]\\
&L_f^k h(\underline{x}) = \nabla[L_f^{k-1} h(\underline{x})]\underline{f}(\underline{x}) = L_f^1[L_f^{k-1} h(\underline{x})].
\end{aligned}$$

The first step in input-output linearization is to differentiate the output function to find an explicit relation to input. Every derivation yields a new state. The new states are used to form a linearizing control law. This is generally the inner loop of the control structure. As the dynamics are transformed to be linear, the last step is to design a linear controller. This control constructs the outer loop of the system and it is performed according to system requirements. The output of the outer loop is called virtual control and it acts as an input to the inner loop.

Considering the general system representation in Eq. 3.1, the derivative of the output equation with respect to time is

$$\dot{y} = \frac{dy}{dt} = \frac{\partial h(\underline{x})}{\partial \underline{x}}\frac{d\underline{x}}{dt} = \nabla h(\underline{x})\dot{x} \tag{3.4}$$

replacing $\dot{x}$ with the equation in Eq. 3.1a yields

$$\dot{y} = \nabla h(\underline{x})[\underline{f}(\underline{x}) + \underline{g}(\underline{x})u]. \tag{3.5}$$

Using the definition of Lie derivative, Eq. 3.5 is rewritten as

$$\dot{y} = L_f h(\underline{x}) + L_g h(\underline{x})u. \tag{3.6}$$

Even though, in the first derivation input $u$ appears in the equation, $L_g h(\underline{x}) \neq 0$ should be satisfied for the input-output relation to be exist. It is also possible that some values of $\underline{x}$ satisfies the condition whereas some does not. A global controller is achieved when all the points do. If this is not the case, a controller can be designed with singularities at some points. Assuming the condition is satisfied, the control input transformation is stated as

$$u = \frac{1}{L_g h(\underline{x})}[\nu - L_f h(\underline{x})] \tag{3.7}$$

where the virtual input $\nu$ is defined as $\dot{y} = \nu$. Hence, a direct linear relationship is formed between $y$ and $\nu$ that a linear controller can be designed.

If the condition $L_g h(\underline{x}) \neq 0$ is not satisfied then $\dot{y} = L_f h(\underline{x})$ and a successive derivation is needed to make input $u$ apparent in the equation. The second derivative of output is

$$\begin{aligned}
\ddot{y} &= \frac{\partial[L_f h(\underline{x})]}{\partial \underline{x}} \frac{dx}{dt} \\
&= \nabla\Big[L_f h(\underline{x})\Big]\Big[\underline{f}(\underline{x}) + \underline{g}(\underline{x})u\Big] \\
&= \nabla\Big[L_f h(\underline{x})\Big]\underline{f}(\underline{x}) + \nabla\Big[L_f h(\underline{x})\Big]\underline{g}(\underline{x})u \\
&= L_f^2 h(\underline{x}) + L_g L_f h(\underline{x})u
\end{aligned} \tag{3.8}$$

In this case, condition to have an input-output relation changes to be $L_g L_f h(\underline{x}) \neq 0$. If it is satisfied, the control input is written as

$$u = \frac{1}{L_g L_f h(\underline{x})}[v - L_f^2 h(\underline{x})] \tag{3.9}$$

and the outer loop dynamics with the virtual control happens to be a double integrator

$$\ddot{y} = v \tag{3.10}$$

If $L_g L_f h(\underline{x}) = 0$, input-output relation requires further investigation with additional differentiation. Assume that, this relation is found after $r$ times differentiation such that $r$ is the minimum number where $L_g L_f^{r-1} h(\underline{x}) \neq 0$ is satisfied. This yields

$$y^{(r)} = L_f^r h(\underline{x}) + L_g L_f^{r-1} h(\underline{x})u \tag{3.11}$$

where $y^{(r)}$ is $r^{\text{th}}$ order time differentiation of $y$. The control input is obtained generically as

$$u = \frac{1}{L_g L_f^{r-1} h(\underline{x})}[v - L_f^r h(\underline{x})]. \tag{3.12}$$

The outer linear controller is designed based on the integrator dynamics. The control law of a tracking control problem for a double integrator as in Eq. 3.10 is

$$v = \ddot{y}_d - k_1 e - k_2 \dot{e} \tag{3.13}$$

where $y_d$ is the desired output or commanded output and $e = y - y_d$. The controller gains are $k_1$ and $k_2$ are tuned according to system requirements. The general control structure of NDI control is shown in Fig. 3.1.

## 3.3. INTERNAL DYNAMICS

In the general case as in Eq. 3.11, the relation between the input and the output is found after $r$ times differentiation. The systems, which do not yield the relationship after infinite differentiation, are not feedback linearizable. A feedback linearizable system order of $n$, input-output relation is obtained at most after $n$ times differentiation, hence $r \leq n$ for all the systems. The number of differentiation $r$ defines the number of system dynamics that is controlled through NDI and this is called relative degree of the plant. If $r = n$, then every mode of the system is controlled, these dynamics are called external dynamics. A system that requires less number of differentiation than the order such that, $r < n$, contains $n - r$ modes that are unobservable, these are referred as internal dynamics and they cannot be controlled by NDI controller.

For NDI controlled system to be practical, internal dynamics should be stable. The systems are gen-

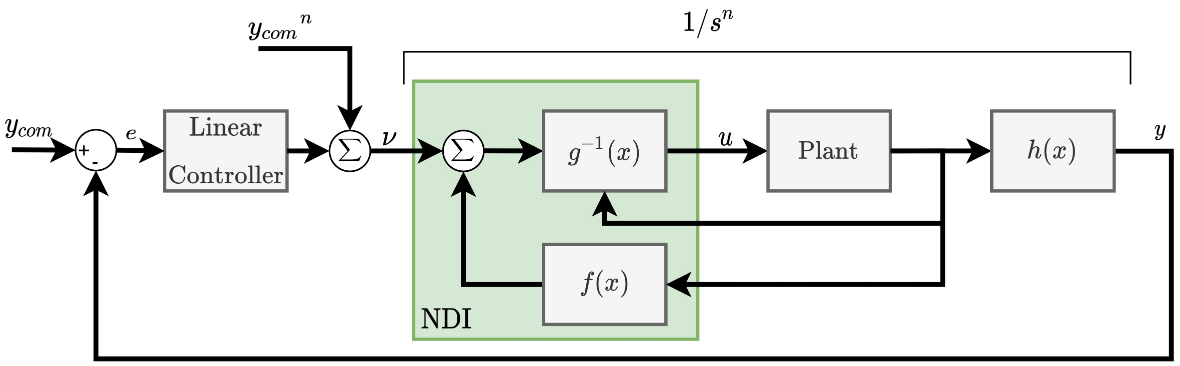


Figure 3.1: A general Block Diagram of NDI Control Structure

erally nonlinear and coupled with the external dynamics, this causes difficulty in evaluation of the stability of internal dynamics. A method is to observe linear approximation of the systems. Relative degree corresponds to excess number of poles over number of zeros for linear system. If the system has zeros on the left half plane of complex coordinate system, i.e. minimum phase system, the internal dynamics are bounded. For non-minimum phase systems the internal dynamics are unstable, therefore NDI is not practical. Even though there are existing solutions, they are only applicable for specific type of systems [38]. When the controlled variables are selected, stable dynamics should be left to be internal dynamics, if possible.

## 3.4. TIME SCALE SEPARATION

In a dynamical system, effectiveness of control input on every variable is not the same. Some variables respond to input faster whereas some others reach the steady state value slower. Dynamic equations of aircraft is naturally faster than the kinematic equations. For example, effect of elevator surface deflection on pitch rate would be faster than its effect on pitch angle. Therefore, it is very common in aerospace field to separate angular rates from attitude angles and control in cascaded loop structure [39]. Stability analysis of nonlinear dynamic inversion control using time scale separation has been studied in [40] and it is found that the system is stable when the selection of gains are appropriate.

As the dynamics are separated they are considered as individual dynamics and treated in this way. In the control structure, a single loop is divided into multi-loop structures that the overall inputs and outputs are in fact the same. The fast dynamics is formed in the inner loop. The output of the outer loop happens to be the input for the inner loop. Since the outer loop is slower, the inner loop assumes that its input is constant. Similarly, outer loop assumes that inner loop has reached steady state since the inner loop is faster. This structure eases mathematical complexity of controller design. In addition, cascaded design is more robust to disturbances in fast dynamics.

## 3.5. ROBUSTNESS ANALYSIS

Mathematical models of systems can never perfectly describe the real system itself. Engineers work with the models that are inaccurate at some points. The controller is designed based on this inaccurate model but it is desirable that the controller works on the real system as well. This ability is called robustness to model inaccuracies and an analysis would give an idea about the performance of the controller even before testing on a real system. The general nonlinear system equation given in Eq. 3.1a is assumed to be the nominal system. The real system is defined as

$$\dot{\underline{x}} = \underline{f}(\underline{x}) + \Delta\underline{f}(\underline{x}) + \left[\underline{g}(\underline{x}) + \Delta\underline{g}(\underline{x})\right]u. \tag{3.14}$$

This equation symbolizes set of functions that is possible to encounter in the real system. $\Delta \underline{f}(\underline{x})$ and $\Delta \underline{g}(\underline{x})$ are set of functions that are bounded and show the deviation of the real system from modeled one. A robust controller would perform sufficiently well within this set of nonlinear equations. Assuming that the input-output relation is found in the first derivation $\dot{\underline{y}} = \nu$ and the output is $\underline{y} = \underline{x}$, the control law that is designed for the nominal system is

$$u = \underline{g}^{-1}(\underline{x})\left[\nu - \underline{f}(\underline{x})\right]. \tag{3.15}$$

Applying the control law on the modeled dynamics yields

$$\dot{\underline{x}} = \underline{f}(\underline{x}) + \underline{g}(\underline{x})\underline{g}^{-1}(\underline{x})\left[\nu - \underline{f}(\underline{x})\right] \tag{3.16}$$

$$\dot{\underline{x}} = \nu \tag{3.17}$$

which is a linear dynamical equation whereas applying the control law on real system with uncertain dynamics in Eq. 3.14 yields

$$\dot{\underline{x}} = \underline{f}(\underline{x}) + \Delta \underline{f}(\underline{x}) + \left[\underline{g}(\underline{x}) + \Delta \underline{g}(\underline{x})\right]\left[\underline{g}^{-1}(\underline{x})\left[\nu - \underline{f}(\underline{x})\right]\right] \tag{3.18}$$

$$\dot{\underline{x}} = \left[I + \Delta \underline{g}(\underline{x})\underline{g}^{-1}(\underline{x})\right]\nu + \Delta \underline{f}(\underline{x}) - \Delta \underline{g}(\underline{x})\underline{g}^{-1}\underline{f}(\underline{x}). \tag{3.19}$$

Introduction of uncertain terms cause nonlinear terms not to be canceled completely. The inner closed loop dynamics is still a nonlinear one that linear controller is not suitable anymore. Model mismatch is an issue that needs to be overcome in the applications of NDI and this led many researches to be conducted to improve robustness.

Earlier works on NDI is generally blended with robust control techniques in frequency domain. In [41], NDI is coupled with structured singular value synthesis and in [42] the outer loop that involves errors due to system uncertainty is shaped using $H_\infty$ technique. Another research uses Linear Quadratic Gaussian outer loop to improve robustness [43]. In this study, a simple example is given to show that inner linearization loop is not linearized under uncertainties. A further development of robustness analysis is given in [44] in which uncertain dynamics are included in linear fractional transformation manner and linearization loop results are given for a general case. The paper considers a reentry vehicle and presents the stability degradation by the uncertainty and investigates the worst case scenarios in order to gain insights when developing controller design for nominal system. A similar approach is applied in [45], structured singular value is used for evaluation of robustness of the closed loop dynamics and paper reveals the sensitivity to model uncertainties and methods to decrease it to improve robustness.

Another approach is taken in [46] in which artificial neural networks are used to correct errors of NDI due to model inaccuracies and disturbances as well for a traditional missile system. A reference model is formed that involves ideal behaviour of missile and autopilot is designed to mimic this behaviour. A similar Adaptive NDI method is used for spacecraft attitude control that fuel sloshing effects of the system dynamics [47].

# 4

# INCREMENTAL NONLINEAR DYNAMIC INVERSION

This chapter consists of four sections. In Section 4.1 derivation of INDI control law is given and robustness analysis of the method is discussed. The next section reviews INDI literature in detail. This section answers the research question 1, presents known strengths and weaknesses of the method. Section 4.3 derives the Model-Based INDI. The section partially answers research question 2 by giving general structure of the control law but does not go into details of questions 2b and 2c. Lastly, Section 4.4 presents overview of possible sensor-model integration giving examples from literature. The section partially answers research question 4.

## 4.1. INDI FORMULATION

A general nonlinear system that is given in Eq. 3.1a is repeated here

$$\underline{\dot{x}} = \underline{f}(\underline{x}) + \underline{g}(\underline{x})\underline{u}. \tag{4.1}$$

This function is approximated by Taylor series expansion at the current value of state $x_0$ and control value $u_0$. The second derivatives and higher terms are assumed to be negligible and they are not included

$$\underline{\dot{x}} \approx \underline{f}(\underline{x}_0) + \underline{g}(\underline{x}_0)\underline{u}_0 + \frac{\partial}{\partial \underline{x}}\left[\underline{f}(\underline{x}) + \underline{g}(\underline{x})\underline{u}\right]_{\underline{u}_0,\underline{x}_0}\left(\underline{x} - \underline{x}_0\right) + \frac{\partial}{\partial u}\left[\underline{f}(\underline{x}) + \underline{g}(\underline{x})\underline{u}\right]_{\underline{u}_0,\underline{x}_0}\left(\underline{u} - \underline{u}_0\right). \tag{4.2}$$

The addition of first two term is simply $\dot{x}_0$. Control surface deflection occurs much faster than the changes in the states. Due to time scale separation between states and inputs the last term in the equation becomes dominant and the states are assumed to be constant hence $\underline{x} = \underline{x}_0$. The increment in control input is defined as $\Delta\underline{u} = \underline{u} - \underline{u}_0$. Therefore, the equation reduces to

$$\underline{\dot{x}} \approx \underline{\dot{x}}_0 + g(\underline{x}_0)\Delta\underline{u} \tag{4.3}$$

The incremental control input law is formed based on this relation. For a system that state variable is also the output, the first derivative yields relation of output and input as $\underline{\dot{x}} = \underline{\dot{y}} = \underline{v}$. Thus the control increment is

$$\Delta\underline{u} = g^{-1}(\underline{x}_0)(\underline{v} - \underline{\dot{x}}_0). \tag{4.4}$$

The new control input is found using previous time step control input as

$$\underline{u} = \underline{u}_0 + g^{-1}(\underline{x}_0)(\underline{v} - \underline{\dot{x}}_0). \tag{4.5}$$

This result shows that either measuring or estimating the current value of the derivative of state would be sufficient for control input calculation. Comparing Eq. 4.5 with Eq. 3.6, it is seen that dependence on accurate model is limited with control effectiveness. Therefore, accuracy of model is trade off with accuracy of measurement or estimation of state variables. Robustness of NDI against modeling uncertainties are investigated in Section 3.5. Similarly, INDI is analysed for robustness. The real system equation with unknown uncertainties

$$\underline{\dot{x}} = \underline{f}(\underline{x}) + \Delta\underline{f}(\underline{x}) + \left[\underline{g}(\underline{x}) + \Delta\underline{g}(\underline{x})\right]\underline{u}. \tag{4.6}$$

Assuming that $\underline{\dot{x}}_0$ is accurately available, the control input in Eq. 4.5 is inserted into the equation which yields

$$\underline{\dot{x}} = \underline{f}(\underline{x}) + \Delta\underline{f}(\underline{x}) + \left[\underline{g}(\underline{x}) + \Delta\underline{g}(\underline{x})\right]\left[\underline{u}_0 + g^{-1}(\underline{x}_0)(\underline{v} - \underline{\dot{x}}_0)\right] \tag{4.7}$$

expanding the equation

$$\underline{\dot{x}} = \underline{f}(\underline{x}) + \Delta\underline{f}(\underline{x}) + \underline{g}(\underline{x})\underline{u}_0 + \underline{v} - \underline{\dot{x}}_0 + \Delta\underline{g}(\underline{x})\underline{u}_0 + \Delta\underline{g}(\underline{x})g^{-1}(\underline{x}_0)\left[(\underline{v} - \underline{\dot{x}}_0)\right]. \tag{4.8}$$

The assumption of negligible state change is applicable for this equation as well. Since $\underline{x} \approx \underline{x}_0$, most of the terms cancel and the remaining is

$$\underline{\dot{x}} = \underline{v} + \Delta\underline{g}(\underline{x})g^{-1}(\underline{x}_0)\left[(\underline{v} - \underline{\dot{x}}_0)\right]. \tag{4.9}$$

The robustness of INDI method is reduced to accuracy of control effectiveness. For the nominal system where $\Delta\underline{g}(\underline{x_0}) = 0$, the relation $\underline{\dot{x}} = \underline{v}$ is obtained. There has been several assumptions in order to achieve this result. The assumptions are

1. Second order and higher order dynamics are excluded from Taylor series expansion

2. The change in states are assumed to be negligible. The validity of this assumption increases as the sampling frequency of the system increases. Less change is expected to be observed in less time.

3. The controls change relatively fast compared to states.

4. It is assumed that the measurement $\underline{x}_0$ is accurately available.

Besides the control effectiveness uncertainty, these assumptions are the subject of robustness tests of INDI method. For the real system it is not possible to obtain $\underline{\dot{x}}_0$ since sensors are used and they have their own dynamics. With these dynamics and other additional ones which are detailed in Section 5.3 the corresponding measurement has time delay. The measurement corresponds to a previous time $\underline{\dot{x}}_d$. The subscript $d$ indicates a known time delay. This time is also subject to uncertainty, hence more accurately $\underline{\dot{x}}_{d+\Delta t}$ is used where $\Delta t$ is unknown time delay. Measurement is used for cancellation of many nonlinear parameters stated in Eq. 4.8. Among these terms cancellations based on $\underline{u}_0$ are dominant compared to state related ones. The best performance is obtained when time of control increment matches with the time of the measurement so that $\underline{u}_{d+\Delta t}$ should be used. The challenge is to estimate or restrict the magnitude of uncertain term $\Delta t$.

## 4.2. REVIEW ON INDI

This section presents literature of Incremental Nonlinear Dynamic Inversion. Theoretical and robustness studies are separated in order to increase the readability. The other papers contribute to these areas as well but the focus is regarded to be different.

### 4.2.1. THEORETICAL DEVELOPMENT OF INDI

Incremental Nonlinear Dynamic Inversion (INDI) is established to overcome robustness issues of NDI. The term *incremental* is merged into NDI in the aerospace community in [12]. The idea of INDI is first presented as *simplified* NDI in [42]. The proposed method is based on manipulations of basic equations of flight mechanics. Smith has found that feeding back angular accelerations decrease the sensitivity to model mismatches and thus performance is enhanced when subjected to uncertainties [42]. The method is tested on a test aircraft VAAC Harier and the importance of pitch rate and pitch acceleration matching and sensor drifting effect are highlighted [48]. The succeeding studies [49, 50] improved the method by using a reconfigurable approach and testing it with several failure scenarios. In [51], angle of attack tracking controller is designed referring to their method as *implicit* NDI. Robust NDI techniques are model-dependent and in Adaptive NDI for example numerical computations are required to derive aerodynamic coefficients. In addition, the methods are complex and the complexity of Adaptive NDI and Robust NDI causes them to be time consuming and difficult to derive, furthermore clearance of the flight controller gets more challenging.

The basic principle of INDI is feeding angular accelerations and control surface deflections back to the system. It is primarily shown that feeding sensor information eliminates sensitivity to model mismatch [12]. In addition, paper concludes insensitivity to center of gravity and inertia as well. However, desensitising closed-loop system to uncertainties comes with the costs of sensitivity to time delays of measurement. A linear predictive filter is proposed that uses angular rates to solve sensor time delay problem. This enables INDI to be applicable to practical systems by only using inertial measurement unit, although this causes actuator signals to be delayed in order to synchronize all feedback signals. However, it is shown that with the current technology using angular accelerometer sensor directly does not yield better results [52].

Initially, INDI is formulated specifically for UAV attitude control and it is proposed as a method that is easy to apply and less dependent on the system model. The assumptions of INDI may affect stability of the system. A study by van 't Veld et al. investigates stability and robustness analysis of closed INDI by deriving discrete time INDI and testing on a system with continuous time plant and discrete time controller [4]. It is shown that as the sampling time gets as higher the region that the system is stable gets smaller. These results are shown in Fig. 4.1. This is basically due to assumption of fast changes in states lose its strength. Paper includes the results of simulation tests for the effect of time delay, control gain, uncertainty and controller frequency on the stability and proposes solutions for problems caused by sensor bias, noise and time delays.

Wang et al. derived INDI control law without time scale separation assumption for a general arbitrary degree system, in order to perform stability analysis of the closed loop system in presence of external disturbances [53]. The paper also derives general closed loop equations in time domain for output tracking and for input to state linearized system that is under disturbance. Robustness analysis includes disturbances, model inaccuracies and singular perturbations.

In [54], the assumptions are not made and a new method formulated which is referred as Extended INDI method. Instead of linearizing the system equations by Taylor expansion, time derivative of virtual control $\nu$ is calculated so that neglecting higher order terms are not necessary anymore. Relation of virtual control and control input is first determined in Laplace domain and then transferred back to time domain and the theory is tested on VTOL drone.

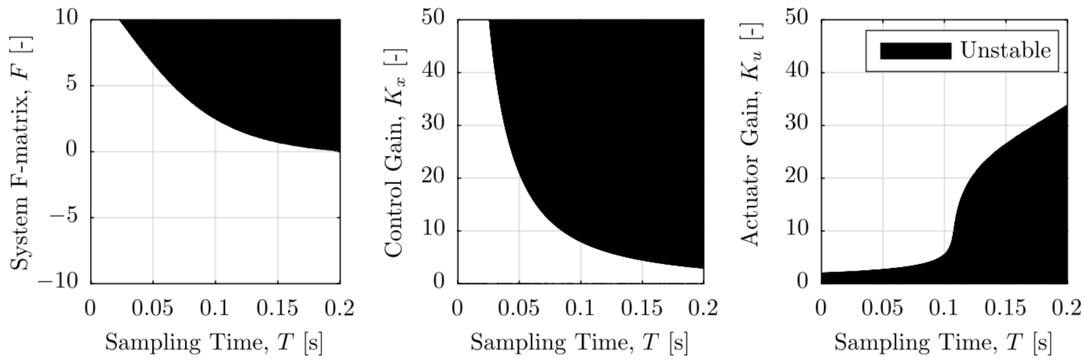


(a) $K_u = 13$, $K_x = 7$ (b) $F = 2$, $K_u = 13$ (c) $F = 2$, $K_x = 7$

Figure 4.1: The stable regions of system with INDI controller reduces as the sampling time increases [4]

### 4.2.2. ROBUSTNESS OF INDI

Simplicio presents a similar robustness analysis given in previous section [55] . It states when sampling frequency of the controller is high enough the uncertainties on the control effectiveness does not affect the closed loop system significantly. Therefore, there is less need to robustify the system, meaning that less effort is required compared to NDI applications. To highlight the significance of INDI against NDI, robustness test include uncertainties in model parameters. Final tests are performed for lower sampling rates and it is found that INDI assumption loses its strength after 60 Hz. The study also states that unsynchronized signals are found to be tolerated until 50 ms. Even though oscillations are introduced to the system, satisfactory tracking performance is obtained. Smeur shows that noise filtering delays angular acceleration signal and unsynchronized signals cause significant issues in the performance [5]. The oscillations due to time delay of the measurement are shown in Fig. 4.2.

A research by Acquatella aims to design completely model free control law by eliminating control effectiveness term as well [56]. INDI and PI controllers are related to each other and gains of PI controller is selected based on this relation. This is done by reformulating the dynamical equation of the system by introducing an additional scheduling parameter that acts as proportional gain which should be chosen according to performance requirements.

INDI trades off the importance of system model to sensor measurement. Sensors include various phenomenon that can prevent them yielding accurate results. Especially, significance of sensor delays are crucial for stability and performance of the systems. Therefore, in [8] multiplicative uncertainty is added to time delay of sensors since there could be additional delays that are known or expected in real systems. Furthermore, robustness is addressed in terms of parametric uncertainties by including the worst case perturbations of inertia values and aerodynamic coefficients on nominal model.

Robustness of INDI flight control against external disturbance showed promising results. As INDI control is tested on a rigid aircraft model and a flexible model, sufficient gust load alleviation and tracking performance are achieved [57, 58]. Disturbance rejection performance of INDI control has been tested on a MAV. First experiments showed that three times better performance is achieved in terms of position error when compared to PID [59]. Later on, INDI is improved with a cascaded version which increased the performance to be seven times better then classical PID controller [60].

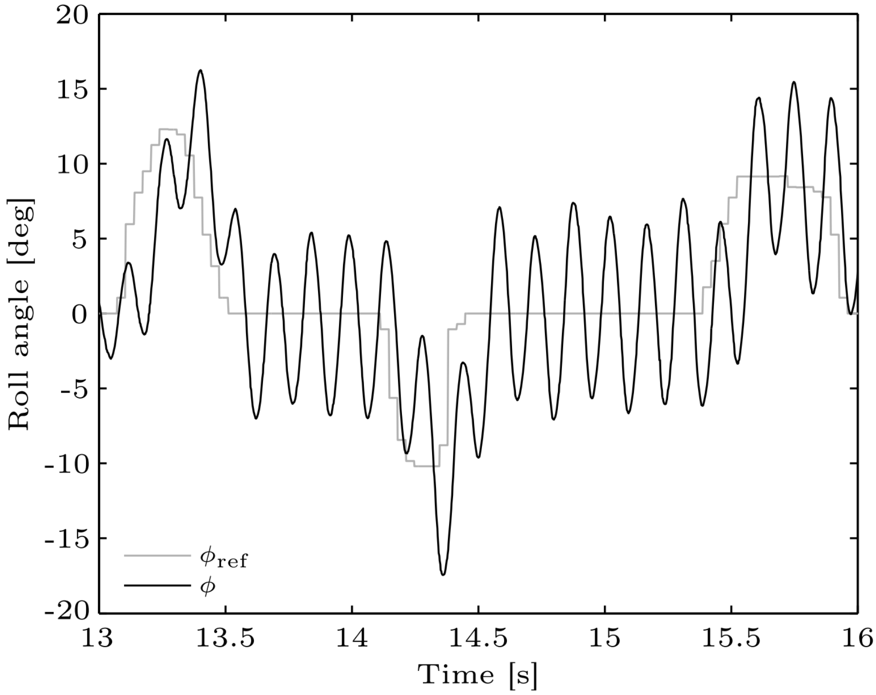


Figure 4.2: Noise filtering cause angular acceleration to be delayed. Signal mismatches yields oscillations in large magnitudes [5]

### 4.2.3. OTHER APPLICATIONS OF INDI

INDI has found itself a large number of applications on various aerospace systems. In [61], attitude tracking performance of a spacecraft is presented using INDI. The method is concluded to be more suitable than identification or model-based adaptive control architecture. By simulations the performance of INDI is compared to PI and regular NDI and the results showed that INDI has better stability and performance in nominal case and in the presence of external disturbances, time-delay and parametric uncertainties. In [55], INDI is used for helicopter flight control, attitude and navigational controllers are designed. This study offered using pseudo-control hedging which is pioneered in [62] to overcome actuator saturation problems. Actuator dynamics need to be carefully handled since the problem of oscillations is frequently encountered in INDI applications. In order to overcome this challenge suitable actuator modeling has been proposed in [63].

INDI showed effectiveness on lateral control of an under-actuated airship [64] and also on attitude control of a tiltwing aircraft where fixed-wing coordinate system is used [65]. Silva blends gain scheduling, NDI and INDI to stabilize VTOL during all stages [66]. In addition, INDI is a promising tool for urban air mobility since it has effective applications on electrical VTOL [67]. Due to the nature of VTOL, tiltwing and tiltrotor, control laws need to be blended with control allocation methods since these systems are over-actuated and contains effector redundancy. Hence, flight control for tiltrotor is designed with a control allocation algorithm [68, 69]. In these studies, INDI proved its ability to decouple control variables. A similar result is achieved in [70] where improvement in control allocation speed is emphasized as well. In [71], an INDI baseline controller is designed for another redundant aerospace vehicle, F-16 assuming readily available angular accelerations.

Aerospace systems are relatively heavy, have six degrees of freedom, include many components and they are assigned to perform various tasks. Therefore they are vulnerable for structural damages and changes. Considering faults on the systems are another area of focus. In the study [72], Lu et al. uses INDI as a fault tolerant method and its performance in the presence of actuator fault is appreciated. The study includes comparison with existing methods in three scenarios and efficient performance of INDI is observed without sufficient excitation and threshold selection which is a drawback of adaptive NDI based on online system identification procedure. In [55], the actuator of tailrotor is assumed to be stuck at certain fixed deflections. The performance degradation is limited for the deflections at low degrees and INDI controller is able to keep the system stable. In [73], anti-windup scheme for INDI is proposed to overcome actuator faults. In addition, fault tolerant performance of INDI is tested in a quadrocopter that reach 9 m/s speed when a single rotor is lost [74]. A recent study considers complete loss of two opposing rotors and tests the performance of INDI controller [75]. Bayer in [76] shows that a passenger aircraft can use use INDI adaptively to compensate a partial failure of the high lift system during landing.

INDI is also strengthened by blending the control architecture with other methods, such as augmentation with model reference adaptive control and differential flatness [77, 78]. INDI based flight control is shown to be capable of converting Cessna Citation II aircraft into a variable stable system [19]. The effectiveness of INDI is also validated by aircraft flight tests on a CS-25 certified passenger aircraft [8]. Another flight test is performed to make INDI compatible with a new type electromechanical actuation [79].

## 4.3. MODEL-BASED INDI

Model-based controllers generally encounter with issues about model mismatches and they are vulnerable in conditions that are uncertain for the designer. This situation is presented in Section 3.5 that NDI is not robust for model mismatches. INDI on the other hand is robust for these mismatches and it requires feedback signal of derivative of its states as shown in Eq. 4.5. The model of a system can be used to extract the state derivative term. A general nonlinear system dynamics is given in Eq. 3.1 which could be directly used to obtain state derivative. By using the modeled dynamics, $\underline{\dot{x}}_0$ is given as

$$\underline{\dot{x}}_0 = \underline{f}(\underline{x}_0) + \underline{g}(\underline{x}_0)\underline{u}_0 \tag{4.10}$$

Plugging this into the INDI control law yields

$$\underline{u} = \underline{u}_0 + g^{-1}(\underline{x}_0)\big(\underline{\nu} - \underline{f}(\underline{x}_0) - \underline{g}(\underline{x}_0)\underline{u}_0\big) \tag{4.11}$$

This new control law can be simplified further by distributing inverse of control effectiveness as

$$\underline{u} = \underline{u}_0 + g^{-1}(\underline{x}_0)\underline{\nu} - g^{-1}(\underline{x}_0)\underline{f}(\underline{x}_0) - \underline{u}_0 \tag{4.12}$$

$$\underline{u} = g^{-1}(\underline{x}_0)\underline{\nu} - g^{-1}(\underline{x}_0)\underline{f}(\underline{x}_0) \tag{4.13}$$

$$\underline{u} = g^{-1}(\underline{x}_0)\big(\underline{\nu} - \underline{f}(\underline{x}_0)\big) \tag{4.14}$$

This control method is a modification of INDI using model parameters instead of sensor measurement. The final result is the same as NDI controller that is given in Eq. 3.12. The form given in Eq. 4.11 is referred as Model-Based INDI control, because this form calculates the control increment so that it is an incremental approach. The robustness of this approach is same as NDI. One of the main difference of Model-Based INDI with Sensor-Based INDI is the Model-Based INDI does not need to deliberately delay control input to match with the measurement. The measurements used in this approach are only state related and they are negligible compared to control input related terms. The input used for model computation is precisely known which indicates that the cancellation of the input related terms always hold.

## 4.4. HYBRID CONTROL APPROACHES

This section presents the literature that integrates model output with the measurement. Additionally, papers based on multiple controllers are presented. The aim of the section is to partially answer research question 4 which requires to investigate existing hybrid approaches, identify their weaknesses and strength. Applicability of these approaches for Hybrid INDI will be determined in further studies.

The main goal of this research is to be able to use Model-Based and Sensor-Based INDI together. This requires merging these two control laws or their utilization of each other. Even though this specific combination of control laws has not been a subject of a study, there are many researches that involve multiple controllers. For this purpose, existing hybrid approaches are investigated.

Model and sensor integration is not rare in INDI control designs. Formulation of INDI for over-actuated system yields over-determined problem. To obtain best performance with least effort, control allocation is frequently applied [71, 80]. Initially, these studies consider local linearization of dynamical equations in the form of Eq. 4.2 and virtual control is derived. Then, assumption of slow change in states applied. This assumption does not cancel model dependence completely. Control effectiveness appears in the equation as expected. Partial derivative of $\underline{f}(\underline{x})$ with respect to controlled variables is required for control allocation. Therefore, onboard plant models are implemented for the calculation of these values.

Sun et al. handles a fault tolerant flight control application that combines NDI with Sensor Based Backstepping (SBB) method [81]. The paper treats NDI as outer controller that produces desired angular rates and SBB as inner loop angular rate controller which yields required actuator deflection. In this combination, NDI output feeds SBB controller. This approach is referred as hybrid control, although it is fundamentally different than the approach of this study where the controllers are used to calculate inputs independently.

In [82], a literature overview of hybrid control is presented, stating the closed loop improvements by hybrid controllers. A bang bang controller causes problems such as high frequency oscillations when the control error is small. This can be avoided by a linear controller once the system is brought near the equilibrium point. The combination of two controllers forms a closed loop system that has a high response speed and no steady state error. Hybrid controllers achieve better optimality measures in terms of cost functions and, control and state constraints are guaranteed not to be violated. Robustness and disturbance attenuation performance can also be increased.

A common hybrid controller approach is to switch between controllers. A supervisor or a switching algorithm decides which of the designed controller will be used. A general representation of control architecture is given in Fig. 4.3. In [83], switched controllers are studied with a focus on linear controllers. Fundamental properties are discussed in terms of stability, controllability, observability and optimality.

In aerospace field, switching controllers are used for various objectives. One of the reasons why controller loses its effectiveness is a significant change in the system. This change is generally caused by a damage or a fault. Therefore, switching of controllers is used to form a fault-tolerant system. In [84], two controllers are designed, one of them only includes elevator and the other utilizes thrust vector for F-16 aircraft. Different than the other approaches, the proposed solution is not based on the architecture given in Fig. 4.3 where there is a discrete selection between controllers. On the contrary, Lu and Wu, uses both of the controllers by a weighting function depending on the severity of the fault. This is done to eliminate one of the drawbacks of switching control that is discontinuity caused by logic based switching. Another solution proposed in [6] presents a smooth transition algorithm for the control of aircraft engine that requires a multi-controller structure.

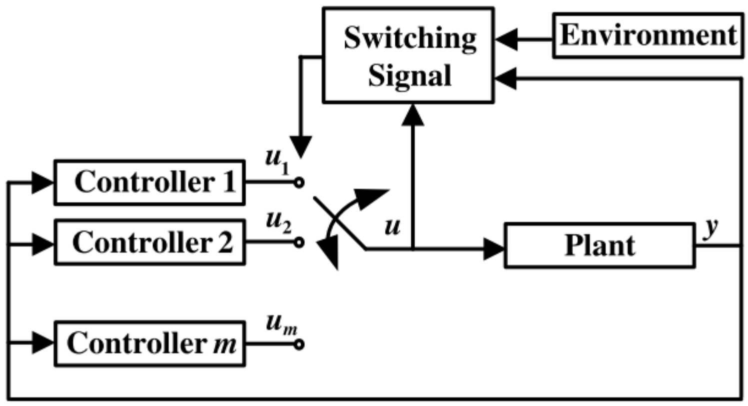


Figure 4.3: Hybrid Control Architecture - Switching controller based on a decision mechanism [6]

# 5

# Application to Missile Longitudinal Motion Dynamics

The preliminary study aims to develop an intuition for the application of the proposed methods and answer research questions 2 and 3 in detail. Missile equations of motion are selected for primary applications. The chapter introduces dynamical equations that are interest. Control laws are designed for Sensor-Based and Model-Based INDI. The dynamics of additional components to form a closed loop system are presented. The control design is improved by considering the error dynamics for tracking purposes, disturbance rejection, control gain optimization and modification in feedforward signal. Lastly, robustness tests are performed which reveal strengths and weaknesses of the approaches compared to each other.

## 5.1. Missile Dynamics

Missile equations of motion are nonlinear and time varying. This nature makes linear controllers to ignore fundamental behaviour of missiles which a nonlinear controller would include. It is generally difficult and time consuming to obtain accurate aerodynamic parameters. Due to modeling errors missile models have uncertainties. Missiles need to be designed to be maneuverable and robust. The full equations of motion are complex and multivariable. Pitch plane equations are used in order to have a good understanding of the methods before distracted by the other performance specifications introduced by multivariable systems. There has been extensive studies using pitch plane equations of motion. This assists validating the results and observing the performance enhancements [85–87].

Body-fixed and earth fixed coordinate sysetems are shown in Fig. 5.1. Longitudinal flight dynamics deal with longitudinal plane that only includes $X_B$ and $Z_B$ axes in body coordinate system. State space is formed by missile velocity $V$, angle of attack $\alpha$, pitch rate $q$ and pitch angle $\theta$. For a rigid body aircraft longitudinal dynamics include two complex eigenmotions; one with short period and another with long period (phugoid). A missile with constant altitude at 6000 m and constant speed does not the need for velocity and pitch angle to be state variables. The states reduce to angle of attack and pitch rate. These two states constitute the pitch plane. The dynamics are approximated such that only short period mode is kept. Nonlinear equations of motion of the approximated generic air to air missile is given as

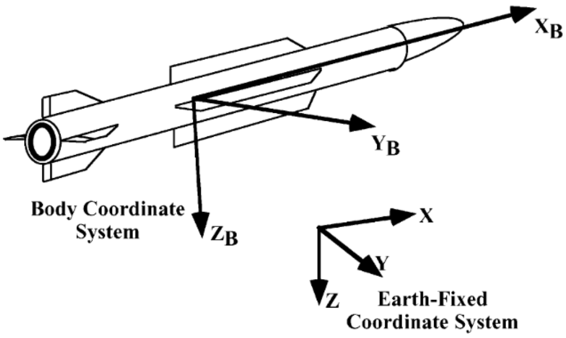


Figure 5.1: Missile Coordinate System [7]

$$\dot{\alpha} = q + \frac{1}{mV}(mg\cos\gamma - L - T\sin\alpha) \tag{5.1}$$

$$\dot{q} = \frac{M}{I_{yy}} \tag{5.2}$$

The parameters $M$,$L$ and $T$ are pitching moment, lift force and thrust, respectively. Furthermore, $I_{yy}$ is pitch moment of inertia, $m$ is mass and $\gamma$ is flight path angle. The aerodynamic moments and forces are function of control surfaces, angle of attack and Mach number. Mach number is constant since the flight velocity and altitude is kept constant. The equations of motion are expanded to show the effects of control surfaces and angle of attack on aerodynamic values:

$$\dot{\alpha} = q + \frac{1}{mV}QS\,[C_z(\alpha) + b_z\delta] \tag{5.3}$$

$$\dot{q} = \frac{1}{I_{yy}}QSd\,[C_m(\alpha) + b_m\delta] \tag{5.4}$$

In this equation, $Q$ represents dynamic pressure, $S$ is surface area, $d$ is reference distance. Aerodynamic coefficients for the control effectiveness are constant and donated by $b_z$ and $b_m$. Other aerodynamic coefficients, denoted by $C_z$ and $C_m$, are third order polynomial functions and dependent on angle of attack. The equations of motion are valid for $1.8 < M < 2.6$. Mach number during flight is constant at $M = 2$. Furthermore, the equations are valid for $-10° < \alpha < 10°$. This form of equations is more convenient for a more general state representation as $\alpha = x_1$ and $q = x_2$:

$$\dot{x}_1 = x_2 + f_1(x_1) + g_1 u \tag{5.5}$$

$$\dot{x}_2 = f_2(x_1) + g_2 u \tag{5.6}$$

The entire aerodynamic contribution of Eq. 5.3 is measurable through linear accelerometers. Therefore, angle of attack state equation can be stated as

$$\dot{\alpha} = q + \frac{A_z}{V} \tag{5.7}$$

Given these equations, the system has three outputs, first two of them are controlled outputs, $\alpha$ and $q$ and the last one is $\frac{A_z}{V}$. In fact, $A_z$ and $V$ are measured with different sensor and in reality these sensor outputs would be post processed to be used as a feedback term. In this case, it is assumed $\frac{A_z}{V}$ is measured directly. Nonlinear dynamics of the system can be linearized at equilibrium point ($\alpha = 0, q = 0$) by Jacobian linearization. This yields a standard Linear Time Invariant system dynamics which is in general form shown as

$$\begin{aligned} \dot{x} &= Ax + Bu \\ y &= Cx + Du \end{aligned} \tag{5.8}$$

The resulting linear approximated state space matrices are

$$\begin{gathered} \begin{bmatrix} \dot{\alpha} \\ \dot{q} \end{bmatrix} = \begin{bmatrix} -0.0982 & 1 \\ -19.8344 & 0 \end{bmatrix} \begin{bmatrix} \alpha \\ q \end{bmatrix} + \begin{bmatrix} -0.022 \\ -27.305 \end{bmatrix} \delta \\ \begin{bmatrix} \alpha \\ q \\ \frac{A_z}{V} \end{bmatrix} = \begin{bmatrix} 1 & 0 \\ 0 & 1 \\ -0.0982 & 0 \end{bmatrix} \begin{bmatrix} \alpha \\ q \end{bmatrix} + \begin{bmatrix} 0 \\ 0 \\ -0.022 \end{bmatrix} \delta \end{gathered} \tag{5.9}$$

## 5.2. CONTROLLER DESIGN

NDI and INDI control design techniques, and time scale separation assumption are introduced in the preceding chapters. The control laws are determined for given missile equations.

### NDI CONTROLLER

Since the control variable is $\alpha$, the relation between angle of attack and control deflection $\delta$ needs to be formed. The first derivative of angle of attack is

$$\frac{d\alpha}{dt} = q + \frac{A_z}{V}. \tag{5.10}$$

Because of the use of measurement instead of Eq. 5.3. The control deflection does not appear directly. To find input-output relation, the equation is differentiated

$$\frac{d^2\alpha}{dt^2} = \dot{q} + \frac{d}{dt}(\frac{A_z}{V}) \tag{5.11}$$

Plugging into the Eq. 5.4 would yield the desired input-output relation as

$$\frac{d^2\alpha}{dt^2} = \frac{QSd}{I_{yy}}[C_m(\alpha) + b_m\delta] + \frac{d}{dt}(\frac{A_z}{V}) \tag{5.12}$$

The pseudo control is the second derivative of the angle of attack since the relationship is found after the second derivative.

$$\ddot{\alpha} = \nu \tag{5.13}$$

Now, the controller law is formed as

$$\delta = \frac{I_{yy}}{QSdb_m}[\nu - \frac{QSd}{I_{yy}}C_m(\alpha) - \frac{d}{dt}(\frac{A_z}{V})]. \tag{5.14}$$

This equation is used as inner linearization loop and since a linearized dynamics is obtained the outer loop can be designed using a PD controller as

$$\nu = K_p(\alpha_d - \alpha) + K_d(\dot{\alpha}_d - \dot{\alpha}) + \ddot{\alpha}_d \tag{5.15}$$

### NDI CONTROLLER WITH TIME SCALE SEPARATION

Pitch rate responds faster than the angle of attack to controller deflection. There is a time scale separation between angle of attack and pitch rate. The approach is to find a desirable value for pitch rate that leads angle of attack to the commanded value. This constructs a cascaded loop structure. The outer loop gets commanded angle of attack as input and calculates the desired pitch rate and the inner loop gets desired pitch rate as input and calculated control deflection. Each loop needs a virtual control. Initially $\nu_1 = \dot{q}$ is considered and it is seen that input - output relation is given by the first derivative in the system equations. The control law is

$$\delta = \frac{I_{yy}}{QSdb_m}[\nu_1 - \frac{QSd}{I_{yy}}C_m(\alpha)] \tag{5.16}$$

Pseudo control $\nu_1$ is designed according to a single proportional control with a feedforward term:

$$\nu_1 = K_{p_1}(q_d - q) + \dot{q}_d \tag{5.17}$$

Desired pitch rate value is given as $(q_d)$ and it is calculated by the outer loop. The second virtual control is defined as $\nu_2 = \dot{\alpha}$ and using Eq. 5.10 yields

$$q_d = \nu_2 - \frac{A_z}{V} \tag{5.18}$$

furthermore the virtual control is

$$\nu_2 = K_{p_2}(\alpha_d - \alpha) + \dot{\alpha}_d. \tag{5.19}$$

### INDI CONTROLLER

Time scale separated system consists of two one-degree dynamics. The outer loop is used to calculate the desired pitch rate value while controlling angle of attack as shown in Eq. 5.18. Inner loop is used to calculate elevator actuator input, given in Eq. 5.16. INDI also make use of time scale separation. In this regard, the outer loop does not need any modification since $A_z/V$ is already a sensor measurement and the dynamics is linear. Inner loop needs to be modified according to the linearization law given in Eq. 4.5. The control effectiveness for the pitch rate is given in Eq. 5.4 and is stated as

$$g_2 = \frac{QSdb_m}{I_{yy}} \tag{5.20}$$

INDI inner loop is used to calculate the increment of control deflection as

$$\Delta\delta = \frac{I_{yy}}{QSdb_m}[\nu_1 - \dot{q}_o)] \tag{5.21}$$

The increment of control $\Delta\delta$ can also be expressed as the difference between current time step control input and previous time time step input, which is $\delta - \delta_0$. This change finalizes the control law as

$$\delta = \delta_0 + \frac{I_{yy}}{QSdb_m}[\nu_1 - \dot{q}_o)]. \tag{5.22}$$

One can see that, the last term is switched to pitch rate measurement and the equation only contains model information about control effectiveness where $C_m(\alpha)$ term disappears which decreases the dependence of control method on system model. Using the linear controller used for virtual controller $v_1$ and plugging it into Eq. 5.22 gives the overall control in time domain as

$$\delta = \delta_0 + \frac{I_{yy}}{QSdb_m}[K_{p_1}(q_d - q) + \dot{q}_d - \dot{q}_o)]. \tag{5.23}$$

Control gains $K_{p1}$ and $K_{p1}$ are two control gains that require tuning. Their value depends on the performance requirements. A further discussion about the selection of these values is given in Section 5.4.

#### MODEL BASED INDI CONTROLLER

Model based INDI uses system model in order to determine $\dot{q}_0$. As it is given in the system dynamical equations pitch acceleration is a function of angle of attack and control surface deflection. The measurement of angle of attack is satisfactory to determine pitch acceleration and so direct measurement or estimation through pitch rate measurement of the parameter is not necessary anymore. State derivative equation for pitch rate given in Eq. 5.4 is written as

$$\dot{q}_0 = \frac{1}{I_{yy}} QSd\left[C_m(\alpha_0) + b_m\delta_0\right] \tag{5.24}$$

Substituting this equation into Eq. 5.22 and rearranging the terms as

$$\delta = \delta_0 + \frac{I_{yy}}{QSdb_m}\left[v_1 - \frac{1}{I_{yy}} QSd\left[C_m(\alpha_0) + b_m\delta_0\right]\right] \tag{5.25}$$

This equation can be simplified further to eliminate current control surface deflection as

$$\delta = \frac{I_{yy}}{QSdb_m}\left[v_1 - \frac{QSd}{I_{yy}}\, C_m(\alpha_0)\right] \tag{5.26}$$

Both of these equations yield the same results and they construct the form of Model-Based INDI control. For a hybrid approach, it is desirable for the control laws to be similar to each other as much as possible to ease combination of the signals. Therefore, the form given in Eq. 5.25 is used in further analysis and simulation.

## 5.3. SYSTEM COMPONENTS

There are additional components that needs to be integrated with plant in order to form a feedback structure. Control surfaces are parts of a missile and their effect on the system is aerodynamically modeled within the plant dynamics. Control surfaces are deflected by actuators. Actuator dynamics need to be modeled to observe a more practical response of the plant to inputs. Missiles also need sensors that measure the states of itself to make the judgement whether they are as commanded. A perfect sensor would have infinitely small sampling time and would show exact value of the state. The sensor measurements are generally not perfect and need to modeled as well. In this study, noise of these sensor measurements are included to the system which requires to have a noise filtering method. Next, synchronization of the commanded control surface deflection and system dynamics measurement are explained. Lastly, a realizable filter for derivation operation is presented. These additional dynamics are investigated and detailed in this section.

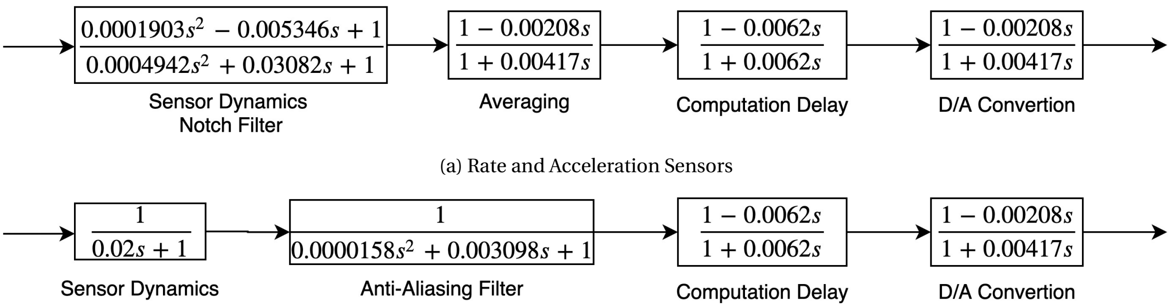


(a) Rate and Acceleration Sensors

(b) Air-data Sensors

Figure 5.2: Linearized Measurement Dynamics

### 5.3.1. SENSORS

The closed loop system involves three sensors for angle of attack, pitch rate and linear acceleration. An air to air missile system is expected to be highly maneuverable and agile. These features would also be expected to be in a fighter jet. Hence, a similar set of sensors are equipped in the missile. A model of a combat aircraft is presented for the research of robust control by the Group for Aeronautical Research and Technology in Europe (GARTEUR) [88]. The same sensor models are used in this study. Accelerometer and attitude rate sensors are located in IMU and they assumed to have the same dynamics. Rate and acceleration measurement dynamics comprise sensor dynamics, averaging, computational delay and analog to digital converter. For the air-data measurements which is used for angle of attack measurement, averaging dynamics is replaced with anti-aliasing filter. Furthermore, rate sensor dynamics include notch filter as well. The linearized dynamics are represented in Laplace domain and corresponding block diagrams are given in Fig. 5.2

### 5.3.2. ELEVATOR ACTUATOR

As shown in Fig. 5.1, the missile has four stationary surfaces on the center for stabilization. There are four dynamic surfaces on the tail. These are the control surfaces since they generate moment for the control. The effect of four surfaces are comparable to regular aircraft's aileron, elevator and rudder. The surfaces act together to have specific effects. For instance, moment generated on $X_B$ and $Z_B$ axes cancel each other and only moment on $Y_B$ axis remains. This action is comparable to elevator deflection in conventional aircraft. In this study, the motion is restricted only in the pitch plane. It is assumed that aileron and rudder effects of the missile always cancel within themselves.

The additional component that needs to be modeled is elevator actuator that transmits the flight controller's command to the control surface. For this phase of the study, it is decided to focus on effects of actuator dynamics in later stages. Nevertheless, for integrity, a simple actuator dynamics is involved that a first order lag dynamics with low time constant which affects the performance of the system very slightly. The dynamics is given as

$$H_{\text{act}}(s) = \frac{1}{0.01s+1} \tag{5.27}$$

This is a fast dynamics that can only affect the system's behaviour in high frequencies.

### 5.3.3. NOISE FILTERING

Sensor measurements contain perturbations around the actual signal that is referred as noise. A noisy signal fluctuates around the true value. Measurement noise has generally characteristics that its magnitude changes in frequency. In this study, it is assumed that noise is constant for every frequency. This means that white noise is used for simulations. The variance of noise parameters

Table 5.1: Variances of white noise of sensors. Values are taken from [8]

| Signal | | | Noise Variance ($\sigma^2$) |
|---|---|---|---|
| Angle of Attack | $\alpha$ | (rad) | $7.5 \cdot 10^{-8}$ |
| Pitch Rate | $q$ | (rad/s) | $4.0 \cdot 10^{-7}$ |
| Normal Acceleration | $A_z$ | (g) | $1.5 \cdot 10^{-5}$ |

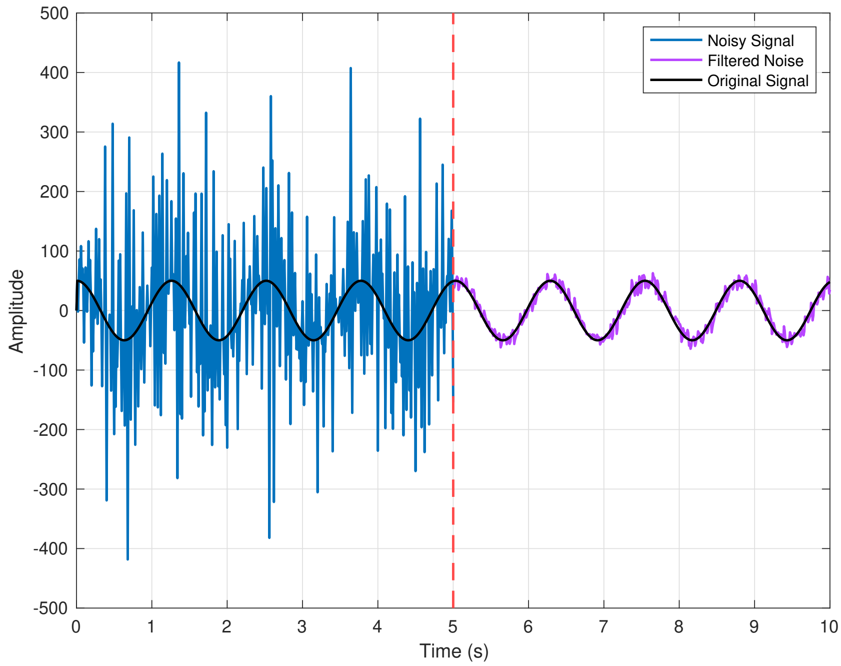


Figure 5.3: Noise with standard deviation of 1 is added to a sinusoidal signal with amplitude 10. The signal is differentiated and the noise contribution is amplified. A second order filter is activated after 5 seconds.

are taken from [8] where INDI controller is tested for Cessna Citation II aircraft. These values are presented in Table 5.1. Noisy measurements degrade the performance of the closed loop system. A control design is expected to alleviate effect of noise therefore a noise filter is added to the closed loop dynamics.

Noise can be filtered through different ways. Filtering low frequency signals deteriorates tracking performance of the system and should be avoided. Noise filtering causes additional lag in the system. Introduction of high signal lag on the feedback signal should be avoided since it also limits the performance.

INDI controller given in Eq. 5.22 requires pitch acceleration $\dot{q}$. This variable is not directly measured and generally found through differentiation of pitch rate measurement signal. Derivation of a noisy signal causes the effect of the noise to be amplified. Numerical derivation techniques use previous sample points to estimate current derivation value. As the number of sample points used for derivation increases more accurate results are gathered. Using more sample points also amplifies the effect of noise on the signal. The effectiveness of a second order filter on a differentiated signal is shown in Fig. 5.3. A more detailed analysis is given in Appendix A. Therefore, a signal that is differentiated requires to have more rigorous filtering than the ones that are directly used.

First order lag filters are used for three measurements that are directly measured by the sensors. A second order filter is used for the pitch acceleration. The bandwidth of the noise filters are selected according to bandwidth of the sensors. Any higher frequencies cannot be measurement by sensor

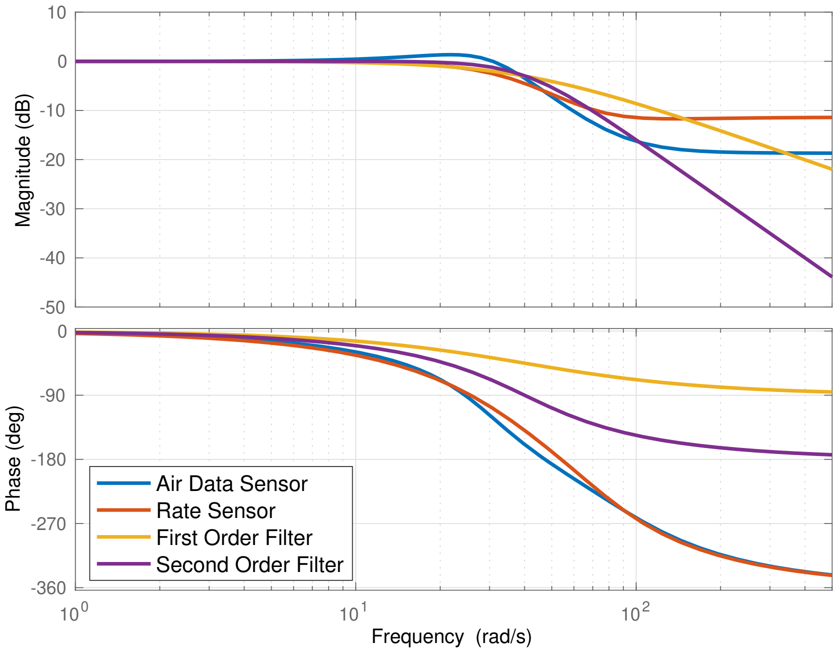


Figure 5.4: Bode Plots of Sensors and Noise Filters

therefore they are regarded as noise. The natural frequency is set to 40 rad/s and for the second order filter damping coefficient is selected as 0.7. The transfer functions are

$$H_{N_1}(s) = \frac{1}{1/40s+1} \tag{5.28}$$

(5.29)

$$H_{N_2}(s) = \frac{1600}{s^2+56s+1600} \tag{5.30}$$

The Bode plots of sensor dynamics and noise filters are given in Fig. 5.4. $H_{NF2}(s)$ is used to filter differentiated signal in Fig. 5.3.

### 5.3.4. SYNCHRONIZATION

INDI control determines the next control input based on current state of the system and current commanded control input. The input is known but there is possibility that this is not realized as expected due to actuator dynamics. In this case actuator dynamics can be used to obtain real control input or more directly deflections are measured. Both of the approach give good estimation of control input. This means $u_0$ is readily available for further calculation. On the other side, the source of system's state information is sensor measurement. It is not practically possible to measure the current states. The measurements are gathered with a time delay and with noise. As discussed previously, noise is attenuated by filtering high frequency components of the signal. Filtering comes with cost of additional time delay and thus by the time system knows about it's state current state differs already. Our best knowledge of state is represented as filtered variable $\underline{x}_d$. Therefore, the form of Sensor-Based INDI given as

$$\underline{u} = \underline{u}_0 + g^{-1}(\underline{x}_0)(\underline{v} - \dot{\underline{x}}_0) \tag{5.31}$$

is not practical unless perfect sensors are assumed. Therefore, time that the Taylor expansion is applied should be delayed as much as the delay of the state signal. This requires delaying control input and using $\underline{u}_d$. The new Sensor-Based INDI control is

$$\underline{u} = \underline{u}_d + g^{-1}(\underline{x}_d)(\underline{\nu} - \dot{\underline{x}}_d). \tag{5.32}$$

This process is called synchronization and it is essential to obtain satisfactory results. This synchronization requires transferring the signal $\underline{u}_0$ to $\underline{u}_d$. Another synchronization method would be transferring $\underline{x}_d$ to $\underline{x}_0$ and thus no modification would be required in control law. The problem with this type of synchronization is that it requires prediction of the future states which may not be obtained accurately. On the other side, previous values of control deflections are known accurately.

The first step that needs for the synchronization is keeping the previous commanded control surface in memory. This would mean obtaining $\underline{u}_0$. Then, this signal should be delayed as much as the measurements. The added delay can be pure time delay due to sensor dynamics and noise filtering or another approach is to filter the signal through the same signals. The drawback of this procedure is that the sensor dynamics need to be known accurately. In addition there might be unexpected delays or faults in the measurement.

A single step time delay of a function $f(t)$ is represented as $f(t-dt)$ where $dt$ is the time increment. The sensor dynamics and noise filtering are given in Laplace domain, thus time delay is transferred into Laplace domain:

$$\mathscr{L}(f(t-\Delta t)) = e^{-\Delta ts} \tag{5.33}$$

Having a Laplace variable in the exponential format causes computational problems in the linear analysis. A common approach is to approximate the time delay. Pade approximation that is formed by ratio of two power series is frequently used for approximation. The first order is given by

$$e^{-\Delta ts} = \frac{\frac{e^{-\Delta ts}}{2}}{\frac{e^{\Delta ts}}{2}} \approx \frac{1 - \frac{\Delta ts}{2} + \frac{dt^2s^2}{8} \ldots + \frac{((\frac{(-dt)s}{2})^k}{k!}}{1 + \frac{\Delta ts}{2} + \frac{dt^2s^2}{8} \ldots + \frac{((\frac{-dt)s}{2})^k}{k!}} \tag{5.34}$$

This approximation allows limited value of k which determines order and accuracy of the approximation. The computational delay given for the sensor dynamics in Fig. 1.2 is an example of first order Pade approximation. Another approximation is given in the form of

$$e^{-\Delta ts} \approx \frac{1}{\left[1 + \frac{\Delta ts}{n}\right]^n} \tag{5.35}$$

First two orders of these approximations are compared in Fig. 5.5 with respect to their performance for a delayed step signal. The signal is delayed 0.1 s.

As the order increases, the approximations approach to pure time delay faster and with less error. In this regard, second order Pade approximation is selected to be used in Laplace domain analysis. This approximation shows good performance in frequency domain as well especially in low frequencies. The overall synchronization transfer function is given as

$$H_{\text{sync}} = H_{\text{Pade}} * H_q * H_{N_2} \tag{5.36}$$

Unsynchronized signals do not affect the performance of Model-Based INDI. Even though, the form that is used in this study includes the current control input, this signal cancels itself. In the case the signal synchronized, it still cancels itself; hence there is no compromise in performance. This form is suitable for an hybrid approach because switching between control types require less change.

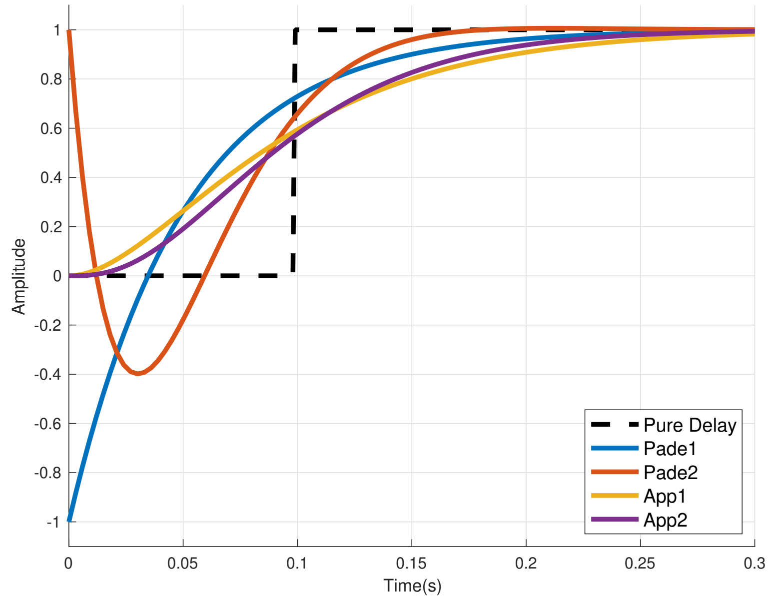


Figure 5.5: Delayed Step Response

### 5.3.5. REFERENCE MODEL

The internal dynamics of a system prevents the response for a command to be infinitely fast. A reference model is planted to shape the commanded input. This improves the tracking error and input command becomes more realistic for the system to follow. The model is selected to be a first order system with relatively fast response that the missile can realistically follow. The dynamics is given as

$$H_{\mathrm{RM}}(s) = \frac{1}{\frac{1}{4.5}s+1}. \tag{5.37}$$

This function is selected because it yields the fastest response without any overshoot.

### 5.3.6. DERIVATIVE FILTER

There are several occasions that the signals are differentiated, for instance to obtain angular acceleration from angular rate measurements. Derivative signal of the control input is used as the feedforward and in addition derivative of the error signal can be used as feedback controller. In order to avoid noise application, derivation is performed via a filter. This filter also makes the derivation a realizable operation. It does not differentiate high frequencies since the magnitude rolls off. The operation is performed with

$$H_{\mathrm{d}}(s) = \frac{s}{30s+1}. \tag{5.38}$$

With this transfer functions every additional components and transfer functions are presented to construct a closed loop system which will be discussed in the following section.

## 5.4. CLOSED LOOP SYSTEM

Given the dynamics of the additional components the closed loop systems are formed. The block diagrams for Sensor-Based INDI and Model-Based INDI are given in Fig. 5.6. There are two disturbances ($d_1$, $d_2$) added to the system, to be used in the selection of proportional gains. The other inputs are noise $n$ and angle of attack command $\alpha_{\mathrm{ref}}$. The innermost loop is the linearization loop

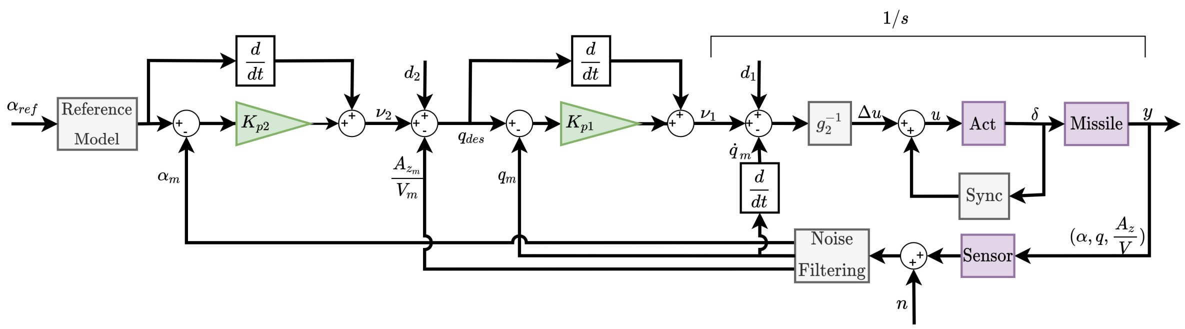


(a) Sensor-Based INDI Closed Loop System

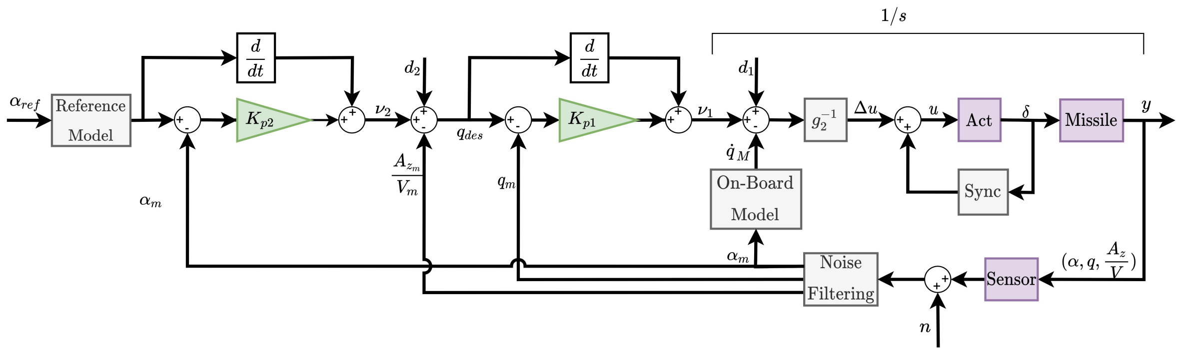


(b) Model-Based INDI Closed Loop System

Figure 5.6

going from $\nu_1$ to $q$. This relation is marked as an integrator in Fig. 5.6 which is true if the linearization loop is perfect. First, a non-perfect transfer function which includes additional dynamics is derived for Sensor-Based INDI.

The are two dynamics in the block diagram that are not linear. The missile dynamics and inverse of control effectiveness. For this example, the control effectiveness does not depend on any state, therefore it is constant and be regarded as static gain. The state space form of the missile dynamics which is linearized at equilibrium point is given in Eq. 5.9. The transfer function representation is

$$G_\alpha(s) = \frac{-0.022s - 27.3}{s^2 + 0.0982s + 19.83} \tag{5.39}$$

$$G_q(s) = \frac{-27.3s - 2.245}{s^2 + 0.0982s + 19.83} \tag{5.40}$$

$$G_{\frac{A_z}{V}}(s) = \frac{-0.022s^2 + 2.245}{s^2 + 0.0982s + 19.83} \tag{5.41}$$

where subscripts are used to indicate the output signal. The synchronization loop that involves actuator dynamics and synchronization is given by

$$TF_{\Delta u \to \delta} = \frac{H_{\text{act}}}{1 - H_{\text{sync}} H_{\text{act}}} \tag{5.42}$$

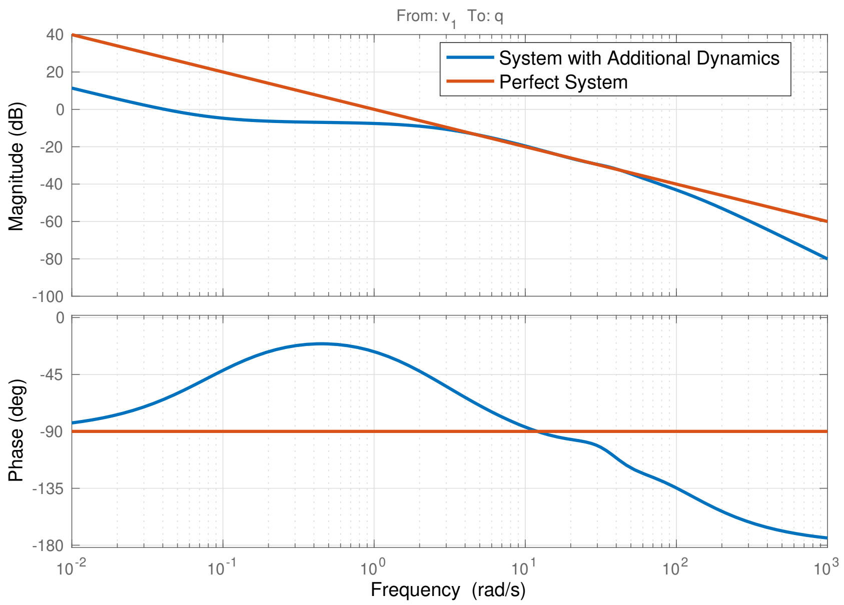


Figure 5.7: Bode plots of transfer function from virtual input $v_1$ to pitch rate $q$ of a perfect system (Integrator Dynamics) and a system with additional dynamics included are compared

Transfer function from $v_1$ to $q$ is

$$TF_{v_1 \to q} = \frac{g_2^{-1}\, H_{\text{act}}\, G_q}{1 - H_{\text{act}}\, e^{-\Delta ts}\, H_q\, H_{N_2} + g_2^{-1}\, G_q\, H_{\text{act}}\, H_q\, H_{N_2} s} \tag{5.43}$$

An approximation to a perfect system assumes sensors and actuators can transmit the signals as they are. In addition, no noise is added to system which eliminates the need for noise sensors. Lastly, time delay's magnitude approaches to unity at low frequencies and also for small time steps. With these assumptions, the overall transfer function reduces to

$$TF'_{v_1 \to q} = \frac{g_2^{-1}\, G_q}{g_2^{-1}\, G_q s} = \frac{1}{s} \tag{5.44}$$

which is indeed a single integrator. INDI controller is designed based on perfect linearization which yields this integrator dynamics. Even though, the additional dynamics deviate the system from being perfect, a good level of linearization is achieved when they are included. The bode diagrams of transfer function given in Eq. 5.43 is compared with integrator dynamics in Fig. 5.7. The linearization is close to integrator dynamics around 10 rad/s. Deviation is caused by time delay in low frequencies and other additional dynamics in higher frequencies.

The outer loop dynamics that is from $v_2$ to $\alpha$ is easier to observe when assuming a successful control of linearization dynamics. The time scale assumption between angle of attack and pitch rate loop states inner loop reaches at steady state much faster than the outer loop and assumption of a successful controller yields $q_{des} = q$. Using this equality, the system dynamics equation is given by

$$v_2 = \frac{A_z}{V} - q = \dot{\alpha} \tag{5.45}$$

Therefore, the transfer functions from $v_2$ to $\alpha$ is also a single integrator. The term $A_z/V$ is measured through a sensor. With an ideal sensor, the relation between pitch rate and angle of attack is also an integrator dynamics. These assumptions form a new block diagram, given in Fig. 5.8, that is suitable

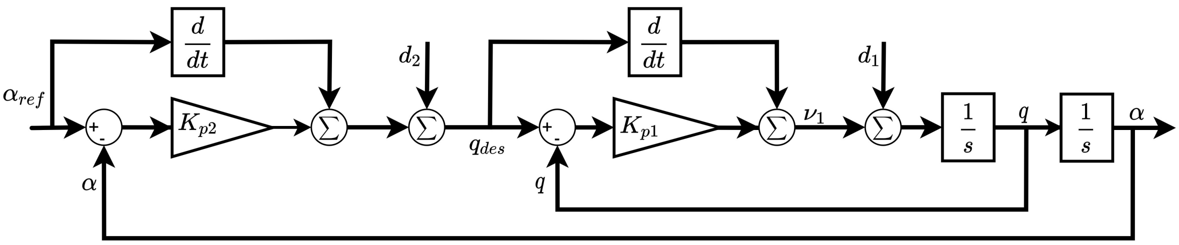


Figure 5.8: Model-Based INDI Closed Loop System

for linear control gains determination.

The linear controllers have the same form and given as

$$\nu_1 = K_{p2}(\dot{q}_d - q) + \dot{q}_d \tag{5.46}$$

$$\nu_2 = K_{p1}(\dot{\alpha}_d - \alpha) + \dot{\alpha}_d \tag{5.47}$$

There are two proportional gains that needs to be tuned. There has been different criteria and methods used in order to select the parameters. van 't Veld assess the success of the controller according to root mean square of the error signal [4]. Grondman sets an optimization algorithm by first selecting gains according to tracking performance and disturbance rejection [8]. Mooij finds integrated control effort and state derivation, and selects the gains that are satisfactory on both parameters [89]. Acquatella uses a cost function to minimize tracking error and control effort [61]. In this study, the error signal is investigated for disturbance rejection and reference tracking. Two disturbances are included $(d_1, d_2)$ in the inner and outer loop. The effects are studied for both of the states. Therefore, four transfer functions from disturbances derived. First, the disturbance transfer function from $d_1$ to $q$ is derived as

$$\frac{q(s)}{D_1(s)} = \frac{1}{s + K_{p1}} \tag{5.48}$$

Note that, $d_1$ is considered as the only input. Desired pitch rate, $q_{des}$, is assumed to be zero. Feedforward signal does not contribute to this disturbance transfer function. The error dynamics, with no reference input, represented as

$$E(s) = q_{des}(s) - q(s) = -q(s) = -D_1(s)\frac{q(s)}{D_1(s)}. \tag{5.49}$$

For step disturbance, the error dynamics is

$$E(s) = -\frac{1}{s}\frac{1}{s + K_{p1}} \tag{5.50}$$

by applying final value theorem steady state error is found as

$$\lim_{s \to 0} sE(s) = e_{ss} = -\frac{1}{K_{p1}}. \tag{5.51}$$

This result shows that disturbance can be rejected up to a finite value that is determined by the proportional gain. The disturbance $d_1$ is also effective on angle of attack. This transfer function is given as

$$\frac{\alpha(s)}{D_1(s)} = \frac{1}{s^2 + (K_{p1} - K_{p2})s + K_{p1}K_{p2}} \tag{5.52}$$

The steady state error for angle of attack is

$$\lim_{s\to 0} sE(s) = e_{ss} = -\frac{1}{K_{p1}K_{p2}}. \tag{5.53}$$

As both of the proportional gains are effective on the performance of the angle of attack, $K_{p2}$ being larger than 1 yields a better disturbance rejection compared to inner loop. The outer loop disturbance is a better tuning criterion for the linear control gains. This disturbance input directly determines the desired pitch rate value. It can also be regarded as the tracking command to the inner loop. The feedforward term in this loop happens to be effective. The error dynamics is directly extracted as

$$\dot{e} + eK_{p1} = 0. \tag{5.54}$$

This shows that the outer loop disturbance is tracked by the pitch rate without any error. The dynamics is stable for any $K_{p1} > 0$. The gain value determines the location of the pole and the how fast the error dynamics responds. The disturbance, $d_2$ is directly transmitted to pitch rate which makes the outer loop identical to inner loop except the gain changes from $K_{p1}$ to $K_{p2}$. Disturbance transfer function to the angle angle attack happens to be similar to Eq. 5.48 as

$$\frac{\alpha(s)}{D_2(s)} = \frac{1}{s + K_{p2}}. \tag{5.55}$$

Final value theorem is applied again to determine the steady state error for step disturbance which yields $e_{ss} = 1/K_{p2}$ Lastly the tracking error dynamics of the outer loop is given by

$$\dot{e} + eK_{p2} = 0 \tag{5.56}$$

since the inner loop is considered to be a static transfer function. These results show that, gains can be increased for faster response and lower disturbance rejection. As the side effect, the increase causes overshoot and higher control effort which limits the gains. The initial values for these are selected as $K_{p1} = 5$ and $K_{p2} = 2$. The disturbance rejection performances are shown in Fig. 5.9 that the results comply with the theoretical findings.

In terms of tracking performance Eq. 5.54 and Eq. 5.56 indicate that as long as positive gains are selected the system is stable, if the linearization is perfect. The final value theorem shows that there is no steady state error. This is an achievement of feedforward term. Two criteria are set in order to evaluate tracking performance. These are control effort and root mean square (RMS) of the angle of attack error. An additional one can be set for pitch rate error, though the designed controller determines the pitch rate input whereas angle of attack reference is an external signal.

The control effort is based on deflection angle of the actuator and it is calculated as

$$\delta_E = \int_0^{t_s} |\delta(t)|\, dt \tag{5.57}$$

where $t_s$ is simulation time. The simulation is based on discrete time increment thus this continuous formulation is modified as

$$\delta_E = \sum_{k=0}^{N} |\delta(k)|\, dt \tag{5.58}$$

where $N$ is number of sampled data. RMS of angle of attack error is given by

$$\epsilon_\alpha = \sqrt{\frac{\sum_{k=0}^{N} \left(\alpha_{ref}(k) - \alpha(k)\right)^2}{N}} \tag{5.59}$$

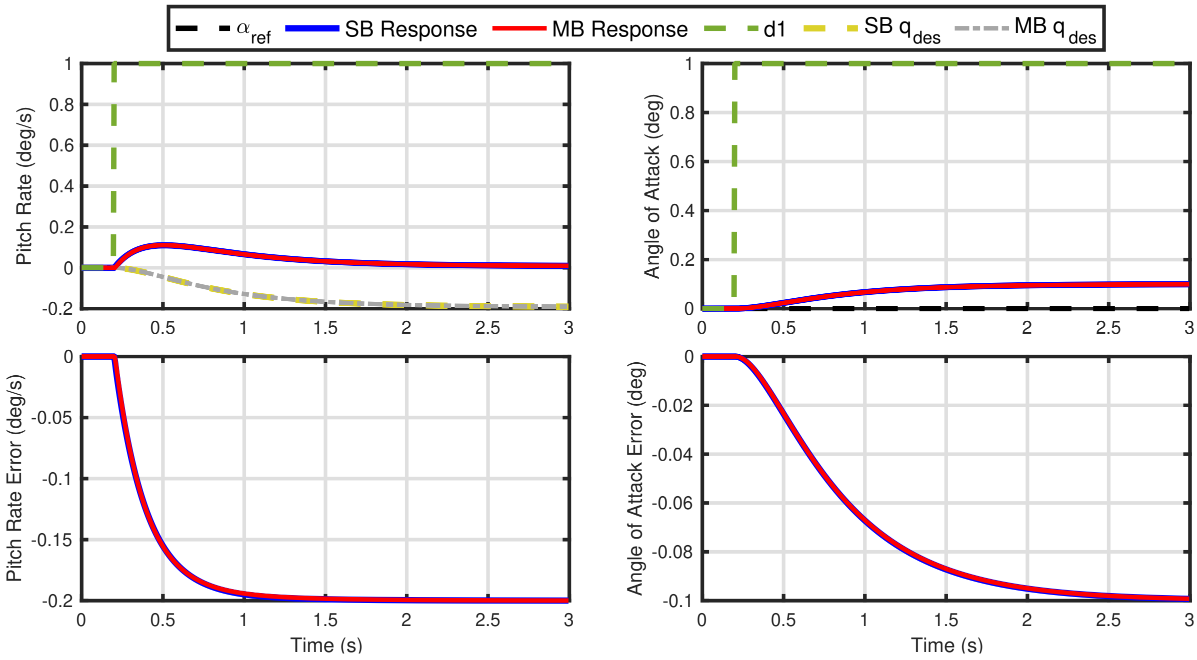


(a) System and Error Response to Inner Loop Disturbance

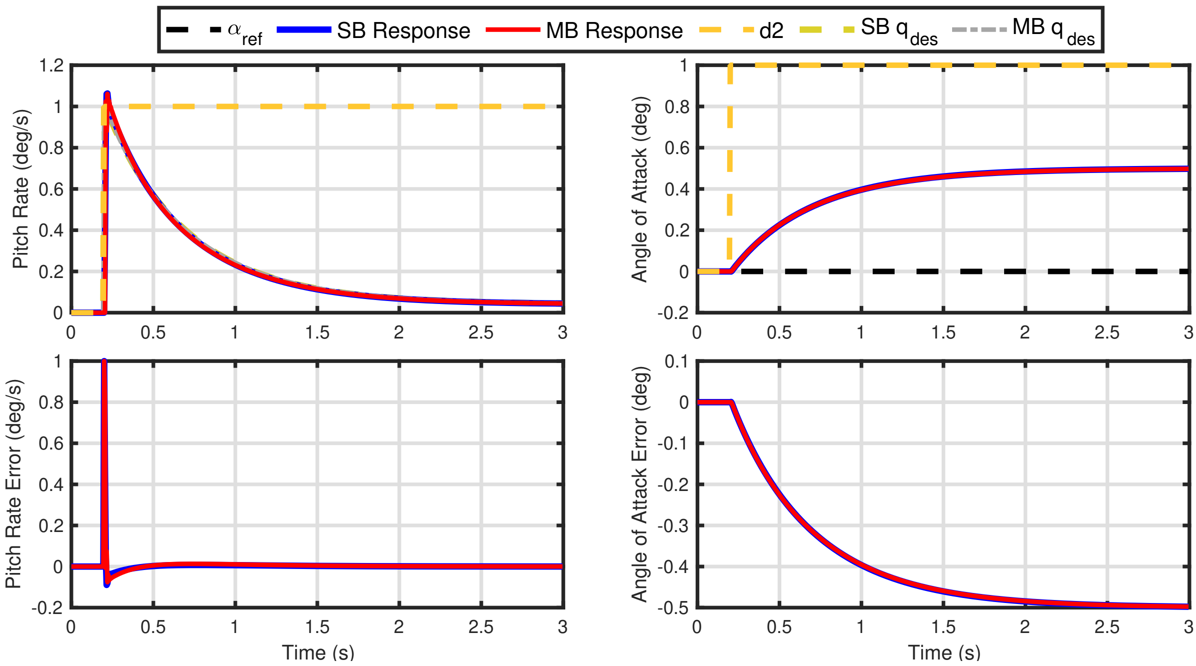


(b) System and Error Response to Outer Loop Disturbance

Figure 5.9: Response to Disturbances

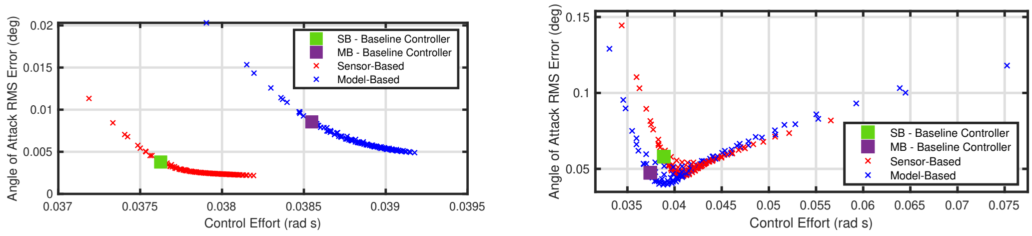


(a) Sensor Dynamics not Included (b) Sensor Dynamics Included

Figure 5.10: Time Domain Simulations with Various Gain Values

These calculations yield single values that the performance can be evaluated. In order to observe the step response for various gains, simulations are run within a gain limit such that gains are selected with linear spacing. The simulation time is determined to be 3 seconds since this time is sufficient to respond a step input and reach a steady state value. The gains that are used for disturbance rejection are selected as baseline values and the lower limit is set to half of these values and the upper values are three times of the values, $2.5 < K_{p1} < 15$ and $1 < K_{p1} < 6$. Simulation is repeated with 200 values and the results are shown in Fig. 5.10a with control effort in the x-axis and RMS error is in the y-axis. Sensor-Based INDI results are better than Model-Based even though they are relatively close to each other. This changes when sensors are included in the simulation which results Model-Based INDI to have better performance values. The results are given in Fig. 5.10b. One of the research questions is to compare the nominal performance of the methods. Fig. 5.10 presents this comparison and answers research question 3a. As expected nominal performances are close to each other. This helps a fair comparison when the methods are tested for robustness.

The results show that there is a global minimum within the range of gains such that the performance can be optimized. For the optimization, a cost function is set as

$$J = a \cdot \delta_E + b \cdot \epsilon_\alpha \tag{5.60}$$

The constants $a$ and $b$ are the weights for the criteria and $J$ is the overall cost. In order to equally weight the importance for this cost function $a = 1$ and $b = 1$ are selected. The optimization penalizes extra control effort and additional error and determines the gain values that these are minimized. Using the gains $K_{p1} = 5$ and $K_{p2} = 2$, the cost value for the Sensor-Based approach is 0.0437 and the optimization finds the gains as $K_{p1} = 8.77$ and $K_{p2} = 5.96$ which yields the cost value as 0.0428. As the weights of the cost function changes, different gains could be the optimum values. The upper boundary can be extended as well to obtain even more optimized results but this might cause undesirably high control deflection rates.

As it is seen in the Fig. 5.10a, additional dynamics impact the response of the system to be altered for the gain values. The optimum values that are selected for the system without sensors do not perform well for a system with sensors. The performances are shown in Fig. 5.11. Oscillations are introduced and the result is not desirable anymore. Therefore, it is essential to consider sensor dynamics when the gains are optimized. The same optimization procedure could be followed in order to find a new set of gains. Although, the controller can be adjusted such that knowledge of sensor dynamics is used for controller design.

The success of INDI controller mainly based on achievement of linearization loop in forming integrator dynamics. As it is shown in Fig. 5.7, additional dynamics causes deviation of inner loop from being integrator dynamics. The feedforward differentiator term can form a unity closed loop system without additional dynamics. This term can be adjusted to compensate additional sensor dynamics [90]. The effect of sensor dynamics on transfer function from virtual input $v_1$ to pitch rate $q$ is

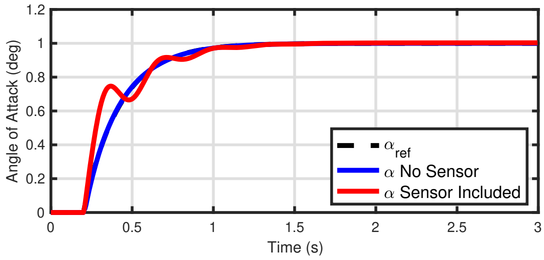


Figure 5.11: Performance Degradation Using Gains Optimized for System without Sensors on the System with Sensors

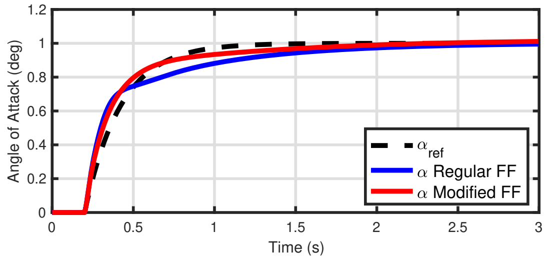


Figure 5.12: Effect of Modifiying Feedforward Term

$$TF_{v_1 \to q} = \frac{1/s}{1 + H_q(s)/s} \tag{5.61}$$

Feedforward term is designed as the inverse of the transfer function

$$F_r(s) = s + H_q(s) \tag{5.62}$$

where $s$ is the differentiator that has already been included. The derivative filter given in Eq. 5.38 is used to make the signals realizable. $H_q(s)$ is the pitch rate sensor dynamics. The improvement of this modification is shown in Fig. 5.12, where step response of angle attack is plotted. The cost function improves from 0.1036 to 0.0905. As the optimization is applied to this form of control structure, cost value decreases to 0.0772.

## 5.5. ROBUSTNESS ANALYSIS

There are various elements that affect the performance of control system. A robust system can handle those elements without a significant reduction in the performance. Initially, an indication on the robustness can be made based on the previous results. Different gains are used within a range to observe the change in the performance based on two design performance metrics. Those results are shown in Fig. 5.10. It is seen that when sensors are not included Sensor-Based INDI performance metrics are better than the Model-Based INDI. As the sensor dynamics are added in the simulation, Model-Based INDI in general performs better. There is no model mismatches hence the on-board model acts as perfect sensor. This shows the dependence of Sensor-Based INDI on sensors. As the sensors get perfect, better results are obtained.

Observation of different gains on the system performance also reveals another result that the selection of gains are more important for the Model-Based INDI. Sensor-Based INDI results are in compact region that the cost value does not change significantly. Model-Based INDI results spread more. This is shown with a 3-D plot in Fig. 5.13. Gains are in the X-Y axes and the cost value is in Z-axis. Maximum cost value of Model-Based INDI is 0.68, for Sensor-Based INDI, this value is 0.18.

A control system is desired to perform under uncertain and unexpected conditions such as time delays, parametric uncertainties and model mismatches. The range and likelihood of these conditions can be predicted at some level. Robust systems compensate uncertain conditions. In this section, ability of INDI methods to handle uncertain situations is investigated. This section answers research question 3b. The methods are expected to be robust against different issues. These issues are desired to be kept in the hybrid approach.

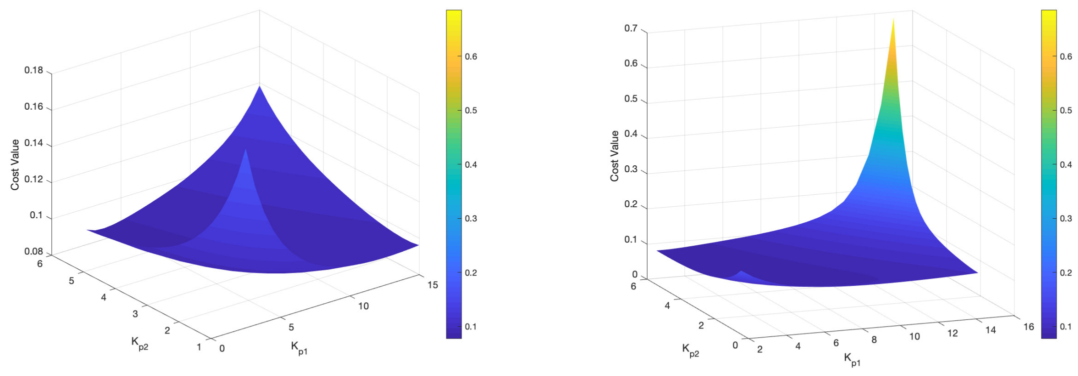

(a) Sensor-Based INDI

(b) Model-Based INDI

Figure 5.13: Change in Cost Value For Gains

### 5.5.1. TIME DELAYS

INDI control law calculated the next control input based on previous control input $u_0$ and state derivative $\dot{x}_0$. To obtain $u_0$ is relatively easy. The signal passes through the actuator dynamics. Modeling actuator dynamics give a good estimate of $u_0$. Another method is to measure control surface deflection. The second term, $\dot{x}_0$, is used by the control law after some process for instance noise filtering which causes time delays. To prevent time differences between these signals control law is updated as in Eq. 5.32. Asynchronous signals do not affect the performance of Model-Based INDI, because control law equations cancels control input feedback $u_0$. This subsection is dedicated to indicate the effect asynchronous signals and unexpected time delays on state derivative.

Depending on the time difference between the signals, unsynchronized system becomes unstable. The linearized transfer function has complex poles on the Right-Hand-Plane. Synchronizing the signals makes the inner linearization loop stable that eases the design of a controller and increases its performance. The poles shift to the stable region after the signals are synchronized.

A time-domain simulation is performed to observe the effect of additional time delay in the feedback signals. In this scenario control input is not delayed accordingly such that it is leading the state derivative. Pure time delay of 0.04 second is introduced to the system that corresponds to 8 time steps. Its effect on the performance of controllers are shown in Fig. 5.14a for Sensor-Based INDI and in Fig. 5.14b for Model-Based INDI. The delay that is introduced is the maximum delay that Sensor-Based INDI can handle before becoming unstable. Model-Based INDI is more tolerant to unsynchronized time delays. Its performance degrades very limited compared to Sensor-Based INDI.

In the previous case, unsynchronization is designed such that control signal is leading. The same simulation is performed with state derivative signal, $\dot{x}_0$, is leading. This is shown in figure Fig. 5.14d for Sensor-Based INDI. Even though, the oscillations in the response still exists, their amplitude is very small and decay quickly. This indicates that, when the control input is the lagging signal it does not have a severe affect. In practice, this is rarely the case because it is easier to obtain control input value compared to measurements.

Two approaches behave similar when the additional delay is synchronized. The system easily handles 0.04s of latency. This simulation is shown in Fig. 5.14c. It shows Sensor-Based and Model-Based controllers affected similarly from synchronous time delays.

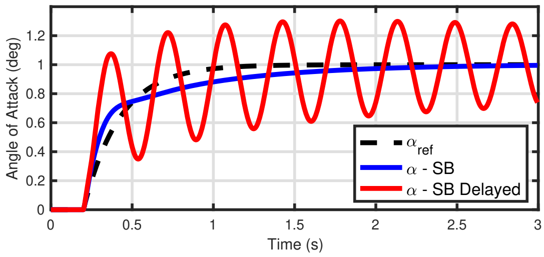


(a) Additional Delay on Measurement Signals - Control Input Unsynchronized - Sensor-Based INDI

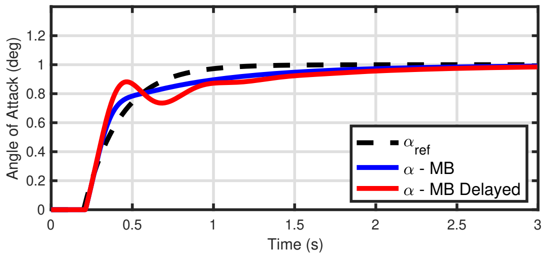


(b) Additional Delay on Measurement Signals - Control Input Unsynchronized - Model-Based INDI

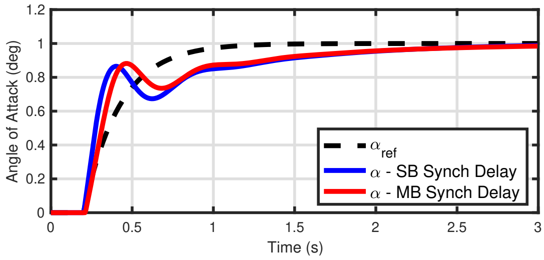


(c) Additional Synchronized Time Delay - Sensor-Based and Model-Based INDI

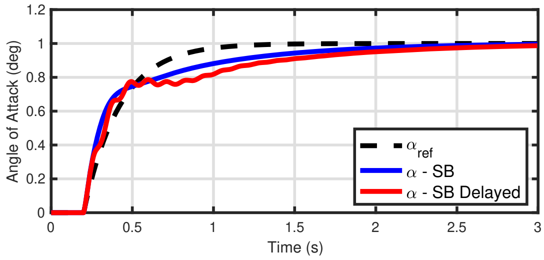


(d) Additional Delay on Control Input Feedback - Measurements Unsynchronized

Figure 5.14: Synchronization Related Time Domain Simulations

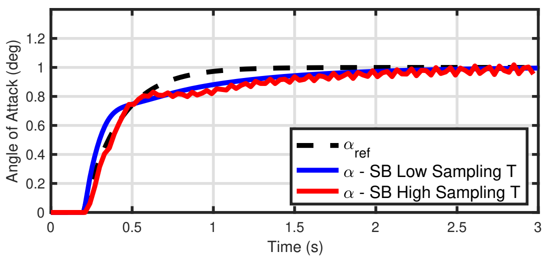


(a) Sensor-Based INDI

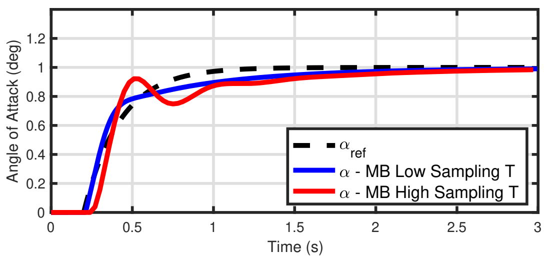


(b) Model-Based INDI

Figure 5.15: Effect of Increasing Sampling Time

### 5.5.2. SAMPLING TIME

An assumption in derivation of INDI controller states that the change of system states between each sampling time is negligible. This assumption is more accurate as the sampling time is small. If the next measurement reaches very late this assumption would not be correct anymore. In this subsection, tolerance of the methods to sampling time is investigated.

Initially, sampling time is set to 0.005 s which corresponds to 200 Hz. Sampling time is increased up to 0.03 s. Starting from this value Sensor-Based INDI becomes unstable whereas Model-Based stays in the stable region even though performance decreases as expected. The simulation results are shown in Fig. 5.15. Sensor-Based INDI results have oscillations and the amplitudes increase in time.

Based on the assumption 2 listed in Section 4.1, the state increment term has been eliminated from the INDI formulation. As the sampling time increases the increment increases as well. This term is included in order to observe the change in its value as the sampling time increases. When sampling time is 0.005 s, the maximum value of the term is 0.005° whereas for 0.03s of sampling time the value reaches at 0.5°. Considering the input is 1° this value is significant. In addition, this value increases

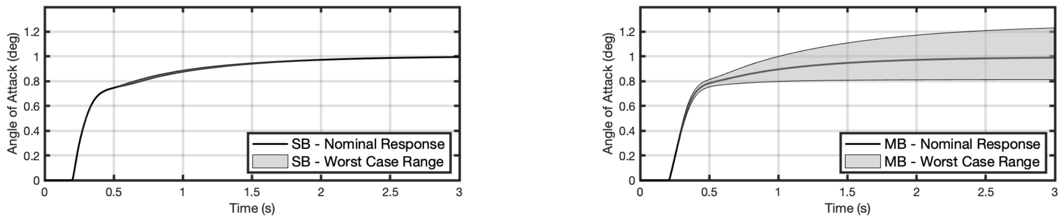


(a) Sensor-Based INDI

(b) Model-Based INDI

Figure 5.16: Performance under uncertain aerodynamic coefficients and control effectiveness, the parameters are assumed to have 5% uncertainty. The range of performance is shown in the figures

almost 10 times whereas sampling time is increased by 6 times.

### 5.5.3. MODEL MISMATCHES

One of the main motivations of INDI controllers to reduce the dependence on system model. Determination of aerodynamic coefficients is a time consuming process. Moreover, in case of structure damage or change aerodynamic coefficients are not reliable. Sensor-Based INDI only requires the control effectiveness of the control surfaces although, Model-Based INDI utilizes system related aerodynamic coefficients as well.

It is decided to observe performance of the control systems with the aerodynamic coefficients having 5% of maximum uncertainly. Therefore, the expectation is that the real values the system would encounter in a flight are between 5% less and 5% more of the values that are used to design the controllers. The performances are shown in Fig. 5.16. The graph includes the nominal performance and the boundary of worst case scenarios.

From the results of Sensor-Based INDI, the advantages of eliminating the use of model is apparent. Within the limit of uncertainty Sensor-Based INDI's performance is almost the same whereas Model-Based performance significantly changes and the range of expected performance is very broad compared to Sensor-Based.

Other sources of model mismatches are in parametric terms such as mass of the system or mass inertia. These terms are present in the dynamical equations given in Eq. 5.1 and Eq. 5.2. Both of the approaches can handle the uncertainties on these parameters as a simulation test is performed with 20% of uncertainty. The worst case and nominal performances are very close to each other and they are not distinguishable. For this reason, the response plots are shown here.

## 5.6. RESULTS AND DISCUSSION

The preliminary example is mainly fed from the studies in the literature. The issues that has been encountered are applied on the system and the literature is verified. In addition, it has been an opportunity to compare the performances of two approaches. First of all, it was shown that Model-Based control law is fundamentally same as NDI method depending on the selection of control increment. The way it has been formulated allows to use delayed control inputs to be increment which makes the formulation close to Sensor-Based INDI. This formulation is suitable for comparison and combination as hybrid approach.

To improve the control design several issues were handled. Initially, the control scheme that is generally used in the literature is used. This scheme includes two proportional gains that can be tuned. At first, disturbance rejection and error response for tracking purposes were considered and a pair of baseline control gains were decided. Control effort and tracking error were set to be performance criteria. The performance is improved by minimization of cost function that is the addition of the criteria. Another improvement was done by modifying feedforward dynamics which depends on the idea of making the linearization loop close to integrator dynamics as much as possible. These improvements increased the performance around 25% in the nominal conditions since the cost value reduces from 0.1036 to 0.0772.

The robustness analysis revealed how the performances differ for two approaches. The performance of the Model-Based INDI alters more based on the selection of proportional gains whereas for Sensor-Based INDI, performance metric stays within a much more narrow region. On the other side, performance of Sensor-Based INDI degrades when the assumption of perfect sensor measurement is eliminated. This result is expected since Sensor-Based INDI trades off dependence on the model with the sensors.

Both of the methods are capable of handling time delays in the feedback signals as long as the signals are synchronized. Model-Based INDI does not need synchronization of the signals since control increment cancels. Only 0.04 seconds of additional time delay in the state measurements leads Sensor-Based INDI to be unstable. The method is more tolerant for the control input time delay but this case is less likely in a real system. Moreover, high sampling rate of the measurements also causes instability for the Sensor-Based INDI whereas Model-Based INDI remains stable for the same sampling rate.

Lastly, it was shown that tracking performance of the Sensor-Based INDI is significantly superior of Model-Based INDI in existence of aerodynamic uncertainty. Only 5% of uncertainty resulted with 20% of steady state error whereas Sensor-Based INDI affected in a very negligible level.

# 6

# CONCLUSION

The thesis report presents the answers research questions 1 to 6. In this chapter, main results are concluded and the questions are revisited. It is discussed that to what extent the questions are answered.

This paper has presented a new approach of INDI by modifying the linearization loop via a complementary filter. The filter supplies an angular acceleration estimation based on sensor measurement and on-board model output. By formulating Hybrid INDI it is shown that the approach includes characteristics of both Model-Based INDI and Sensor-Based INDI. The fast response of on-board model is presented as the key feature for the elimination of drawbacks of sensor measurement delays. Hybrid INDI persists to be robust against model mismatches and external disturbances by utilizing low frequency characteristics of measurements.

The effectiveness of the Hybrid INDI has been demonstrated by two types of simulation analysis. The initial analysis considers a simple system and only the linearization loop of INDI is investigated. This analysis compares Sensor-Based INDI and Hybrid INDI in terms of tracking performance in nominal conditions, and in the existence of measurement delays. Consequently, it is shown that Hybrid INDI yields less overshoot and faster settling time when the measurements delays are underestimated. Further details are presented about the synchronization filter, which is given as a modified transfer function of the complementary filtering of sensor measurement. Moreover, change in closed loop characteristics with respect to filter gains and measurement delays are presented.

This thesis is validated by designing an attitude controller for the F-16 aircraft using Hybrid INDI, and showing its robustness against measurement delays and its ability to maintain the sensor-based nature of INDI. Simulation results indicated that Hybrid INDI loses very little tracking performance in nominal conditions. This is compensated by having low control effort. Simulation scenarios with uncertainties in aerodynamic coefficient indicates that the on-board model of Hybrid INDI does not have to be accurate for the control system to be robust against model mismatches. This finding is strengthened by the successful rejection of gust disturbance. Finally, measurement delays are introduced and the aircraft is commanded by doublets of pitch angle and roll angle. As a result, Hybrid INDI insignificantly deviates from the nominal performance whereas the performance of Sensor-Based INDI becomes undesirable due to oscillations in the commanded channel as well as other channels.

1. *What is the state of the art of INDI?*

   The state of the art of INDI has been reviewed in Chapter 4. The chapter examines the method in various perspectives. Some studies focus on theoretical development and some mainly considers robustness of the method. The method has been introduced in 2010 and within this time period, it has been applied many kinds of aerial vehicles. Literature review enlightens the issues of the method. Most of the issues are investigated in the preliminary study. In addition, assumptions of the INDI are highlighted and throughout the study, the assumptions have been examined to observe whether they are valid or weak under certain situations.

2. *How can Model-Based INDI be structured?*

   Model-Based INDI has been formulated in Section 4.3. The formulation is based on obtaining state derivative from an on-board model instead of measurement. The final control law is the same as NDI control law, which is also a model dependent control law. It is highlighted that no measurement is needed to be differentiated for Model-Based INDI, which is one of the main advantages of utilizing the system model.

   (a) *How should the synchronization method be modified?*

      In Section 4.3, it is shown that the control input term disappears. Therefore, there is no need for supplying control input feedback and thus no need for synchronization.

   (b) *How should the noise filter be modified?*

      Noise filtering issue is treated in subsection 5.3.3. It is shown that differentiation causes amplification in the amplitude of the noise thus Sensor-Based INDI needs a more advanced sensor filtering. A second-order noise filter is used for Sensor-Based INDI. For Model-Based INDI, first-order filter is sufficient for noise reduction.

   (c) *What other considerations should be taken for disturbance rejection or tracking performance?*

      A cost function is presented in Section 5.4 which considers the control effort that is spend by the actuators and root mean square of the tracking error. These perspectives are determined to be sufficient to derive fair control gains. The simulation results in Section 5.4 show that similar disturbance rejection and tracking performance are achieved in nominal conditions, although this changes as the model mismatches are introduced in Section 5.5.

3. *How do Model-Based INDI and Sensor-Based INDI perform compared to each other?*

   (a) *What are the differences in the nominal performance?*

      The nominal performances are compared in two ways. One with sensor dynamics included, another without the sensor dynamics. Both of the method has comparable nominal performances. The performance values are shown in Fig. 5.10a. As expected inclusion of sensor dynamics affect the performance of Sensor-Based INDI more than Model-Based INDI. This is due to achieving the state derivative values with a time lag.

   (b) *How do the methods perform in robustness analysis?*

      There has been various time domain simulations to compare the methods for different situations. In Section 5.5, robustness of the methods against, aerodynamic uncertainties, time delays and sampling time are tested. The results are summarized in Section 5.6, stating that the model mismatches, even in small percentages, significantly degrades the performance of Model-Based INDI. On the other side, it is shown that measurement delays cause oscillations in tracking performance of Sensor-Based INDI. These results are especially important for the design of Hybrid INDI.

4. *What are the existing methods of hybrid controllers?*

   Hybrid controllers are reviewed in Section 4.4. The main focus has been in the methods that are applied for aerospace vehicles and two of the promising solutions are discussed.

   (a) *What are the problems that are encountered with combining the control systems?*

   One of the considered hybridization method has been switching between control approaches. Guaranteeing the stability has been regarded as the main challenge of such controllers. Especially, switching within the methods causes jumps or irregularities in the control input at the instance of switching. Another issue is to determine the switching algorithm. Occasionally, the system oscillates around the commanded value, this causes the switching from one of the approaches to another repeatedly which yields more oscillations. Due to these problems a frequency based combination is selected which fuses the approaches based on their frequency components.

   (b) *Can the existing methods of hybrid controllers be applied to form Hybrid INDI?*

   As the hybrid approach an existing solution is determined to be the best option. The angular acceleration estimation based on a specific complementary filtering is used. Although this approach is not presented as a control law, it shown to be suitable for INDI applications.

5. *How can Model-Based INDI and Sensor-Based INDI be combined into a hybrid method and what are the considerations of the combination?*

   (a) *How is the information from processed sensor signal integrated with the one coming from the onboard model?*

   The preliminary study results show the success and failure of the methods for various conditions. Both of the methods perform well in nominal conditions; therefore, Hybrid INDI focuses on the robustness issues. Sensor-Based and Model-Based approaches are formulated to be similar to each other for easier combination. Hybrid INDI includes beneficial frequency domain of the methods. The bandwidth of the filter is designed based on noise filtering, response time, robustness against measurement delays.

   (b) *How are the signals synchronized?*

   It is shown that Model-Based INDI is not affected by unsynchronized signals. Hybrid INDI is designed based on this feature of the method. Model-Based INDI can respond instantly to the given commands and does not have to wait for the measurement. As shown in Chapter 2, for Hybrid INDI, instead of using noise filtering, complementary filter function that is applied to angular rate measurement is used. This function is integrated and zero of it is removed to supply sufficient phase lag.

   (c) *What is the effect of hybridization to stability margins?*

   It is shown that the method is stable for higher range of measurement delays. As shown in Chapter 2, for F-16 aircraft application, Hybrid INDI stays in the stable region up to 0.13 s of time delay whereas Sensor-Based INDI becomes unstable with 0.07 s of time delay. The stability of the method does not affected by uncertainties in aerodynamic coefficient maintains.

6. *Which of the challenges of INDI is solved by Hybrid INDI and what are the challenges of Hybrid INDI?*

The performances of all three approaches are compared. The results are presented in Chapter 2. Hybrid INDI is found to be more robust for sensor faults and the degradation in nominal performance is negligible. Measurement delays which is seen as one of the main challenges of INDI can be compensated by using Hybrid INDI. The noise filtering capability of Hybrid INDI is emphasized as the one of the main restrictions of the method. To achieve the same level of noise filtering, a lower bandwidth is required to be set for the complementary filter, although this causes the response time to be slower. A trade-off between noise filtering and response time has to made for good performance.

# 7
# Recommendations and Future Research

Hybrid INDI is not without drawbacks which future studies might overcome. One of the main limitations of Hybrid INDI approach is the noise filtering capability. The bandwidth of the filter design is determined based on the trade-off between the noise filtering and fast response. To achieve the same noise filtering of Sensor-Based INDI, the bandwidth of the complementary filter is required to be set to lower value which slows the response of the system dramatically. The noisy angular acceleration estimation is directly reflected to the actuator. The actuator itself filters the noise as well and the magnitude of the noise is very low such that the control effort is not affected. However, in real life applications, this limitation might lead to actuator failures. A future study can investigate the importance of the excess of noise and focus on mitigating it.

Different hybridization or estimation techniques could be used for Hybrid INDI. One possible modification that is worth investigating is to use angular accelerometers instead of gyroscopes. In this study, an angular acceleration estimation method is used for Hybrid INDI since this method has advantages such as being simple and easily adaptable to system requirements. The use of accelerometers can be implemented with a slight change in the complementary filter. A future study may consider Kalman filtering as one of the possible methods which exploits both measurement and model simultaneously.

A variant of Hybrid INDI is presented as a fault-tolerant system. The approach includes a logical switch that is fed by an FDI algorithm, which can switch the system to become Model-Based INDI by avoiding sensor measurement innovation. This variant is not tested in the F-16 aircraft application because of a lack of FDI algorithm. A future study may implement an FDI algorithm to show the applicability of this feature on an aerospace system.

This study has shown that an on-board model can be used without introducing robustness problems. Additional benefits of on-board models can be used to achieve better performance by Hybrid INDI. One of the possible improvements is implementation of online delay estimation. The comparison of measurement with the model output supply a clue for the measurement delays. However, for accurate delay detection, high computational power and an accurate model are required. By feeding this estimated delay value, unexpected measurement delays can be handled.

It is recommended to have in depth analysis of the effects of aerodynamic uncertainties on Hybrid INDI. This study shows that the approach is robust against aerodynamic uncertainties. The investigation is limited with only changes in magnitudes but not in signs. Having an opposite sign of aerodynamic coefficient in the on-board model can lead to the undesirable performance. A following study could investigate whether incorrect coefficient signs cause degradation in the robustness against measurement delays.

One of the assumptions that is held through the study is the accurate knowledge of control surface deflection. This assumption is not valid in real life applications. In case of unknown delays in the measurement of actuator deflection, the synchronization filter causes the incremented control input to belong to a previous time. Previous papers studied these effects for Sensor-Based INDI, which have not been addressed for Hybrid INDI in this study. The investigation of these effects for Hybrid INDI is left for a future study.

The study considers a single operating point of F-16 aircraft. Even though the results are expected to be valid over the flight envelope, this expectation can be verified in a further study by selecting various operating points. Lastly, it is observed that in case of delayed measurements, Sensor-Based INDI shows coupling between attitude channels. The explanation of this phenomenon is also left to be investigated further.

# A

# NUMERICAL DIFFERENTIATION

The numerical differentiation techniques developed from Taylor series approximation, for the value at $f(t_{i-1})$ the expansion is

$$f(t_{i-1}) \cong f(t_i) + f'(t_i)(t_{i-1} - t_i) + \frac{f''(t_i)}{2!}(t_{i-1} - t_i)^2 + ... \tag{A.1}$$

where $t_{i-1} - t_i = -\Delta t$ is the time increment. This equation yield the derivative at time step $t_i$ as

$$f'(t_i) = \frac{f(t_{i-1}) - f(t_i)}{-\Delta t} + O(h) = \frac{f(t_i) - f(t_{i-1})}{\Delta t} + O(\Delta t) \tag{A.2}$$

The $O(\Delta t)$ is the error term that symbolizes that the error is related to the time step. To derive the approximation with three point, first find the second derivative approximation;

$$f(t_{i-2}) \cong f(t_i) + f'(t_i)(t_{i-2} - t_i) + \frac{f''(t_i)}{2!}(t_{i-2} - t_i)^2 + ... \tag{A.3}$$

Multiplying Eq. A.1 by two and subtracting from this equation yields

$$f(t_{i-2}) - 2f(t_{i-1}) = -f(t_i) + f''(t_i)(\Delta t)^2 + ... \tag{A.4}$$

Solving this for the second derivative:

$$f''(t_i) = \frac{f(t_i) - 2f(t_{i-1}) + f(t_{i-2})}{(\Delta t)^2} + O(\Delta t) \tag{A.5}$$

An additional term for the first order derivative approximation in Eq. A.2 is written by addition of second derivative term as

$$f'(t_i) = \frac{f(t_i) - f(t_{i-1})}{\Delta t} + \frac{f''(t_i)}{2}\Delta t + O(\Delta t)^2 \tag{A.6}$$

The order of error is changed to be $O(\Delta t)^2$ and inserting the second derivative approximation to this equation:

$$f'(t_i) = \frac{f(t_i) - f(t_{i-1})}{\Delta t} + \frac{f(t_i) - 2f(t_{i-1}) + f(t_{i-2})}{2(\Delta t)} + O(\Delta t)\Delta t + O(\Delta t^2) \tag{A.7}$$

$$f'(t_i) = \frac{3f(t_i) - 4f(t_{i-1}) + f(t_{i-2})}{2\Delta t} + O(\Delta t^2) \tag{A.8}$$

The order of error is $O(\Delta t)^2$ since the multiplication of $O(\Delta t)\Delta t$ is the second order as well. Therefore, using additional point increases the accuracy.

Using additional points amplifies noise as well. Assume a randomly distributed variable with mean $\mu = 0$ and variance $\sigma^2 = 1$ is added on a smooth function. Let at time $t_i$ the added noise is $n_i$. Two-point differentiation yields;

$$f'(t_i) = \frac{f(t_i) + n_i - f(t_{i-1}) - n_{i-1}}{\Delta t} + O(\Delta t) \tag{A.9}$$

In order to show the effect of noise contribution on the derivation, noise terms are added up

$$n_a = \frac{n_i - n_{i-1}}{\Delta t} \tag{A.10}$$

The terms $n_i$ and $n_{i-1}$ are both linearly independent random variables with same characteristic as the noise. A linear function of random variable yields the variance as $\text{var}(aX) = a^2\text{var}(X)$. Therefore expected value would remain at 0, but the variance of the difference of the random variables is $(\sigma_i^2 + \sigma_{i-1}^2 /)(\Delta t)^2$. Hence the noise contribution is a random variable with 0 mean and variance is $2/(\Delta t)^2$.

For three-point differentiation the noise contribution is

$$n_a = \frac{3n_i - 4n_{i-1} + n_{i-2}}{2\Delta t} \tag{A.11}$$

This random variable has zero mean as well, we use the variance relationship $\text{var}(aX) = a^2\text{var}(X)$, therefore variance happens to be $(3^2 * \text{var}(n) + 4^2 * \text{var}(n) + 1^1 * \text{var}(n))/(2 * \Delta t)^2$. This confirms that the noise contribution is amplified, as more numbers are used for differentiation. Three-point differentiation yields 3.25 times more variance than two-point method. Moreover, as the time step decreases this contribution increases. The contribution of time step is quite significant. For a smooth signal without noise, as time step decreases the error decreases as well but when considering noise, the error is amplified by a factor of $1/\Delta t$ and this value is very large for small time step. Therefore, noisy signals should be first smoothed then differentiated or filtered after differentiated.

# BIBLIOGRAPHY


[1] Space Exploration Technologies Corp., *Falcon heavy & starman,* (2018), online: accessed 17-March-2020.

[2] Collins Aerospace, *Air data systems,* (2020), online: accessed 17-March-2020.

[3] *Flutter Free FLight Envelope eXpansion for ecOnomical Performance improvement (FLEXOP),* (2019), Horizon 2020 research and innovation programme of the European Union, grant agreement No 636307. `https://flexop.eu/`.

[4] R. C. van't Veld, E.-J. van Kampen, and Q. P. Chu, *Stability and robustness analysis and improvements for incremental nonlinear dynamic inversion control,* AIAA Guidance, Navigation, and Control Conference, 2018 (2018), 10.2514/6.2018-1127.

[5] E. J. Smeur, Q. P. Chu, and G. C. De Croon, *Adaptive incremental nonlinear dynamic inversion for attitude control of micro air vehicles,* Journal of Guidance, Control, and Dynamics **39**, 450 (2016).

[6] X. Liu and S. An, *Smooth Switching Controller Design for Multiobjective Control Systems and Applications,* Journal of Aerospace Engineering **29**, 1 (2016).

[7] P. K. Menon and E. J. Ohlmeyer, *Integrated design of agile missile guidance and autopilot systems,* Control Engineering Practice **9**, 1095 (2001).

[8] F. Grondman, G. H. Looye, R. O. Kuchar, Q. P. Chu, and E.-J. van Kampen, *Design and flight testing of incremental nonlinear dynamic inversion based control laws for a passenger aircraft,* AIAA Guidance, Navigation, and Control Conference, 2018 **0** (2018), 10.2514/6.2018-0385.

[9] B. Stevens, F. Lewis, and E. Johnson, *Aircraft Control and Simulation: Dynamics, Controls Design, and Autonomous Systems* (Wiley, 2015).

[10] J. Foust, *SpaceX's Space-Internet Woes,* IEEE Spectrum **56**, 50 (2019).

[11] D. McLean, *Automatic Flight Control Systems*, Prentice-Hall international series in systems and control engineering (Prentice Hall, 1990).

[12] S. Sieberling, Q. P. Chu, and J. A. Mulder, *Robust flight control using incremental nonlinear dynamic inversion and angular acceleration prediction,* Journal of Guidance, Control, and Dynamics **33**, 1732 (2010).

[13] J.-F. Magni, S. Bennani, and J. Terlouw, *Robust flight control: a design challenge*, Vol. 110 (Springer, Berlin, Heidelberg, 1997).

[14] T. Lombaerts, *Fault Tolerant Flight Control A Physical Model Approach* (Cambridge University Press, Delft, 2010) arXiv:1011.1669 .

[15] B. Etkin, *Turbulent wind and its effect on flight,* Journal of Aircraft **18**, 327 (1981).

[16] W. Xuerui, *Incremental Sliding Mode Flight Control (PhD thesis)* (TU Delft, 2019).

[17] C. Edwards, T. Lombaerts, H. Smaili, *et al.*, *Fault tolerant flight control*, Lecture Notes in Control and Information Sciences, Vol. 399 (Springer-Verlag Berlin Heidelberg, 2010) pp. 1–560.

[18] F. W. Burcham, T. a. Maine, C. G. Fullerton, and L. D. Webb, *Development and Flight Evaluation of an Emergency Digital Flight Control System Using Only Engine Thrust on an F-15 Airplane,* NASA Technical Paper (1996).

[19] P. A. Scholten, M. M. V. Paassen, Q. P. Chu, and M. Mulder, *A Variable Stability In-Flight Simulation System using Incremental Non-Linear Dynamic Inversion,* AIAA Scitech 2020 Forum , 1 (2020).

[20] L. Blackmore, *Autonomous precision landing of space rockets,* in *Frontiers of Engineering: Reports on Leading-Edge Engineering from the 2016 Symposium* (National Academies Press, 2017).

[21] S. A. Jacklin, *Closing the certification gaps in adaptive flight control software,* AIAA Guidance, Navigation and Control Conference and Exhibit , 1 (2008).

[22] S. Bhattacharyya, D. Cofer, D. Musliner, J. Mueller, and E. Engstrom, *Certification considerations for adaptive systems,* 2015 International Conference on Unmanned Aircraft Systems, ICUAS 2015 , 270 (2015).

[23] D. J. Leith and W. E. Leithead, *Survey of gain-scheduling analysis and design,* International Journal of Control **73**, 1001 (2000).

[24] M. Spillman, P. Blue, S. Banda, and L. Lee, *A Robust Gain-Scheduling Example Using Linear Parametervarying Feedback,* (1996).

[25] A. Helmersson, *$\mu$ Synthesis and Lft Gain Scheduling With Real Uncertainties,* International Journal of Robust and Nonlinear Control **8**, 631 (1998).

[26] J. S. Shamma and M. Athans, *Gain scheduling: potential hazards and possible remedies,* IEEE Control Systems **12**, 101 (1992).

[27] M. Oosterom and R. Babuška, *Design of a gain-scheduling mechanism for flight control laws by fuzzy clustering,* Control Engineering Practice **14**, 769 (2006).

[28] R. Brockett, *Feedback Invariants for Nonlinear Systems *,* IFAC Proceedings Volumes **11**, 1115 (1978).

[29] A. Isidori, A. J. Krener, and S. Monaco, *Nonlinear Decoupling via Feedback: A Differential Geometric Approach,* IEEE Transactions on Automatic Control **26**, 331 (1981).

[30] A. J. Krener, *Feedback linearization,* in *Mathematical Control Theory*, edited by J. Baillieul and J. C. Willems (Springer New York, New York, NY, 1999) pp. 66–98.

[31] J.-J. E. Slotine and W. Li, *Applied nonlinear control*, Vol. 199 (Prentice Hall Inc. Englewood Cliffs, NJ, 1991).

[32] A. Isidori, *Nonlinear Control Systems II* (Springer-Verlag London, 1995).

[33] S. Sastry, *Nonlinear Systems: Analysis, Stability, and Control* (Springer-Verlag New York, 1999).

[34] D. J. Bugajski, D. F. Enns, and M. R. Elgersma, *A dynamic inversion based control law with application to the high angleof-attack research vehicle,* Guidance, Navigation and Control Conference, 1990 , 826 (1990).

[35] Y. Ochi and K. Kanai, *Design of restructurable flight control systems using feedback linearization,* Journal of Guidance, Control, and Dynamics **14**, 903 (1991).

[36] S. A. Snell, D. F. Enns, and W. L. Garrard, *Nonlinear inversion flight control for a supermaneuverable aircraft,* Guidance, Navigation and Control Conference, 1992 **15**, 808 (1992).

[37] D. Enns, D. Bugajski, R. Hendrick, and G. Stein, *Dynamic inversion: An evolving methodology for flight control design,* International Journal of Control **59**, 71 (1994).

[38] J. Rajput and Z. Weiguo, *Fundamental methodologies for control of nonlinear nonminimum-phase systems: An overview,* Proceedings of the Institution of Mechanical Engineers. Part I: Journal of Systems and Control Engineering **228**, 553 (2014).

[39] R. R. Da Costa, Q. P. Chu, and J. A. Mulder, *Reentry flight controller design using nonlinear dynamic inversion,* Journal of Spacecraft and Rockets **40**, 64 (2003).

[40] C. J. Schumacher, P. P. Khargoneka, and N. H. McClamroch, *Stability analysis of dynamic inversion controllers using time-scale separation,* 1998 Guidance, Navigation, and Control Conference and Exhibit , 1217 (1998).

[41] J. Reiner, G. J. Balas, and W. L. Garrard, *Flight control design using Robust dynamic inversion and time-scale separation,* Automatica **32**, 1493 (1996).

[42] P. R. Smith, *A simplified approach to nonlinear dynamic inversion based flight control,* 23rd Atmospheric Flight Mechanics Conference , 762 (1998).

[43] D. Ito, D. T. Ward, and J. Valasek, *Robust dynamic inversion controller design and analysis for the X-38,* AIAA Guidance, Navigation, and Control Conference and Exhibit (2001), 10.2514/6.2001-4380.

[44] S. Juliana, Q. P. Chu, J. A. Mulder, and T. J. Van Baten, *The analytical derivation of non-linear dynamic inversion control for parametric uncertain system,* Collection of Technical Papers - AIAA Guidance, Navigation, and Control Conference **1**, 342 (2005).

[45] H. P. Lee, S. E. Reiman, C. H. Dillon, and H. M. Youssef, *Robust nonlinear dynamic inversion control for a hypersonic cruise vehicle,* Collection of Technical Papers - AIAA Guidance, Navigation, and Control Conference 2007 **4**, 3380 (2007).

[46] R. Hindman and W. M. Shell, *Missile autopilot design using adaptive nonlinear dynamic inversion,* Proceedings of the American Control Conference **6**, 3918 (2005).

[47] E. De Weerdt, E. Van Kampen, D. Van Gemert, Q. P. Chu, and J. A. Mulder, *Adaptive nonlinear dynamic inversion for spacecraft attitude control with fuel sloshing,* AIAA Guidance, Navigation and Control Conference and Exhibit , 1 (2008).

[48] P. Smith and A. Berry, *Flight test experience of a non-linear dynamic inversion control law on the VAAC harrier,* Atmospheric Flight Mechanics Conference , 132 (2000).

[49] B. J. Bacon and A. J. Ostroff, *Reconfigurable flight control using nonlinear dynamic inversion with a special accelerometer implementation,* AIAA Guidance, Navigation, and Control Conference and Exhibit (2000), 10.2514/6.2000-4565.

[50] B. J. Bacon, A. J. Ostroff, and S. M. Joshi, *Reconfigurable NDI controller using inertial sensor failure detection & isolation,* IEEE Transactions on Aerospace and Electronic Systems **37**, 1373 (2001).

[51] H. B. Chen and S. G. Zhang, *Robust dynamic inversion flight control law design,* 2008 2nd International Symposium on Systems and Control in Aerospace and Astronautics, ISSCAA 2008 , 1 (2008).

[52] C. Cakiroglu, E.-J. Van Kampen, and Q. P. Chu, *Robust incremental nonlinear dynamic inversion control using angular accelerometer feedback,* AIAA Guidance, Navigation, and Control Conference, 2018 (2018), 10.2514/6.2018-1128.

[53] X. Wang, E.-J. van Kampen, Q. P. Chu, and P. Lu, *Stability Analysis for Incremental Nonlinear Dynamic Inversion Control,* Journal of Guidance, Control, and Dynamics **42**, 1116 (2019).

[54] S. A. Raab, J. Zhang, P. Bhardwaj, and F. Holzapfel, *Consideration of Control Effector Dynamics and Saturations in an Extended INDI Approach,* in *AIAA Aviation 2019 Forum*, June (American Institute of Aeronautics and Astronautics, Reston, Virginia, 2019) pp. 1–13.

[55] P. Simplício, M. Pavel, E. van Kampen, and Q. Chu, *An acceleration measurements-based approach for helicopter nonlinear flight control using Incremental Nonlinear Dynamic Inversion,* Control Engineering Practice **21**, 1065 (2013).

[56] P. Acquatella B., W. van Ekeren, and Q. P. Chu, *PI(D) tuning for Flight Control Systems via Incremental Nonlinear Dynamic Inversion,* IFAC-PapersOnLine **50**, 8175 (2017), arXiv:1701.08981 .

[57] X. Wang, E.-J. Van Kampen, and Q. P. Chu, *Gust load alleviation and ride quality improvement with incremental nonlinear dynamic inversion,* AIAA Atmospheric Flight Mechanics Conference, 2017 , 1 (2017).

[58] X. Wang, E.-J. Van Kampen, Q. P. Chu, and R. De Breuker, *Flexible aircraft gust load alleviation with incremental nonlinear dynamic inversion,* Journal of Guidance, Control, and Dynamics **42**, 1519 (2019).

[59] E. J. Smeur, G. C. De Croon, and Q. P. Chu, *Gust disturbance alleviation with incremental nonlinear dynamic inversion,* IEEE International Conference on Intelligent Robots and Systems **2016-Novem**, 5626 (2016).

[60] E. J. Smeur, G. C. de Croon, and Q. P. Chu, *Cascaded incremental nonlinear dynamic inversion for MAV disturbance rejection,* Control Engineering Practice **73**, 79 (2018), arXiv:1701.07254 .

[61] P. B. Acquatella, W. Falkena, E.-J. Van Kampen, and Q. P. Chu, *Robust nonlinear spacecraft attitude control using incremental nonlinear dynamic inversion,* AIAA Guidance, Navigation, and Control Conference 2012 (2012), 10.2514/6.2012-4623.

[62] E. N. Johnson and A. J. Calise, *Pseudo-Control Hedging : a New Method for Adaptive Control,* Advances in Navigation Guidance and Control Technology Workshop (2000).

[63] F. Binz and D. Moormann, *Actuator Modeling for Attitude Control Using Incremental Nonlinear Dynamic Inversion,* 11th International Micro Air Vehicle Competition and Conference , 25 (2019).

[64] J. R. Azinheira, A. Moutinho, and J. R. Carvalho, *Lateral Control of Airship with Uncertain Dynamics using Incremental Nonlinear Dynamics Inversion,* IFAC-PapersOnLine **48**, 69 (2015).

[65] F. Binz, T. Islam, and D. Moormann, *Attitude control of tiltwing aircraft using a wing-fixed coordinate system and incremental nonlinear dynamic inversion,* International Journal of Micro Air Vehicles **11** (2019), 10.1177/1756829319861370.

[66] N. B. Silva, J. V. Fontes, R. S. Inoue, and K. R. Branco, *Dynamic Inversion and Gain-Scheduling Control for an Autonomous Aerial Vehicle with Multiple Flight Stages,* Journal of Control, Automation and Electrical Systems **29**, 328 (2018).

[67] T. Lombaerts, J. Kaneshige, S. Schuet, B. L. Aponso, K. H. Shish, and G. Hardy, *Dynamic Inversion based Full Envelope Flight Control for an eVTOL Vehicle using a Unified Framework,* in *AIAA Scitech 2020 Forum*, January (American Institute of Aeronautics and Astronautics, Reston, Virginia, 2020) pp. 1–30.

[68] G. Di Francesco, E. D'Amato, and M. Mattei, *INDI control with direct lift for a tilt rotor UAV,* IFAC-PapersOnLine **28**, 156 (2015).

[69] G. D. Francesco and M. Mattei, *Modeling and incremental nonlinear dynamic inversion control of a novel unmanned tiltrotor,* Journal of Aircraft **53**, 73 (2016).

[70] Z. Liu, J. Guo, M. Li, S. Tang, and X. Wang, *VTOL UAV transition maneuver using incremental nonlinear dynamic inversion,* International Journal of Aerospace Engineering **2018** (2018), 10.1155/2018/6315856.

[71] J. Zhang, J. Wang, F. Zhang, and F. Holzapfel, *Modeling and incremental nonlinear dynamic inversion control for a highly redundant flight system,* AIAA Scitech 2019 Forum , 1 (2019).

[72] P. Lu, E.-J. van Kampen, C. de Visser, and Q. P. Chu, *Aircraft fault-tolerant trajectory control using Incremental Nonlinear Dynamic Inversion,* Control Engineering Practice **57**, 126 (2016).

[73] S. Zhang and Q. Meng, *An anti-windup INDI fault-tolerant control scheme for flying wing aircraft with actuator faults,* ISA Transactions **93**, 172 (2019).

[74] S. Sun, L. Sijbers, X. Wang, and C. De Visser, *High-Speed Flight of Quadrotor Despite Loss of Single Rotor,* IEEE Robotics and Automation Letters **3**, 3201 (2018).

[75] S. Sun, X. Wang, Q. Chu, and C. de Visser, *Incremental Nonlinear Fault-Tolerant Control of a Quadrotor with Complete Loss of Two Opposing Rotors,* arXiv preprint (2020), arXiv:2002.07837 .

[76] Y. Beyer, A. Kuzolap, M. Steen, J. H. Diekmann, and N. Fezans, *Adaptive nonlinear flight control of STOL-aircraft based on incremental nonlinear dynamic inversion,* 2018 Modeling and Simulation Technologies Conference (2018), 10.2514/6.2018-3257.

[77] P. Bhardwaj, V. S. Akkinapalli, J. Zhang, S. Saboo, and F. Holzapfel, *Adaptive augmentation of incremental nonlinear dynamic inversion controller for an extended f-16 model,* AIAA Scitech 2019 Forum , 1 (2019).

[78] E. Tal and S. Karaman, *Accurate Tracking of Aggressive Quadrotor Trajectories Using Incremental Nonlinear Dynamic Inversion and Differential Flatness,* Proceedings of the IEEE Conference on Decision and Control **2018-Decem**, 4282 (2019), arXiv:1809.04048 .

[79] T. S. Pollack, G. H. Looye, and F. L. van der Linden, *Design and flight testing of flight control laws integrating incremental nonlinear dynamic inversion and servo current control,* AIAA Scitech 2019 Forum , 1 (2019).

[80] S. A. Raab, J. Zhang, P. Bhardwaj, and F. Holzapfel, *Proposal of a unified control strategy for vertical take-off and landing transition aircraft configurations,* 2018 Applied Aerodynamics Conference (2018), 10.2514/6.2018-3478.

[81] L. G. Sun, C. C. de Visser, Q. P. Chu, and W. Falkena, *A hybrid sensor based backstepping control approach with its application to fault-tolerant flight,* AIAA Guidance, Navigation, and Control (GNC) Conference (2013), 10.2514/6.2013-4777.

[82] N. McClamroch and I. Kolmanovsky, *Performance benefits of hybrid control design for linear and nonlinear systems,* Proceedings of the IEEE **88**, 1083 (2000).

[83] Z. Sun and S. S. Ge, *Analysis and synthesis of switched linear control systems,* Automatica **41**, 181 (2005).

[84] B. Lu and F. Wu, *Switching-based fault-tolerant control for an F-16 aircraft with thrust vectoring,* Proceedings of the IEEE Conference on Decision and Control , 8494 (2009).

[85] R. T. Reichert, *Dynamic scheduling of modern-robust-control autopilot designs for missiles,* IEEE Control Systems **12**, 35 (1992).

[86] R. A. Hull, D. Schumacher, and Z. Qu, *Design and evaluation of robust nonlinear missile autopilots from a performance perspective,* Proceedings of the American Control Conference **1**, 189 (1995).

[87] E. R. Van Oort, L. Sonneveldt, Q. P. Chu, and J. A. Mulder, *Modular adaptive input-to-state stable backstepping of a nonlinear missile model,* Collection of Technical Papers - AIAA Guidance, Navigation, and Control Conference 2007 **3**, 3249 (2007).

[88] J. C. Terlouw, S. Scala, E. Muir, D. Moormann, P. Lambrechts, R. Hyde, S. Bennani, and J. Schuring, *Technial Publication TP-088-3, Group for Aeronautical Research and technology in EURope GARTEUR-FM(AG08),* Tech. Rep. (GARTEUR, 1996).

[89] E. Mooij, *Robust Control of a Conventional Aeroelastic Launch Vehicle,* AIAA Scitech 2020 Forum (2020), 10.2514/6.2020-1103.

[90] K. J. Åström and R. M. Murray, *Feedback systems: an introduction for scientists and engineers* (Princeton university press, 2010).